γ-Cyclodextrin-based carrier in ocular drug delivery

Suppakan Sripetch

Thesis for the degree of Philosophiae Doctor

September 2022

School of Health Sciences

FACULTY OF PHARMACEUTICAL SCIENCES

UNIVERSITY OF ICELAND

γ-Cyclodextrin-based carrier in ocular drug delivery

Suppakan Sripetch

Thesis for the degree of Philosophiae Doctor

Supervisor
Prof. Thorsteinn Loftsson

Doctoral committee
Prof. Einar Stefánsson
Prof. Hákon Hrafn Sigurdsson
Assoc. Prof. Phatsawee Jansook
Dr. Sunna Jóhannsdóttir

September 2022

School of Health Sciences
FACULTY OF PHARMACEUTICAL SCIENCES
UNIVERSITY OF ICELAND

Augnlyfjaferjur byggðar á γ-sýklódextríni

Suppakan Sripetch

Ritgerð til doktorsgráðu

Leiðbeinandi
Prof. Þorsteinn Loftsson

Doktorsnefnd
Prof. Einar Stefánsson
Prof. Hákon Hrafn Sigurdsson
Assoc. Prof. Phatsawee Jansook
Dr. Sunna Jóhannsdóttir

September 2022

Heilbrigðisvísindasvið
LYFJAFRÆÐIDEILD
HÁSKÓLI ÍSLANDS

ISBN 978-9935-9689-0-6

Printing by Háskólaprent EHF.

Reykjavik, Iceland 2022

Ágrip

γ-sýklódextrín (γCD) hefur nýlega verið notað sem hjálparefni fyrir lyf til staðbundinnar notkunar í auga. Greint hefur verið frá mikilli þéttni barkstera í ýmsum augnvefjum eftir staðbundna notkun augndropa, einkum eftir að meðferðarþéttni hefur verið náð í aftari hluta augna. Þetta gefur tilefni til að kanna frekari notkun γCD við gjöf barkstera í auga og uppgötva nýja notkunarmöguleika γCD sem lyfjalosunarkerfis fyrir önnur hugsanleg lyf við augnsjúkdómum. Það er vel þekkt að eðlisefnafræðilegir eiginleikar gestasameindar, til dæmis fitusækið lyf og/eða γCD, geta breyst þegar þau mynda flóka. Þetta gerist þrátt fyrir að ekkert samgilt tengi taki þátt í myndun efnaflókans milli lyfsins og γCD. Flestir efnaflókar leiða til aukinnar leysni og/eða aukins stöðugleika lyfsins í vatni, sem aftur leiðir til aukins aðgengis lyfsins að marklíffærinu eftir gjöf. Vatnskennda slímlagið sem liggur yfir þekjuvef margra líffæra hindrar yfirleitt upplausn fitusækna lyfsins og dreifingu þess í slímlaginu. Með því að bæta vatnsleysni lyfja sem leysast illa upp í vatni eykst enn fremur aðgengi að lyfjasameindinni á mótum slímlags og þekju. Á svipaðan hátt myndar vatnskennt slímlag tárahimnunnar sem þekur augnþekjuna helstu efnislegu hindrunina fyrir fitusækna lyfið. Við þróun augnlyfja er ekki aðeins mikilvægt að auka leysnieiginleika hjálparefna heldur einnig að bæta gegndræpi lyfja til að lyfjalosunarkerfið komist fram hjá flóknum hindrunum í augum. Þar af leiðandi felur þetta verkefni í sér rannsókn á notkun γCD sem lyfjaferju fyrir staðbundna notkun í augum og að leita hagkvæmra leiða fyrir ný hugsanleg lyf sem γCD getur flutt með sama hætti.

Markmið rannsóknarinnar var að bæta vatnsleysni fitusækna lyfsins dóvitiníbs, sem er óbundinn basi, með því að nota γCD til að rannsaka eðlisefnafræðilega eiginleika lyfsins samhliða γCD og öðrum hjálparefnum með það fyrir augum að ákvarða áhrif γCD á gegndræpi lyfja. Enn fremur var markmiðið að rannsaka þá þætti sem hafa áhrif á gegndræpi lyfja í gegnum fitusæknar himnur og losun lyfs frá γCD-lyfjaferju. Fasaleysniaðferð (e. phase-solubility technique) var notuð á vatnslausn með γCD til að mynda flóka úr fitusæknum lyfjum í líkani (e. model-drugs) (dóvitiníb og dexametasón), ákvarða vatnleysni lyfjanna á viðkomandi rannsóknarformi og að undirbúa sýnislausnir fyrir gegndræpirannsóknir. Metin var virkni stakra aðferða, svo sem myndun γCD-flóka og myndun salta, og samsettra aðferða með myndun γCD-flóka og jónun til að bæta vatnsleysni dóvitiníbs. Fimm sýrur voru notaðar til að rannsaka saltmyndun og jónun dóvitiníb-basa með rannsóknum á leysanleika tengdum sýrustigi (e. pH-solubility). Fimm

mótjónum með þremur mismunandi þéttnigildum var bætt við flókalausnina sem innihélt γCD með tveimur mismunandi þéttnigildum og aukin leysni var svo ákvörðuð út frá því. Auk þess voru fitusækni og stöðugleiki skoðuð bæði með og án hjálparefna, þ.e. γCD, mótjóna, jafnalausna. Enn fremur var eiginleikum brota á föstu formi sem fundust í dreifu með dóvitiníbi/sýru/γCD í mikilli þéttni lýst með hliðsjón af magni dóvitiníbs og γCD með því að nota háþrýstivökvaskiljun, stærð föstu agnanna var lýst með ljósdreifigreiningu með leysigeisla og formi dóvitiníbs og γCD var lýst með Fourier-vörpunarlitrófsgreiningu með innrauðu ljósi. Að lokum var *in vitro* prófun á gegndræpi framkvæmd í lóðréttu Franz dreifihólfi (e. Franz diffusion cell) með efnasmíðaðri fitusækinni himnu og stöku lagi af skilunarhimnu úr sellulósa. Sérstakar tilraunaaðstæður voru hannaðar til að rannsaka sérstaklega áhrif γCD á gegndræpi lyfs, myndunarþætti sem hafa áhrif á gegndræpi lyfs og losun lyfs frá γCD-lyfjaferju.

Rannsóknir á leysni sýndu að saltmyndun með mótjón eykur vatnsleysni dóvitiníbs mun meira en myndun efnaflóka með γCD. Mjólkursýra bætti leysni allt að tugþúsundfalt og var leysniaukning hennar mest af þeim sýrum sem voru notaðar. Þegar tvær aðferðir voru notaðar samhliða jókst leysnin vegna bættrar sýnilegrar og eðlislægrar leysni, eins og búist var við í sumum kerfum. Hins vegar kom á óvart að samverkandi leysniáhrif komu fram þegar dóvitiníb var leyst upp í súrum vatnslausnum sem innihéldu fosfór-/γCD og malín-/γCD þar sem γCD var í lágri þéttni (38,6 mM). Á sama tíma bætti þrígilda kerfið með dóvitiníbi, mjólkursýru og γCD (38,6 mM) leysni gegnum viðbótaráhrif. Við mikla þéttni γCD (154,2 mM) jókst upplausn dóvitiníbs og dóvitiníb-/γCD-flóka í takt við aukna sýruþéttni. Aftur á móti voru nokkur sýni sem innihéldu tiltölulega lága sýruþéttni dreifur. Því var magn dóvitiníbs og γCD í föstu broti ákvarðað og tvær dreifur sem fengust úr mjólkursýru og fosfórsýru voru greindar með hliðsjón af eiginleikum. Niðurstöðurnar leiddu í ljós að fasta brotið innihélt meira af γCD en dóvitiníbi. Föstu agnirnar í þessum dreifum voru nokkrir míkrómetrar að stærð og á formi flóka með γCD. Þetta benti til þess að dreifa með dóvitiníbi, sýru og γCD (154,2 mM) sem fékkst úr mjólkursýru og fosfórsýru innihélt sjálfraðaðar (e. self-assemble) öragnir af dóvitiníb-/γCD-flókum. Auk þess var fitusækni dóvitiníbs ákvörðuð þegar súrar mótjónir voru til staðar við mismunandi sýrustig og henni lýst með $\log_{10}$ af dreifistuðli, log D. Í ljós kom að sýrustigið var helsti þátturinn sem hafði áhrif á log D í jónanlegu dóvitiníbi. Mótjónirnar geta haft áhrif á log D jónaðs dóvitiníbs en þær hafa óveruleg áhrif á log D í ójónaða lyfinu. Rannsóknir á stöðugleika sýndu einnig að γCD getur haldið dóvitiníbi stöðugu við tiltölulega lágt sýrustig. Stöðugleikaáhrif γCD voru greinilegri en áhrif jafnalausnarinnar.

Rannsóknir á gegndræpi lyfsins í gegnum efnasmíðaða fitusækna himnu voru gerðar til að kanna áhrif γCD á gegndræpi dexametasóns og áhrif

myndunarþáttarins á gegndræpi dóvitiníbs. Niðurstöður fyrir gegndræpi dexametasóns sýndu að flæði lyfsins jókst með aukinni upplausn dexametasóns og aukinni þéttni γCD. Flæðið minnkaði verulega eftir að hámarksleysni dexametasóns var náð en hins vegar sást umframmagn af γCD. Þetta benti til þess að mesta gegndræpi hafi komið fram þegar bæði varmafræðileg virkni lyfsins og þéttni uppleysts lyfs voru í hámarki. Hins vegar voru niðurstöðurnar fyrir gegndræpi dóvitiníbs ólíkar. Flæði dóvitiníbs minnkaði og sýnilegur gegndræpistuðull (P_{app}) þess lækkaði þegar sjálfröðuðu nanóagnirnar voru til staðar. Auk þess minnkaði flæðið og P_{app} lækkaði enn frekar þegar nanóagnir voru stærri. Þar af leiðandi skal hafa í huga myndunarþætti á borð við stærð agna við hönnun lyfjasamsetningar.

Rannsóknin á losun lyfsins var framkvæmd með því að nota eitt lag af skilunarhimnu úr sellulósa. Upphaflegur tilgangur þessarar rannsóknar var að kanna áhrif α-amýlasaensíms, sem fundist hefur í táravökva, á losun dexametasóns frá γCD-lyfjaferju við aðstæður sem líkja eftir sýrustigi tára og yfirborðshita augans. Hins vegar fannst óvæntur þáttur sem hefur viðbótaráhrif á virkni α-amýlasa. Samkvæmt niðurstöðum úr losunarrannsóknunum getur þetta skýrt hraðari losun dexametasóns úr vatnslausn sem inniheldur γCD í tiltölulega lágri þéttni, þ.e. 1–4 mM og α-amýlasaensím á þann veg að hraðari losun er tilkomin vegna viðbótaráhrifa þynningar og hvötunar α-amýlasa.

Lokaniðurstaðan er sú að γCD hefur sveigjanlega virkni sem fer eftir þéttni þess og því hvort aukefni eru til staðar eða ekki. Það getur bæði gert fitusækna lyfið dóvitiníb leysanlegt og haldið því stöðugu með því að mynda flóka og sjálfraðaðar γCD-agnir. Jafnvel þó γCD-lyfjaferja geti bæði aukið eða hindrað gegndræpi lyfsins er hægt að hámarka áhrifin. Enn fremur er hægt að auka losun lyfs þegar α-amýlasi er til staðar í þynntri γCD-lausn. Þessar niðurstöður benda til þess að hægt sé að nota γCD sem lyfjaferju fyrir fitusækin lyf til staðbundinnar notkunar í auga.

Lykilorð:

γ-sýklódextrín

Leysni

Fitusækni

Stöðugleiki

Gegndræpi

Abstract

γ-Cyclodextrin (γCD) has been recently used as pharmaceutical excipient in topical formulation for ocular delivery. The high corticosteroid concentration in various ocular tissues has been reported after topical application of aqueous eye drops, especially achieving therapeutic level in the posterior segment of the eyes. This draws attention to expand on the γCD application in ocular corticosteroid delivery and discover new use of γCD as drug carrier for drug candidates in eye disease. It is well known that physicochemical properties of lipophilic drug, e.g., solubility, can be changed when they form complex with γCD without covalent bond involved in the complexation. Most complex formations result in improvement of the drug´s solubility or stability or both in water leading to the enhancement of the drug bioavailability at target organ after administration. Normally, aqueous mucus layer covering epithelium of many organs hampers lipophilic drug to dissolve and partition in this layer. When the aqueous solubility of poorly water-soluble drugs is improved, availability of the drug molecule is greater at mucus-epithelium interface. Similarly, the aqueous-mucin layer of tear film covering ocular epithelium is the frontline physical barrier of the lipophilic drug. In ophthalmic formulation development, not only solubilizing property of excipient but the ability of vehicle to enhance drug permeability is also important for drug delivery system to overcome complicated barriers of the eyes. Therefore, this project will explore into the foundation of the γCD application as a drug carrier for topical delivery to the eye and seek feasibility of incorporation of new drug candidate in γCD-based carrier platform.

The objectives of this study were to improve water solubility of the lipophilic drug, dovitinib free base using γCD; to examine physicochemical properties of the drug in the presence of γCD and other pharmaceutical excipients; to determine the effect of γCD on drug permeation; as well as to investigate the factors affecting drug permeation through lipophilic membrane and drug release from γCD-based carrier.

Phase-solubility technique was used to form complex of the lipophilic model-drugs (dovitinib and dexamethasone) in γCD aqueous media, determine the aqueous solubility of the drugs in relevant studied condition, and prepare sample solutions for the permeation studies. To improve the aqueous solubility of dovitinib, single technique such as γCD complexation and salt formation, and combination techniques of γCD complexation and ionization were evaluated. Five acids were used to investigate salt formation and ionization of dovitinib base by pH-solubility studies. In optimization, three different concentrations of each acid were added to the complexing media

containing two different γCD concentrations and the enhanced solubility was determined. Lipophilicity and stability were also examined in the presence and absence of pharmaceutical excipients, i.e., γCD, counterions, buffers. Furthermore, the solid fraction found in spontaneous suspensions of the dovitinib/acid/high γCD concentration was characterized in terms of the contents of dovitinib and γCD, size of solid particles, and form of dovitinib and γCD using high performance liquid chromatography, laser scattering technique, and Fourier-transform infrared spectroscopy, respectively. Finally, in-vitro permeation studies were carried out using vertical Franz diffusion cells, artificial lipophilic membranes, and a single layer of cellulose dialysis membranes. A particularly experimental condition was designed to separately investigate the γCD effect on drug permeation, formulation factors affecting drug permeation, and drug release from γCD-based carrier.

Solubility studies showed that salt formation with counterions increased the aqueous solubility of dovitinib greatly rather than complexation with γCD. Lactic acid improved the solubility up to many ten-thousand folds and its solubility enhancement was the highest among other acids used. When the combined techniques were used, the total solubility, i.e., the intrinsic solubility of the pure drug and solubility of the drug/γCD complex, was increased due to the improvement of apparent intrinsic solubility as expected. Surprisingly, a synergistic effect of solubilization was found when dovitinib was dissolved in the acidic aqueous solutions containing lactic/γCD, phosphoric/γCD and maleic/γCD at low concentration of γCD (38.6 mM). At high γCD concentration (154.2 mM), the dissolved dovitinib and dovitinib/γCD complex increased with increasing acid concentration. In contrast, some samples containing relatively low acid concentration were suspension. Thus, the contents of dovitinib and γCD in solid fraction were determined and two suspensions obtained from lactic acid and phosphoric acid were characterized. The results revealed that solid fraction contained γCD content more than dovitinib content. The solid particles in those suspensions were in a few micrometers of size and in a complex form with γCD. This indicated that spontaneous suspension of dovitinib/acid/154.2 mM γCD obtained from lactic acid and phosphoric acid contained self-assembled microparticles of dovitinib/γCD complexes. Moreover, lipophilicity of dovitinib in the presence of acidic counterions was determined at different pH and described with $\log_{10}$ of distribution coefficient, log D. It was found that the pH was the main factor influencing the log D of the ionizable dovitinib. The counterions can affect the log D of the ionized dovitinib but have a negligible impact on the log D of the unionized drug. The stability studies also showed that γCD could stabilize dovitinib at relatively low pH. The stabilizing effect of γCD was more noticeable than the buffer effect.

The drug permeation studies through the artificial lipophilic membrane were performed to investigate the γCD effect on permeation of

dexamethasone and the impact of formulation factor on dovitinib permeation. The results of dexamethasone permeation showed that drug flux increased with increasing dissolved dexamethasone and γCD concentration. The dexamethasone flux increased until reaching the maximum at the highest solubility of the drug then decreased dramatically when excess γCD was found in the dexamethasone-saturated solution. This indicated that the highest permeation was obtained when both the thermodynamic activity of the drug and the soluble drug concentration were at maximum. However, the results from dovitinib permeation showed different phenomenon. The dovitinib flux and apparent permeability coefficient (P_{app}) decreased when the self-assembled nanoparticles existed. In addition, the flux and P_{app} further decreased when the nanoparticle was larger in size and concentration. Therefore, the formulation factor such as particle size should be considered during formulation design.

The study of drug release was performed using a single layer of cellulose dialysis membrane. Original intention of this study was to investigate the effect of α-amylase enzyme, which has been found in tear fluid, on dexamethasone release from γCD-based carrier under mimic tear pH and ocular surface temperature. However, unexpected factor was found with additive influence on the α-amylase effect. From the observation in the release studies, it can explain that the faster release of dexamethasone from aqueous solution containing relatively low γCD, i.e., 1–4 mM and α-amylase enzyme was due to the additive effect of dilution and α-amylase catalysis.

In conclusion, γCD showed functional flexibility as an excipient depending upon its concentration and the presence of additives. It could both solubilize and stabilize the lipophilic drug of interest, dovitinib through forming complex and self-assembled γCD particles. γCD-based carrier can either enhance or hamper the drug permeation, but the effect can be optimized. Furthermore, drug release can be enhanced when α-amylase is present in diluted γCD solution. These findings suggest that γCD can be used as a drug carrier for lipophilic drug in topical delivery to the eyes.

Keywords:

γ-Cyclodextrin

Solubility

Lipophilicity

Stability

Permeation.

Acknowledgements

This study was carried out during the period of 2018 – 2022 at Oculis ehf. Laboratory and the Faculty of Pharmaceutical Sciences, School of Health Sciences, University of Iceland. The project was funded by Oculis ehf. and was received the grant from the Bergþóra and Þorsteinn Scheving Thorsteinsson fund.

First and foremost, I would like to express my sincere gratitude to my supervisor Professor Thorsteinn Loftsson for giving me the opportunity to work in his research group as a Ph.D. student as well as being team member of Oculis research and technology. His invaluable advice, assistance, professional guidance, and endless patience throughout my Ph.D. study have been deeply appreciated. I would like to thank for his kindness, understanding, support, and encouragement through all scientific impediments. Also, I am extremely grateful for his meaningful advice 'Keep It Simple' which means that do not complicate the experimental design when we were discussing our challenged research. That was the important key to get precise answers to the research questions.

Beside my supervisor, I would like to thank the members of doctoral committee: Prof. Einar Stefánsson, Prof. Hákon Hrafn Sigurdsson, Assoc. Prof. Phatsawee Jansook, and pay respect to late Dr. Sunna Jóhannsdóttir.

I would like to acknowledge Prof. Kim Lambertsen Larsen from the Faculty of Engineering and Science, Aalborg University for his scientific knowledge and advice on enzymatic reaction. My sincere thanks also go to all professors and staff at the Faculty of Pharmaceutical Sciences for technical support and advice. I am very grateful to Assoc. Prof. Phatsawee Jansook for introducing me to my supervisor and for his helpfulness.

My special thanks to my colleagues at Oculis ehf., Iceland, Gudrun, Pall, Alexey, Tijana, Sirry, Iris, Linda, and Jon for the friendship, assistance, and comprehension. I would like to express my thanks to Manisha, Pitsiree, Vivien, Maonian, Sigga, and Sebastian for their help and companion when I was in Faculty´s lab. I am also thankful to my Thai colleagues and friends in Thailand for their encouragement and support that made my Ph.D. study possible. Special thanks to my best friend, Dr. Ing-orn Prasanchaimontri for her kind assistance and useful advice about the study and living in a foreign country.

Lastly, I would like to express my heartfelt thanks to my parents, my sister, and all my relatives for their endless love, care, support, and cheerfulness throughout my Ph.D. journey and entire life.

Contents

List of abbreviations

γCD	γ-cyclodextrin
CD	Cyclodextrin
CE	Complexation efficiency
DMSO	Dimethyl sulfoxide
FTIR	Fourier-transform infrared spectroscopy
HPγCD	Hydroxypropyl-γ-cyclodextrin
HPLC	Reverse-phase high performance liquid chromatography
HPLC-RI	Reverse-phase high performance liquid chromatography with refractive index detector
J_{ss}	Steady-state flux
$K_{1:1}$	Stability constant of the 1:1 complex
K_c	Stability constant
k_{cat}	Turnover number of enzymes
K_d	Dissociation constant
K_m	Michaelis-Menten constant
MWCO	Molecular weight cut-off
P_{app}	Apparent permeability constant
PPA	Porcine pancreatic α-amylase
RC	Regenerate cellulose
rpm	Revolution per minute
S_0	Intrinsic solubility
SBEγCD	Sulfobutylether-γ-cyclodextrin
UWL	Unstirred water layer
V_{max}	Maximum velocity of enzymes

List of figures

List of tables

List of original papers

This thesis is based on the following original publications:

I. Sripetch, S., Jansook, P., & Loftsson, T. (2020). Effect of porcine pancreatic α-amylase on dexamethasone release from aqueous solution containing natural γ-cyclodextrin. *International Journal of Pharmaceutics, 585*, 119452.

II. Sripetch, S., Ryzhakov, A., & Loftsson, T. (2022). Preformulation studies of dovitinib free base: Solubility, lipophilicity and stability. *International Journal of Pharmaceutics, 619*, 121721.

III. Sripetch, S., Prajapati, M., & Loftsson, T. (2022). Cyclodextrins and Drug Membrane Permeation: Thermodynamic Considerations. *Journal of Pharmaceutical Sciences*, *111*, 2571-2580.

Some unpublished data may be presented.

In addition, other scientific publications:

IV. Jansook, P., Praphanwittaya, P., Sripetch, S., & Loftsson, T. (2020). Solubilization and in vitro permeation of dovitinib/cyclodextrin complexes and their aggregates. *Journal of Inclusion Phenomena and Macrocyclic Chemistry, 97*(3), 195-203.

V. Sripetch, S., & Loftsson, T. (2021). Topical drug delivery to the posterior segment of the eye: Thermodynamic considerations. *International Journal of Pharmaceutics, 597*, 120332.

VI. Soe, H. M. S. H., Sripetch, S., Loftsson, T., Stefánsson, E., & Jansook, P. (2022). Effect of Soluplus® on γ-cyclodextrin solubilization of irbesartan and candesartan and their nanoaggregates formation. *Pharmaceutical Development and Technology, 27*(1), 9-18.

Declaration of contribution

The doctoral student, Suppakan Sripetch planned the research works in these studies, performed all experiments, drafted the manuscripts, and wrote this thesis with the guidance of her supervisor, the doctoral committee, and cooperation with the co-authors of each study.

1 Introduction

1.1 Ocular drug delivery

1.1.1 Anatomy and physiology of the human eye

The eye is an environmentally exposed organ with sophisticated function. Its structure is complicated and composed of various tissues. The eyeball has three layers, i.e., cornea/sclera, uvea, and retina (Cholkar, Dasari, Pal, & Mitra, 2013; Galloway, Amoaku, Galloway, & Browning, 2016). In addition, most clinically divide it into two compartments, anterior and posterior parts (Figure 1). The anterior segment is from the posterior lens to anterior cornea. This segment occupies approximately one third of the eyeball in the front. After the lens toward inside orbital bone is the posterior segment comprising four major structures. To serve as primary organ of visual function, the eye´s tissues are embryonically built to work together facilitating incident light from an object to the retina, producing an image, and transmitting the image to the brain. Like its main function, the defending function of the eye to foreign materials or stimulants is inherent physiological role of the eye´s tissues to protect and secure the organ (Cholkar et al., 2013).

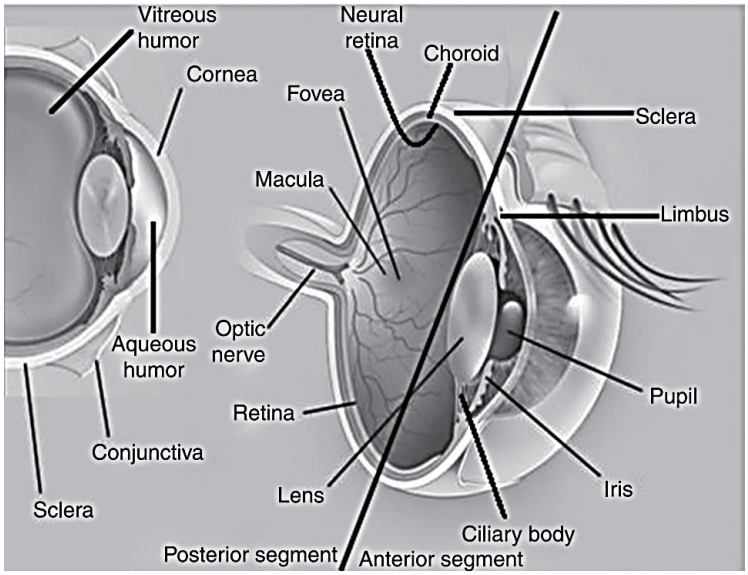

Figure 1. A schematic diagram of human eye modified from Cholkar et al. (2013).

1.1.1.1 Anterior segment

The anterior segment consisting of the cornea, conjunctiva, iris, ciliary body, aqueous humor, and lens, is in front of the eye. Although the cornea and conjunctiva are readily accessible upper and lower eyelids physically protect the eye by closing. Another function of the eyelids, besides protective function (preventing mechanical trauma, extremes of temperature and bright light), is preservation of the tear film which consequently maintains cornea transparency (Galloway et al., 2016).

Cornea

The cornea has a curved shape and is clear, thin, smooth, and very sensitive tissue owing to high innervation and having no blood vessels. The dimensions of a normal cornea after mature growth are approximately 11.8 mm in horizontal diameter and approximately 11.3 mm in vertical diameter (Augusteyn et al., 2012). No significant difference exists between left and right eye, or between male and female eyes (Augusteyn et al., 2012; Rüfer, Schröder, & Erb, 2005). The cornea connects with the conjunctiva; the semi-transparent tissue, and the anterior sclera; the visibly white tissue. The connective border of the clear cornea and the white sclera is limbus where the end of the ciliary arteries supply blood components to the cornea. The thickness of the central cornea is thinner than that of the peripheral cornea. The average thickness was about 523 µm and 660 µm for center and peripheral, respectively (Martola & Baum, 1968). The cornea epithelium is covered with mucus layer of tear film and next to the cornea endothelium is the aqueous humor.

The cornea tissue is composed of five distinct layers (Figure 2) from outer to inner layer, i.e., epithelium, Bowman's layer, stroma, Descemet's membrane, and endothelium. Corneal epithelium consists of five to six layers of non-keratinized epithelial cells. Basal epithelial cells, which are columnar cells, are seated on the basal lamina to form a single layer and two to three layers of wing cells and superficial squamous cells (Willoughby et al., 2010). Upon differentiation, the superficial epithelial cells become flat with tight junction cells. Its membrane at the corneal surface forms microplicae which are covered by very fine charged-glycocalyx. The glycocalyceal microplicae involve in tear film turnover (Cholkar et al., 2013). Although the microplicae increase surface area, the presence of tight cell junctions decreases permeability throughout the epithelium. The superficial cells are renewed every 7 to 10 days by the pluripotent stem cells in the limbus (Cholkar et al.,

2013; Willoughby et al., 2010). Bowman's layer is composed of collagen fibrils in the proteoglycan matrix and forms a boundary of the stroma. This layer maintains the cornea's shape. Corneal stroma is in the middle between Bowman's layer and Descemet's membrane. The mean thickness of the stroma at the central cornea, measured in a population of normal eyes, is approximately 465.4 µm (Reinstein, Archer, Gobbe, Silverman, & Coleman, 2009). The corneal stroma is comprised of collagen fibrils and proteoglycans which are secreted by stromal keratocytes. The fibrils regularly arrange from limbus to limbus. The collagen network is responsible for the strength and transparency of the cornea. Descemet's membrane is the basement membrane of the corneal endothelium. The corneal endothelium consists of a single layer of cuboidal cells with ion transport system. The ion flux regulates an osmotic gradient to control the water in the stroma and is important in maintaining corneal clarity (Willoughby et al., 2010).

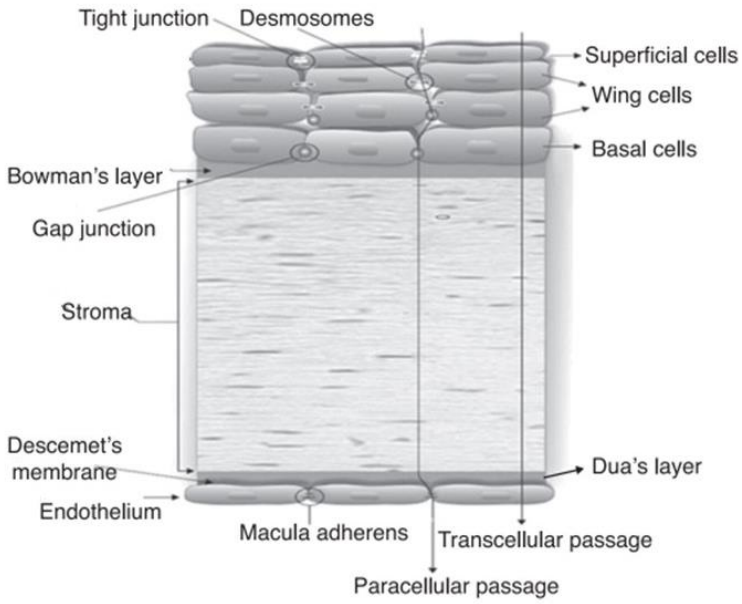

Figure 2. Schematic diagram of the cornea modified from Cholkar et al. (2013).

Conjunctiva

The conjunctiva tissue covers from the anterior sclera to the inner of both upper and lower eyelids and is semi-transparent, vascularized, innervated, and lymphatic. Its thickness and histology depend on the location. A small and thin fraction of conjunctiva tissue, called the bulbar conjunctiva, covers

the anterior sclera, and connects to the cornea. The whole surface area of the conjunctiva is ~17 times greater than that of the cornea (Watsky, Jablonski, & Edelhauser, 1988). The conjunctiva consists of two layers, i.e., epithelium and stroma. The conjunctival epithelium consists of stratified epithelial cells with tight junction and the apical epithelial cells forming microplicae and microvilli (Cholkar et al., 2013; Hosoya, Lee, & Kim, 2005). The conjunctival stroma is a structure integrated with blood vessels, nerves, and lymphatic vessels. Other cells such as goblet cells and melanocytes are present in the bulbar conjunctival epithelium near the limbus (Wanko, Lloyd, & Matthews, 1964). The conjunctiva epithelium plays an important role in tear film system. It secretes tear film elements such as mucin, electrolytes, and fluid as well as supports the attachment of tear film on the eye surface (Diebold & García-Posadas, 2021; Hosoya et al., 2005).

Aqueous humor

Aqueous fluid, located at the posterior corneal endothelium and anterior lens, is called the aqueous humor. The aqueous humor functions as a source of nutrients and some oxygen and a waste collector for the cornea and lens (Cholkar et al., 2013; Galloway et al., 2016). It also maintains intraocular pressure via the outflow of the aqueous humor. The aqueous humor is like blood plasma, except the content of protein and ascorbic acid. It is produced in the ciliary body and secretes into the anterior chamber called the ciliary processes. The ciliary processes consist of diffusion, ultrafiltration, and active secretion. The turnover rate of the aqueous humor is approximately 2.4 µL/min or about 1.0 to 1.5% of the anterior chamber volume per min (Goel, Picciani, Lee, & Bhattacharya, 2010). The aqueous humor is removed from the anterior chamber via the trabecular meshwork/Schlemm's canal pathway and uveo-scleral pathway (Fautsch, Johnson, & Group, 2006).

Ciliary body

The ciliary body is a joining part between the anterior and posterior chambers in the anterior segment. The anterior ciliary body is attached to the sclera spur and the posterior part connects to the choroid and retina at the ora serrata (Goel et al., 2010). The ciliary body consists of ciliary epithelium, i.e., pigmented and nonpigmented epithelial cells, ciliary stroma, and ciliary muscle (Delamere, 2005). The ciliary body looks like a right triangle in cross-section. At the base of the triangle posteriorly is the ciliary muscle where the

suspensory ligaments, zunules, connect to the ciliary body. On other side of the triangle base anteriorly, it connects to the iris. As mentioned above, the ciliary body's function is to form the aqueous humor. Others are a focus adjustment of the lens via ciliary muscle and zunules and an aqueous humor drainage (Armstrong & Cubbidge, 2014; Cholkar et al., 2013).

Iris

The iris is a circular disc with a central aperture or a pupil and is a visibly anterior part of the uvea, comprising an iris, ciliary body, and choroid. The iris is immersed in the aqueous humor at the anterior region of the lens. When the eyes are exposed to bright or dim light, the iris muscle will regulate the pupil's size to adjust the light entering the posterior segment. The inner surface of the iris is covered with cells containing the pigment melanin. The amount of pigmentation is genetically dependent (Armstrong & Cubbidge, 2014; Cholkar et al., 2013; Galloway et al., 2016).

Lens

The lens is a transparent, avascular, non-innervated, biconvex, highly elastic structure and is the most inner part of the anterior segment, close to vitreous humor. It comprises four different parts, i.e., the capsule, epithelium, cortex, and nucleus. A lens capsule is a membrane of the lens to maintain its shape and metabolism. The lens epithelium appears only at the anterior side and next to the capsule inside the lens. The lens epithelium consists of a single layer of columnar epithelial cells. The epithelial cells in the equator part can grow and differentiate throughout life. Upon differentiation, the epithelial cells become new fibers in the cortex part and mature fibers in the nucleus part. The growth is from outer to inner lens (epithelium → cortex → nucleus). An arrangement of the fibers in the cortex and nucleus as well as the removing organelle from the cells play important roles in lens transparency and elasticity. Thus, lens thickness changes continually with age and consequently the lens loses its ability to accommodate (Cholkar et al., 2013; Mochizuki & Masai, 2014; Ruan, Liu, Luo, & Liu, 2020).

1.1.1.2 Posterior segment

The posterior segment is composed of vitreous humor, retina, choroid, and sclera (from the anterior toward posterior eyeball).

Vitreous humor

The vitreous humor is a gel-like fluid filled in the vitreous cavity occupying from the back of the lens to the front of the posterior retina. The vitreous humor consists of 99.9% water and 0.01% collagen fibrils, hyaluronic acid, and ions (Cholkar et al., 2013). It helps to support the globe structure.

Retina

The retina is the innermost layer of the eye, covering the vitreous humor and is divided as the neural retina and the retinal pigment epithelium. The neural retina comprises several parallel layers from the inside (next to the vitreous humor) to the outside (Galloway et al., 2016) as follows:

- Internal limiting membrane is attached to the vitreous humor.
- Nerve fiber layer: axons of ganglion cells and Müllerian glia
- Ganglion cell layer: nuclei of ganglion cells
- Inner plexiform layer: the bipolar and amacrine cells connect to ganglion cells.
- Inner nuclear layer: nuclei of Müllerian glia, the bipolar cells, the amacrine and horizontal cells
- Outer plexiform layer: the photoreceptors connect to bipolar and horizontal cells.
- Outer nuclear layer: nuclei of the photoreceptors
- External limiting membrane
- Photoreceptors (rods and cones) close to the retinal pigment epithelium.

The distribution of photoreceptors depends on the region of the retina such as the macula, fovea, optic disc, and temporal retina. In the center of the macula, the fovea is responsible for the highest visual acuity; therefore, it contains the largest number of cones without rods (Cholkar et al., 2013). The major function of the photoreceptors is phototransduction. When light enters the eye and reaches the retina, the rods and cones convert it to an electric signal, subsequently transmitted to the brain. The photoreceptors' function is maintained by the retinal pigment epithelium which intercalates between the

photoreceptors and the choriocapillaris. The retinal pigment epithelium consists of a single layer of the cuboidal epithelial cells containing melanin and lipofuscin pigments. In addition to the maintenance of the photoreceptors, the retinal pigment epithelium functions include retinal adhesion, storage and metabolism of retinoids, production of growth factors, and wound healing (Willoughby et al., 2010).

Choroid

The choroid is highly vascularized and pigmented tissue in between the outer layer of the retina (retinal pigment epithelium) and the inner layer of the sclera. Three parts of the choroid from the posterior retina to anterior sclera are the suprachoroid, vascular layer, and Bruch's membrane. In the vascular layer are blood vessels, pigmented melanocytes and non-pigmented fibrocytes. The choroid's blood vessels supply the nutrient and oxygen to the retina as well as remove wastes and heat from the retinal cells (Cholkar et al., 2013).

Sclera

The sclera is the outer layer of the posterior segment of the eye. It is avascular and sieve-like elastic tissue consisting of collagenous fibers. The scleral appears as a white tissue due to light scattering the disordered arrangement of collagen fibers. It provides support to the globe and the optic nerve (Cholkar et al., 2013; Galloway et al., 2016).

1.1.1.3 Tear film

Tear film is a thin layer of tear fluid, covering the ocular surface and serving as a defending boundary. Its structure, components, production, function, and clearance are complicated and still investigated. New evidence and details of tear film components have been continually emerging (Pflugfelder & Stern, 2020). Approximate thickness of tear film layers is also under discussion due to the different values from using various methods (King-Smith et al., 2000; Pflugfelder & Stern, 2020). Classically, the tear film consists of three layers toward the cornea/conjunctiva epitheliums, i.e., an outer lipid, middle aqueous, and inner mucus layer (Figure 3) (Rolando & Zierhut, 2001). The lipid layer contains polar and non-polar lipids secreted mostly by Meibomian glands. Over 600 individual lipid species have been identified from 17 distinct lipid classes in tear lipid such as cholesterol, wax esters, hydroxy fatty acid,

phospholipids, and sphingolipids (Svitova & Lin, 2016). A thin polar lipid layer lines the interface between the thick non-polar lipid layer, facing the air, and the aqueous layer. Aqueous tear is produced by lacrimal glands and composed of water and soluble substances including proteins, electrolytes, inorganic salts, glucose, and oxygen (Galloway et al., 2016). The proteins found in the aqueous layer comprise great varieties of enzymes, immunoglobulins, glycoproteins, growth factors etc. The most abundant protein is lysozyme at approximately 2.5 mg/mL (Pflugfelder & Stern, 2020). The lipid and aqueous layer are clearly seen as separated layers, but recently the structure of the aqueous and mucus layers has been proposed as a single aqueous-mucin layer (Rolando & Zierhut, 2001). The aqueous-mucin layer toward the ocular surface consists of a greater number of flexible glycoproteins or mucin. The mucin forms hydrogen bonds with surrounding water molecules, resulting in increased viscosity of tear film and forming an aqueous diffusion barrier to the poorly water-soluble drug (Sripetch & Loftsson, 2021). The innermost part of the aqueous-mucin layer is related to the ocular epithelium. The apical epithelial cells form microplicae with glycocalyx where the tear mucins can hang on.

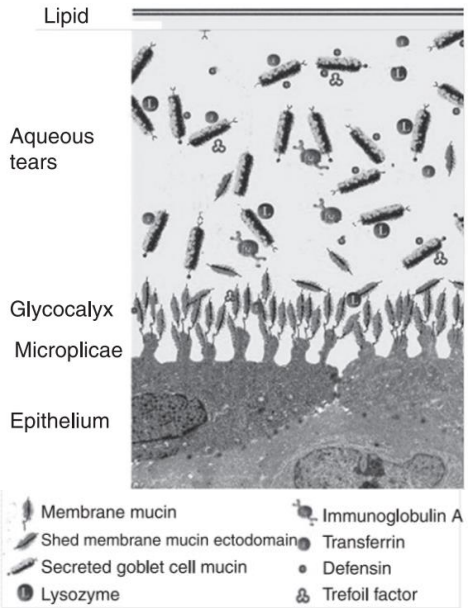

Figure 3. Schematic diagram of tear film modified from Cholkar et al. (2013).

Tear production, delivery and clearance are regulated by the lacrimal functional unit composed of several glands, ocular tissue, an immune system,

and nerves. Briefly, major components of tear film, i.e., aqueous liquid, lipids, and mucins are mainly produced from lacrimal glands, Meibomian glands, and conjunctiva goblet cells. All components are secreted and assembled to form a thin film when the eyelids move over the globe when closing the eye or blinking. Then the tear film breaks up when the eye opens. Tears including residue from tear film breaking and excess volume of tear fluid will be removed via evaporation and the lacrimal drainage system where the fluid flows through the lacrimal puncta → lacrimal canaliculi → lacrimal sac → nasolacrimal duct → inferior nasal meatus (Kels, Grzybowski, & Grant-Kels, 2015; Pflugfelder & Stern, 2020; Rolando & Zierhut, 2001; Tiffany, 2008). The volume of tear fluid depends on many factors, e.g., the thickness of tear film, the area of the film including in measurement and the method. The mean volume of tear fluid is approximately 7 µL. The tear flow rate is about 1.2 µL/min with a turnover rate of 16%/min during an unstimulated state (Mishima, Gasset, Klyce, & Baum, 1966; Tiffany, 2008). The innervation regulating the tear process is very complicated and involves both parasympathetic and sympathetic systems. The eyelids and lacrimal functional unit collaborate to protect the ocular surface when exposing to stimulants, e.g., extreme environments, foreign substrate, and microorganisms. Therefore, tear film will be produced, secreted, removed, and all processes will be repeated continually to lubricate the ocular surface, maintain visual function, prevent infection, suppress inflammation, clear debris, and heal small injuries (Pflugfelder & Stern, 2020; Tiffany, 2008).

The enzymes found in tear fluid play an important role in the antimicrobial function of tears. Lysozyme is a major enzyme in tears and found highest in concentration among all body fluids. It has bacteriolytic activity (Chang & Purt, 2022). Other antimicrobial compounds found in human tears include lactoferrin, lipocalin, secretory immunoglobulin A and complement (McDermott, 2013). Besides lysozyme, amylase is also found in human tear at lower amount than lysozyme and is locally produced and secreted from the lacrimal gland (Anderson & Leopold, 1979; van Haeringen, Ensink, & Glasius, 1975). The physiological function of tear amylase remains unclear. It might be involved in glycogen metabolism of the corneal epithelium and glycogen metabolic process during formation of mucus materials in epithelial cells (Pei & Rhodin, 1971; van Haeringen et al., 1975).

Studies, measuring the normal pH of tear fluid, found that the tear pH ranged from 6.5 to 7.6 which was influenced by eyelid closure, sex, age, pathology etc. (Abelson, Udell, & Weston, 1981; Coles & Jaros, 1984).

1.1.2 Route of drug administration to the eye

The challenge of drug delivery to the eye is overcoming all complicated static and dynamic barriers until achieving a therapeutical concentration of the drug at the target site in ocular tissue. Those barriers depend on the intended target in the eye and route of drug administration. Generally, an ocular drug administration is classified as invasive or non-invasive techniques (Figure 4). An invasive administration includes parenteral, intravitreal, sub-Tenon's, posterior juxtascleral, intracameral, subconjunctival, retrobulbar, peribulbar, suprachoroidal, and subretinal routes (Agrahari et al., 2016; Gaudana, Ananthula, Parenky, & Mitra, 2010; Gote, Sikder, Sicotte, & Pal, 2019; H. M. Kim & Woo, 2021). Some invasive techniques are defined as less invasive such as subconjunctival, sub-Tenon's, retrobulbar, peribulbar, and suprachoroidal injection (Varela-Fernández et al., 2020). An invasive administration must be performed by specialist and precise needle techniques, whereas the non-invasive delivery, i.e., topical, and oral routes, is self-administration. In addition, the routes of ocular drug delivery are divided as local and systemic administration as well as anterior and posterior target sites. Each route has its indication, advantages and disadvantages as summarized in Table 1.

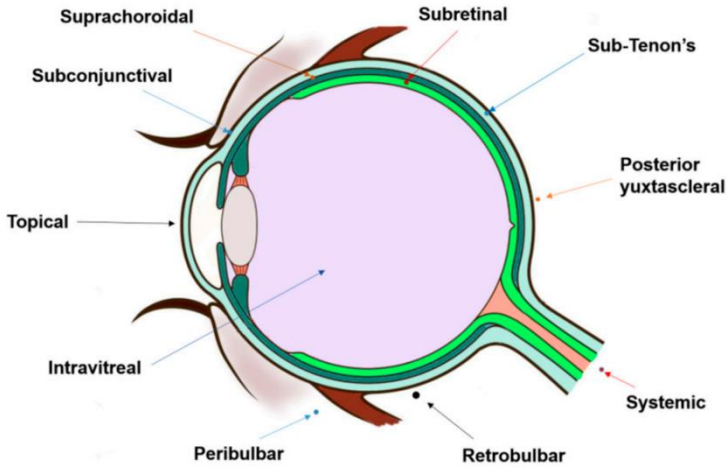

Figure 4. Schematic diagram of the different routes of drug administration to the eye modified from Varela-Fernández et al. (2020).

All invasive techniques are developed to increase bioavailability of the drug in the targeted ocular tissue and bypass barriers reducing the drug concentration. However, it would be inconvenient for the patient leading to

noncompliance and dropping out of treatment. The most favorable route for drug administration to the eye is topical application in terms of patient compliance, low treatment cost, and less adverse effect and complication. Topical administration is commonly used for diseases in the anterior segment and at the ocular surface owing to its low bioavailability of the delivered drug after application. Recently, topical corticosteroid delivery to the back of the eye has been studied among humans. The studies showed that novel γCD-based eye drops were able to deliver and maintain therapeutic concentrations in the posterior segment of the eye among patients with diabetic macular edema (Thorsteinn Loftsson & Stefánsson, 2022; Ohira et al., 2015; Tanito et al., 2011). The studies also proved that drug delivery from the ocular surface to the posterior segment is possible.

Table 1. Summary of routes of administration to the eye (Gaudana et al., 2010; Gote et al., 2019; H. M. Kim & Woo, 2021; Nayak & Misra, 2018; Varela-Fernández et al., 2020; Yeh et al., 2020).

Route	Used	Advantages	Disadvantages
Topical	Keratitis, uveitis, conjunctivitis, scleritis, episcleritis, blepharitis	High patient compliance, self-administration	Very low bioavailability, highly frequent administration
Oral (systemic)	Scleritis, episcleritis, cytomegalovirus retinitis, posterior uveitis	High patient compliance, self-administration	Very low bioavailability, toxicity from high dosing
Parenteral (systemic)	Uveitis, Vitamin B12 deficiency optic neuropathy, scleritis, pseudoscleritis, endophtalmitis	Concomitant therapy for ocular and systemic diseases	Very low bioavailability, toxicity from high dosing
Intravitreal	Age-related macular degeneration, posterior uveitis, branched/central retinal vein occlusion, diabetic/cystoid/uveitic macular edema, cytomegalovirus retinitis	Direct delivery to vitreous humor and retina, sustainable drug level	Retinal detachment, hemorrhage, cataract, endophthalmitis, noncompliance
Intracameral	Anesthesia, prevention of endophthalmitis, inflammation and pupil dilation	High drug level in the anterior chamber, reduction of corneal and systemic side effect of topical steroid treatment	Toxic anterior segment syndrome, toxic endothelial cell destruction syndrome
Subconjunctival	Glaucoma, cytomegalovirus retinitis, age-related macular degeneration, posterior uveitis	Delivery to anterior and posterior segments	Risk of toxicity due to the increase of drug via conjunctival and choroidal circulation
Sub-Tenon's	Diabetic macular edema, age-related macular degeneration, retinal vein occlusion, uveitis	High drug level in vitreous humor, less invasive and fewer complication than intravitreal	Chemosis, subconjunctival hemorrhage
Retrobulbar	Anesthesia	High local doses of anesthetics, minimal influence on intraocular pressure	Retrobulbar hemorrhage, eyeball perforation, oculomotor reflex stimulation, optic nerve trauma, respiratory arrest
Peribulbar	Local anesthesia	Suitable site for local anesthesia in cataract surgery	Less effective for anesthetizing than retrobulbar route, eyeball perforation, oculomotor reflex stimulation, optic nerve trauma, orbital hemorrhage
Posterior juxtascleral	Age-related macular degeneration, endophthalmitis	Safe for delivery of depot formulations, sustainable drug levels (up to 6 months) to the macula, avoidance of endophthalmitis and intraocular damage	Surgery required
Suprachoroidal	Clinical phase 3 noninfectious uveitis complicated macular edema	Direct delivery to the outer retina, potential reservoir for sustained release dosage forms, less ocular complication	Complicated operation, suprachoroidal hemorrhage, choroidal detachment
Subretinal	Clinical phase 3 wet aged-related macular degeneration (Regenxbio)	Minimal invasive injection, safer route in case of bacterial contamination	Transient detachment of retinal pigment epithelium and photoreceptors layer

1.2 Topical drug delivery to the eye

Even though last decade topical eye drops to the posterior segment of eye has been intensively investigated and developed, fewer cases are able to maintain therapeutic level of the drug in the retina due to multiple ocular barriers (Joussen et al., 2019; Thorsteinn Loftsson & Stefánsson, 2022). The drug molecules must permeate into various distinct ocular layers, which are composed of several sequences of aqueous and lipophilic phases, until reaching the innermost layer in the posterior segment. Additionally, the drug will be eliminated from the ocular layers with its physiological function of preventing the entry of foreign material. Hence a high concentration of the drug after applying to the ocular surface will be diluted upon entering different layers and inefficient drug concentration remains in the retina. The most drug loss during topical administration happens at the precorneal area within a few minutes. Less than 5% of the applied dose is absorbed in intraocular tissues (Subrizi et al., 2019; Urtti, 2006; Varela-Fernández et al., 2020). Thus, the drug concentration in tear film and the amount of drug permeating through the first ocular barrier, i.e., corneal, and conjunctival epitheliums, directly affects the consequent drug concentration in further inner ocular layers.

1.2.1 Precorneal barriers

An average volume of the normal droplet of eye drops is about 39 µL, while the eye can transiently hold up to 30 µL. The excess volume will be removed by lacrimal drainage and reflex blinking after instilling the eye drops into the conjunctiva cul-de-sac. The blinking rate is 5 to 7 blinks/min and the tear turnover rate at initial drainage is 1.2 µL/min. The solution will be continually removed until the tear volume returns to normal range, that is approximately 7 to 9 µL. The remaining drug is mixed with the tear fluid and subsequently incorporated in the tear film. Eventually, the dissolved drug is diluted by the lacrimal drainage to the absence of the drug´s presence. Therefore, the contact time of the drug with relatively high concentration is approximately 1 to 2 min based on the constant production of tear fluid (Bachu, Chowdhury, Al-Saedi, Karla, & Boddu, 2018). Moreover, the drug can be metabolized by an enzyme and bound to proteins found in tear fluid leading to drug elimination and further loss. The aqueous-mucin layer of tear film is gel-like fluid containing water (about 90–98%) and mucins. It also forms an aqueous diffusion barrier to the lipophilic drug which permeates into the eye (Sripetch & Loftsson, 2021).

1.2.2 Corneal and/or conjunctival epitheliums

Corneal and conjunctival epitheliums are the outermost layers of the ocular tissue. They serve as a static barrier between the external aqueous layer and internal aqueous layer (corneal and conjunctival stroma). The superficial epithelial cells of both cornea and conjunctiva consist of intercellular tight junctions preventing the entry of substances. The very tight junction of the corneal epithelial cells limits paracellular transport; hence, the corneal epithelium is like a lipophilic barrier and is the preferred pathway of small lipophilic molecules. In contrast, the intercellular spaces of the conjunctiva are wider than those of the cornea. Thus, the conjunctiva is a crucial pathway of hydrophilic compounds (Bachu et al., 2018; Subrizi et al., 2019; Varela-Fernández et al., 2020). The transport of hydrophilic compounds through the conjunctiva is not concentration or direction dependent but depends on molecular size (Hosoya et al., 2005). Furthermore, the pore and surface of corneal epithelium are negatively charged at physiological pH resulting in faster permeation of positively charged ionizable molecules (Bachu et al., 2018; Varela-Fernández et al., 2020).

In addition, the corneal and conjunctival epithelium have been reported to exhibit the expression of efflux pumps including P-glycoprotein and MRP. These proteins can either restrict or enhance drug absorption. However, the clinical relevance of drug transporters in ocular drug delivery remains unclear (Mannermaa, Vellonen, & Urtti, 2006). Pharmaceutical scientists have endeavored to overcome all the obstacles and barriers using a formulation approach. Many strategies are employed to improve drug availability at the ocular surface, for example, solubility enhancement, penetration enhancement, prolongation of drug existence, e.g., mucoadhesive polymer, in situ gel, and nanoparticles (Morrison & Khutoryanskiy, 2014).

1.2.3 Drug transport pathway

After the soluble drug is mixed and saturated in tear film, the drug will partition from the aqueous-mucin layer to the epithelium of the cornea and/or conjunctiva. The permeation pathway of the drug depends on its physicochemical properties. The corneal epithelium has more affinity for small lipophilic drug due to very tight junction of adjacent epithelial cells, whereas the conjunctival epithelium is more selective about hydrophilic molecules due to looser intercellular space (Bachu et al., 2018). The drugs with optimum lipophilicity, that is the log of distribution coefficient of 2 to 3, can penetrate through the cornea by transcellular permeation. The small lipophilic drugs and other drugs such as hydrophilic drugs, ions, and large

molecules will penetrate to the conjunctiva by transcellular and paracellular absorption (Shirasaki, 2008).

Owing to unclear relevance of drug transporters and ocular drug delivery systems, the drug transport into ocular tissue from the ocular surface is thought to be mainly passive diffusion and partition into intraocular tissue. Drugs permeate into the posterior segment of the eye after topical administration using two major pathways. The former is the corneal pathway. Most hydrophobic drugs transcellularly permeate into the cornea → aqueous humor → surrounding tissues (ciliary, iris, lens) → vitreous humor. The latter is the non-corneal pathway. The drugs will permeate via transcellular or paracellular pathways of the conjunctiva and further partition into the sclera → choroid → retina (Shirasaki, 2008; Sripetch & Loftsson, 2021; Varela-Fernández et al., 2020).

In this study, we used in-vitro permeation setup to simplify and simulate the external aqueous layer or unstirred water layer (UWL), lipophilic membrane, and inner aqueous layer. The lipophilic drugs, i.e., ionizable, and non-ionizable drugs, were also used to investigate the formulation factors affecting drug permeation through the biological membrane.

1.3 γCD-based carrier for topical drug delivery to the eye

Numerous studies have investigated the formation, properties, and application of drug/cyclodextrin (CD) aggregates (Jansook, Hnin, Praphanwittaya, Loftsson, & Stefansson, 2022; Jansook, Prajapati, Pruksakorn, & Loftsson, 2020; Jansook, Ritthidej, Ueda, Stefánsson, & Loftsson, 2010; Gauti Jóhannesson et al., 2014; Jóhannsdóttir, Jansook, Stefánsson, & Loftsson, 2015; Konrádsdóttir, Ogmundsdóttir, Sigurdsson, & Loftsson, 2009; Messner, Kurkov, Palazón, et al., 2011; Muankaew, Jansook, Sigurðsson, & Loftsson, 2016; Muankaew, Jansook, Stefánsson, & Loftsson, 2014; Popielec, Agnes, Yannakopoulou, Fenyvesi, & Loftsson, 2018; Prajapati & Loftsson, 2022; Soe, Sripetch, Loftsson, Stefánsson, & Jansook, 2022; Tanito et al., 2011). Some are γCD-based systems with the aim of ocular delivery (Jansook, Praphanwittaya, Sripetch, & Loftsson, 2020; Jansook, Ritthidej, et al., 2010; Muankaew et al., 2016; Tanito et al., 2011). They reported that γCD solubilized several poorly water-soluble drugs by forming inclusion complex with or without a third component (additives). The drug/γCD complexes can also form secondary larger structures such as dimers, trimers, and aggregates of drug/γCD complexes (Thorsteinn Loftsson, 2014). Both simple inclusion complex and complex aggregates

showed solubilization and stabilization effects of γCD on the studied drug (Jansook, Praphanwittaya, et al., 2020; Soe et al., 2022). Additionally, the investigations illustrated that the degree of aggregate formation is γCD concentration dependent and sometimes increases with increasing the additive's concentration. The additives added to improve complexation included water soluble polymer, organic acid and/or its salt, other CDs, and a second drug (Jansook & Loftsson, 2022).

Here we also investigated the complex formation of γCD, ionizable lipophilic drugs, and counterions as well as solubilization and stabilization effect of binary and ternary systems (i.e., drug/γCD and drug/acid/γCD).

1.3.1 Structure and properties of γCD and its derivatives

γCD is a cyclic oligosaccharide of eight glucopyranose monomers. Each glucopyranose unit forms α-1,4-glycosidic bond with adjacent units in a circle, resulting in a particularly molecular shape liked truncated cone with hydrophilic outer surface and hydrophobic central cavity. The γCD has the highest aqueous solubility among three natural CD, i.e., α, β, and γCD. Its central cavity is comparable with ethanolic aqueous solution. It can form an inclusion complex with a lipophilic molecule and increase the aqueous solubility of that molecule without forming a strong molecular bond. In other words, the hydrophobic drug moiety can be inserted in the hydrophobic CD cavity via formation of non-covalent interaction and subsequently the CD/drug (1:1) complex dissolves in water by H-bond formation of CD's exterior OH group with surrounding water molecules, leading to the increase in aqueous solubility of the lipophilic drug. Owing to limited solubility in water of the natural γCD, substituted modification is used to prepare highly water-soluble γCD derivatives such as hydroxypropyl-γ-cyclodextrin (HPγCD) and sulfobutylether-γ-cyclodextrin (SBEγCD) (Table 2) (Jansook, Ogawa, & Loftsson, 2018; Kurkov & Loftsson, 2013; Saokham & Loftsson, 2017).

The natural γCD is susceptible to enzymatic-catalyzed and non-enzymatic hydrolysis. The hydrolytic rate of CDs in aqueous solution depends on the ring size, fraction of free CD, and enzyme activity in the case of enzymatic catalysis (Saokham & Loftsson, 2017). Moreover, source of enzyme and studied condition can affect the hydrolytic rate. An α-amylase enzyme cleaves α-1,4-glycosidic linkage of CDs via multiple attack reactions resulting in forming of maltotriose, maltose, and glucose (Harangi, Béke, Harangi, & Mótyán, 2012; Kondo, Nakatani, & Hiromi, 1990). The α-amylase enzyme is found in many bodily fluids including tear fluid. The enzyme catalysis is done via enzyme-substrate complex. Unlike the drug/CD complexation, the

complex formation of substrate and enzyme is specific reaction. Only matching substrate can bind to the active site of enzyme. In addition, the substrate will be digested after binding to the enzyme. The study found that substituted γCD and bound γCD molecules hamper the α-amylase-catalyzed hydrolysis of the natural γCD (Jansook et al., 2018; Lumholdt, Holm, Jørgensen, & Larsen, 2012). In this study, we also investigated the degradation of unbound and bound γCD by α-amylase enzyme. Unfortunately, the α-amylase from human tear was not commercially available. Thus, the porcine pancreatic α-amylase (PPA) was used instead.

Table 2. Structure and physicochemical properties of γCD, HPγCD, and SBEγCD (Jansook & Loftsson, 2022; Jansook et al., 2018; Saokham & Loftsson, 2017).

Properties	**γCD**	**HPγCD**	**SBEγCD**
Structure		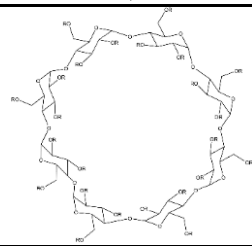	
Substituted group	H	H or C_3H_7O	H or $C_4H_8SO_3$
Degree of substitution	Not applicable	4.2[b]	4.2[b]
Molecular weight (g/mol)	1297	1540[b]	1961[b]
Water solubility at 25 °C	249	>600	>1200
Log $P_{o/w}$[a]	-17	-13	<-10

[a]Logarithm of the octanol/water partition coefficient (calculated value).
[b]From manufacturer certificate of the batch used in this study.

1.3.2 Complexation of γCD and lipophilic drug

Like other CDs, γCD commonly form an inclusion complex with the lipophilic drugs and consequently improve the drug´s solubility in water. The drug/CD complex and its aggregates are fragile. It can easily break apart into free drug and unbound CD. This is because the complex formation is a dynamic equilibrium where the CD and the drug continually associate and dissociate at constant rate. The stability constant (K_c; $K_{m:n}$) and dissociation constant (K_d) of the complexation are necessary to compare CD effects because these values provide an index of change of physicochemical properties of the complex (Brewster & Loftsson, 2007). The K_c and K_d can be described as:

$$mCD + nD \overset{K_{m:n}}{\longleftrightarrow} CD_m \cdot D_n \qquad ; [a - mx][b - nx] \rightarrow [x] \qquad (1)$$

$$K_{m:n} = \frac{[x]}{[a - mx]^m [b - nx]^n} \qquad (2)$$

$$K_d = \frac{[a - mx]^m [b - nx]^n}{[x]} = \frac{1}{K_{m:n}} \qquad (3)$$

Where D is the poorly soluble drug.

Phase-solubility technique is used to determine the K values and evaluate a relationship of the CD and the solubilized drug. In practice, it can be performed by adding an excess amount of the drug to several aqueous solutions containing different CD concentrations from low to high. The samples are agitated under the desired condition until an equilibrium is obtained. The dissolved drug is quantified using an appropriate analytical method. The phase-solubility profile is made from plotting the concentration of dissolved drug against the concentration of added CD. The profile is classified as A-type and B-type (Figure 5) according to Higuchi & Connors (1965).

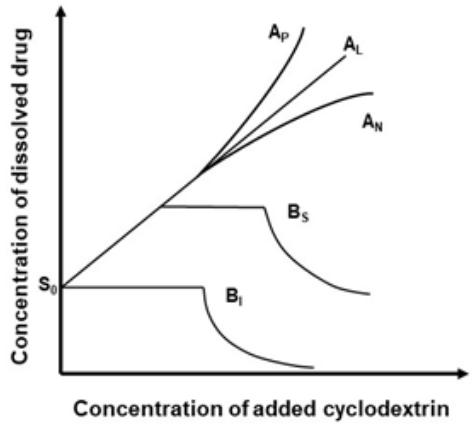

Figure 5. Phase-solubility profiles of A type and B type according to Higuchi & Connors (1965).

In the A-type system, the apparent drug solubility increases with increasing CD concentration. The three subtypes are A_P, A_L, and A_N. The A_L profile indicates a linear increase in solubility as a function of CD concentration. The A_P diagram consists of an initial linear increase and positive deviation from the linearity that makes the CD to be proportionally more effective at higher concentrations. The A_N curve shows a negative deviation from the linearity, i.e., the CD is proportionally less effective at higher concentrations. Taken as a whole, these solubility isotherms indicate

that water-soluble complexes are being formed with solubilities higher than that of the unbound substrate (Brewster & Loftsson, 2007).

The B-type profiles define the formation of complexes with limited water solubility and are traditionally observed with natural CDs. The two subclasses include B_s and B_i. For the B_s profile, an initial increase in drug solubility with increasing soluble complexes is as a function of CD concentration. The maximum solubility of the drug is achieved at a particular point in this linear increase and then the increase in CD concentration rises without increasing the drug solubility which is seen as a plateau. In the plateau phase, the apparent solubility is a limited solubility of the complex and the apparent intrinsic solubility of the drug in the same complexation media. Further addition of the CD concentration results in the formation of additional insoluble complex which precipitates and depletes the total soluble drug concentration showing as a declining profile. Finally, the B_i phase-solubility diagram is similar in form to the B_s profile except that without an initial ascending linearity (Brewster & Loftsson, 2007).

As discussed previously, the complexation is a dynamic equilibrium. When the equilibrium is released from the decrease in CD molecules such as CD degradation, the free lipophilic molecule will be above the ability of the system to solubilize, leading to transient supersaturation and subsequent solid drug precipitation. Thus, in formulation design, CD will be added a bit more than the concentration to solubilize the intended drug concentration. However, the excess solubilizer can prevent the drug absorption in the biological membrane because the drug has less affinity with the membrane compared with the external aqueous phase containing the solubilized drug and CD (Thorsteinn Loftsson, Moya-Ortega, Alvarez-Lorenzo, & Concheiro, 2015). Unlike the loss of complexation equilibrium due to disappearance of substrate, a dilution of the drug/CD complex system with a large volume of media results in the dissociation of the drug/CD and theoretically, a decrease in drug solubility without precipitation. This is because of the constant proportion of the drug to CD in the further diluted system based on the A-type and B_S type of the phase-solubility profile (Brewster & Loftsson, 2007).

The most common complex observed is the 1:1 drug/CD complex (Brewster & Loftsson, 2007) where one drug molecule forms a complex with one CD molecule:

$$CD + D \overset{K_{1:1}}{\longleftrightarrow} CD \cdot D \qquad (4)$$

Such 1:1 complex display A_L-type profile and the initial linearity of further

phase-solubility profiles, i.e., A_P, A_N, and B_s. The stability constant of the complex ($K_{1:1}$) can be calculated from Equation (5).

$$K_{1:1} = \frac{Slope}{S_0(1 - Slope)} \quad (5)$$

Where S_0 is the apparent intrinsic solubility of the drug in complexation media when no CD is present (Jansook et al., 2018; Kurkov & Loftsson, 2013).

When a drug molecule forms a complex with more than one CD molecules, a consecutive complexation is assumed; thus, stability constants of higher order complexes should be calculated using a different model. A_P-types are usually observed under such condition (Brewster & Loftsson, 2007).

The determination of complexation efficiency (CE) is more accurate method to evaluate the solubilizing effect of CD. The CE is calculated from the slope of the linear portion of phase-solubility profiles. It will not be affected when the y intercept is not equal to S_0, for example, in the case that the dissolved drug molecules are unable to form a complex due to forming self-dimers, trimers, and higher order drug aggregates. Also, the CE is more reliable when the effect of various pharmaceutical excipients on the solubilization are being studied. For 1:1 drug/CD complexes, the CE is calculated as follows:

$$CE = \frac{[D \cdot CD_n]}{[CD]} = K_{1:1} \times S_0 = \frac{Slope}{(1 - Slope)} \quad (6)$$

From Equation 6, CE is a product of S_0 and slope; thus, the increase of S_0, slope, and both can improve the CE. Basically, the CE is improved by adding other excipients that can increase intrinsic solubility of the lipophilic drug via ionization or salt formation such as acid or base, can enhance the solubility of the drug/CD complex such as low molecular weight organic acid, and can stabilize the complex such as water-soluble polymer (Thorsteinn Loftsson & Brewster, 2012).

1.3.3 Drug release from cyclodextrin complexes

It has been believed that only free drug will permeate through biological membranes after administering a formulation containing drug/CD complexes to the absorption site, e.g., gastrointestinal tract, intravenous, and ocular surface. Drug release from drug/CD complexes and the effect of CDs on drug pharmacokinetics have been reviewed and discussed mainly concerning parenteral and oral administration (Thorsteinn Loftsson et al., 2015; Stella, Rao, Zannou, & Zia, 1999). Stella at al. (1999) concluded that a simple

dilution is the major driving force for dissociation of weakly to moderately bound drugs, i.e., binding constant below 10^4 M^{-1}, after parenteral administration. For strongly bound drugs, i.e., binding constant of 10^4 M^{-1} or higher, and for those cases where dilution is minimal such as ocular surface, contributions from competitive displacement by endogenous materials, drug binding to plasma and tissues components, drug uptake into tissues, rapid elimination of the cyclodextrin, and possibly pH and temperature effects may also be important. In addition, CD might cause some alterations in the fraction of free drug eliminated in the urine during the same time as the renal clearance of CD. Later, Loftsson et al. (2016) found that for complexes with low to middle binding constant, binding of drug to plasma proteins will mainly dictate the pharmacokinetics. However, for drugs with large CD complex binding constant and low protein binding, significant decrease in distribution volume and enhanced excretion of unmetabolized drug are observed. In the case of oral administration, volume for dilution/dissolution of the complexes is relatively low and hence excess CD can hamper drug absorption from the gastrointestinal tract.

In summary, the drug release from drug/CD complex mainly depends on the binding constant of the complex, route of administration, indicating a dilution effect and endogenous substances that can complete with CD binding. Other factors including drug binding to plasma and tissue components, drug uptake into tissues, rapid elimination of the cyclodextrin, and pH and temperature effects can also influence both drug release and pharmacokinetics.

In case of ocular delivery where the volume for dilution is limited, other factors such as endogenous substances and affinity for ocular epitheliums might play important roles in drug release from drug/γCD complexes. Here, the release of dexamethasone from γCD complexes was studied when α-amylase enzyme was present.

1.3.4 Factors affecting drug permeation though biological membrane

Factors that affect drug permeation into biological membranes can be classified as the factors relating to drugs such as physicochemical properties and formulation factors. Basically, formulation factors result from excipient´s properties and their interaction with the drug and/or with other excipients, for example, pH, particle size, viscosity etc. CDs have been used as pharmaceutical excipients for a lipophilic drug to improve their aqueous solubility and permeability through the aqueous exterior layer of biological

membranes which frequently are referred to as UWL. Due to chemical structure of CD, their large molecular weight, and their very low lipophilicity, i.e., log $P_{o/w}$ below 0, the CDs do not readily permeate the lipophilic membrane (Thorsteinn Loftsson, Jarho, Másson, & Järvinen, 2005). In fact, studies showed that slight amounts of CDs and lipophilic drug/CD complexes can permeate skin, gastrointestinal mucosa, and retinal cell cultures (Furuishi et al., 2017; Prajapati, Christensen, Paquet-Durand, & Loftsson, 2021). CDs can also extract lipophilic endogenous components such as phospholipids and cholesterol which are cell membrane components and alter the integrity of the epithelial layer (Ohtani, Irie, Uekama, Fukunaga, & Pitha, 1989).

As we know, CDs and the CD complex can form self-aggregates from nano to micro size. Studies have shown the deviation of the drug flux from the linear increase at relatively high CD concentrations when the drug permeation through semipermeable membranes was investigated (Jansook, Kurkov, & Loftsson, 2010; Messner, Kurkov, Brewster, Jansook, & Loftsson, 2011). This was found because of self-assembled particles of the drug/CD complexes. In physiological condition, it has been thought that self-assembled drug/CD complexes immediately break apart into free drugs and CD upon dilution. However, in small volumes for dilution of tear film, the size of self-assembled particles of the drug/CD complexes might affect its dissolution, and consequently break slowly. If that occurs, how the self-assembled complexes will affect the drug permeation need to be understood.

1.4 Model drugs

Dovitinib, a multi-tyrosine kinase inhibitor, is an anti-tumor agent, which has been investigated against different types of cancer, such as renal-cell carcinoma, melanoma, breast cancer, gastrointestinal stromal tumor, hepatocellular carcinoma, glioblastoma, and lung cancer (Das et al., 2015; Joensuu et al., 2017; K. B. Kim et al., 2011; Motzer et al., 2014; Musolino et al., 2017; Schäfer et al., 2016; Woei-A-Jin et al., 2021). The free base of dovitinib has a molecular mass of 392.43 Da with 4 H-bond donors and 7 H-bond acceptors (Table 3) and should be suitable for gastrointestinal tract absorption according to the rule of 5 (Lipinski, 2000; Lipinski, Lombardo, Dominy, & Feeney, 1997). However, the dovitinib free base is sparingly soluble in pure water, with a predicted intrinsic solubility of 0.051 mg/mL at 25°C (Table 3). The calculated solubility of dovitinib at pH 6 is quite low and is even lower at pH 7. The aqueous solubility decreases dramatically when the pH changes to above 6 owing to partial protonation, which has been reported (Jansook, Praphanwittaya, et al., 2020; Praphanwittaya, Jansook, &

Loftsson, 2020). Previous studies have found that the solubility of dovitinib free base sharply increases at pH lower than 6 through pH adjustment with hydrochloric acid (HCl). The maximum solubility was observed between a pH of 3 and 4, and then, the aqueous solubility dropped until lower than 1 mg/mL at pH between 6 and 7. The solubility of dovitinib was about 0.036 mM (equivalent to 0.014 mg/mL) at pH 6.5 (Jansook, Praphanwittaya, et al., 2020). Based on oral-dose range of dovitinib in clinical trials between 200 and 600 mg (Angevin et al., 2013; K. B. Kim et al., 2011) and BCS criteria (*M9 Biopharmaceutics classification system-based biowaiver*, 2021), dovitinib free base can be classified as a BCS Class II drug owing to its low solubility above a pH of 6. For the drugs in BCS Class II, solubility is a rate-limiting step in absorption resulting in low drug bioavailability (Löbenberg & Amidon, 2000). To prepare a formulation for an animal study in early drug development, all strategies should be considered, including chemical methods, physical techniques, formulation approaches or/and combination of these strategies (Ku, 2008). Previously, one salt form of dovitinib, dovitinib lactate, was patented and published with the aim of oral administration (Okhamafe et al., 2005). Due to its potential to inhibit several receptor tyrosine kinases, the possibility of other indications and routes of administration is very attractive.

Dexamethasone is a widely used corticosteroid to treat various inflammation disorders of the eye in both anterior and posterior segments. It is almost insoluble in water. Its chemical structure and physicochemical properties are shown in Table 3. The dexamethasone has been used in eye disease since 1960 (Gordon, 1960). Recently, studies have shown that topical dexamethasone in γCD-based eye drops can deliver the drug to the posterior segment of the eye (Jóhannesson et al., 2014; Johannsdottir et al., 2018). Clinical studies also have shown promising results of dexamethasone loaded in γCD-based eye drops among patients with diabetic macular edema (Ohira et al., 2015; Tanito et al., 2011).

Table 3. Structure and physicochemical properties of the model drugs (SciFinder, 2022).

Name	**Dovitinib, TKI-258, CHIR-258**	**Dexamethasone**
Chemical structure	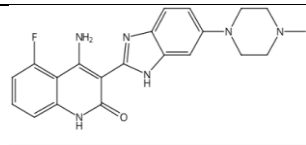	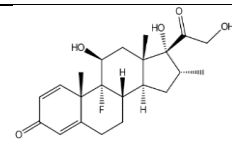
Chemical formula	$C_{21}H_{21}FN_6O$	$C_{22}H_{29}FO_5$
Molecular weight	392.43	392.46
pK_a (at 25 °C)	7.70 ± 0.42, 9.44 ± 0.70	12.13 ± 0.70
Log P (at 25 °C)	1.31 ± 1.22	2.0
H Donors	4	NA
H Acceptors	7	NA
Intrinsic solubility	0.051 g/L (at 25 °C)	0.04 mg/mL (at RT)
Solubility (unbuffered water pH 8.45 at 25 °C)[a]	0.075 g/L	NA
Solubility (pH 6, 7 at 25 °C)[a]	5.5, 0.35 g/L	NA

[a]Calculated using Advanced Chemistry Development (ACD/Labs) Software V11.02 (©1994-2021 ACD/Labs)

2 Aims

The overall aim of this project was to investigate the application of γCD as a drug carrier for topical delivery to the eye. Specific purposes were to improve water solubility of the lipophilic drug using γCD; examine the effect of pharmaceutical excipients on physicochemical properties of the drug; determine the effect of γCD on the permeation of the lipophilic drugs; investigate the factors affecting drug permeation through the lipophilic membrane and study the drug release from a γCD-based drug carrier. These objectives were divided in the specific studies discussed below.

2.1 Preformulation study of dovitinib free base

In this preformulation study, the physicochemical properties of dovitinib free base were determined to provide essential knowledge for developing a γCD-based drug carrier for topical delivery to the eyes. The study included the topic listed below.

- Improvement of aqueous solubility of dovitinib free base using γCD and counterions.
- Effects of acidic counterions on lipophilicity of dovitinib.
- Effects of temperature, pH, and pharmaceutical excipients such as buffer species and γCD on stability of dovitinib.

2.2 Investigation of the γCD effect on the permeation of lipophilic drugs and the formulation factor affecting drug permeation

Drug permeation studies have been used to investigate the factors influencing drug partition across an aqueous diffusion layer and lipophilic barriers and to understand how the drug delivery system works on improving drug absorption. In early states of drug development, an appropriate formulation of drug candidates is designed and selected for further subsequent studies. To reduce cost and unnecessary animal studies as well as increase a successful chance during clinical trials, an in-vitro permeation study of the drug candidate in the designed formulation or excipients is used. The in-vitro permeation is a simple and efficient tool to evaluate the ability of the excipients to promote drug permeation into a biological membrane.

The goals of this research were to determine the effect of γCD on the permeability of the lipophilic drugs and the formulation factor affecting the drug permeation through the lipophilic membrane. The permeation of dexamethasone, unionized lipophilic drug and dovitinib free base, ionized lipophilic drug was carried out when γCD was present, and the thermodynamic activity of the model drugs was considered at maximum. The experimental design intentionally focused on the partition of the lipophilic drug across the UWL and the lipophilic membrane consisting of two cellulose layers with phosphatidylcholine layer inside. This in-vitro setup simulated the situation at the interface between the tear film and the ocular epithelium.

2.3 Study of drug release from γCD-based drug carrier

Only free drug molecules permeate into the biological membrane and γCD can be degraded by α-amylase enzyme, which is found in tear fluid. Because γCD has been used in aqueous eye drops and was mainly used in this project. Therefore, the effect of α-amylase on the drug release from a γCD-based carrier was investigated.

The study investigated the effect of α-amylase on dexamethasone release from a γCD-based drug carrier under mimic tear conditions. The effects were described by these experiments in two aspects detailed below.

- Degradation of γCD by porcine pancreatic α-amylase.
- Release of dexamethasone from aqueous solution containing γCD with the presence and absence of porcine pancreatic α-amylase.

3 Materials and methods

3.1 Materials

3.1.1 Model drugs

Dovitinib free base was purchased from Shanghai Huirui Chemical Technology Co., Ltd. (Shanghai, China). Two lots of dexamethasone base, pharmaceutical grade used in this study were obtained from Unither Pharmaceuticals (Coutances, France) and purchased from Fagron (Rotterdam, the Netherlands).

3.1.2 Cyclodextrins

The γCD, pharmaceutical grade was purchased from Wacker Chemie AG (Burghausen, Germany). HPγCD (DS 4.2, MW 1540) and SBEγCD sodium salt (DS 4.2, MW 1961) were a gift from Chemical Marketing Concepts Europe (Waalwijk, the Netherlands) and Cydex Pharmaceuticals (KS, USA), respectively.

3.1.3 Acidic counterions

Lactic acid solution, ≥ 85 % ACS reagent and maleic acid, ≥ 99 % were purchased from Sigma-Aldrich (MO, USA). D-gluconic acid solution, 49–53 wt% and H_3PO_4, 85 wt% were purchased from Sigma-Aldrich (From China and Switzerland, respectively), and HCl, 37% ACS reagent was purchased from Honeywell (Seelze, Germany).

3.1.4 Buffers

Sodium phosphate monobasic dihydrate ($NaH_2PO_4 \cdot 2H_2O$), analytical grade and N-[2-hydroxyethyl] piperazine-N'-[2-ethanesulfonic acid] (HEPES) were purchased from Sigma-Aldrich (MO, USA). Sodium phosphate dibasic dihydrate ($Na_2HPO_4 \cdot 2H_2O$) and potassium chloride (KCl) were analytical grade and purchased from Riedel-de Haën (Seelze, Germany). Acetic acid (CH_3COOH), Ph.Eur. grade; sodium acetate anhydrous (CH_3COONa), reagent grade; sodium hydroxide (NaOH), Ph.Eur. grade were purchased from Honeywell (Seelze, Germany). Calcium chloride dihydrate ($CaCl_2 \cdot 2H_2O$) was purchased from Merck (Darmstadt, Germany) and sodium chloride (NaCl) was purchased from Honeywell Fluka (Seelze, Germany).

3.1.5 Others

1-Octanol and dimethyl sulfoxide (DMSO), HPLC grade were purchased from Sigma-Aldrich (MO, USA). Porcine pancreatic α-amylase (PPA; Type VI-B, 10 units/mg solid) was purchased from Sigma (MO, USA). Formic acid, 98–100 % ACS reagent, was purchased from Merck KGaA (Espoo, Finland). Acetonitrile, methanol, and tetrahydrofuran, HPLC grade were purchased from Honeywell Riedel-de Haën (Seelze, Germany). Ultrapure water was obtained from Integral Milli-Q water purification system (Merck, Darmstadt, Germany) and used for all preparations and analyses.

Cellulose ester membrane with molecular weight cut-off (MWCO) of 3.5–5 kD (Biotech CE Tubing dialysis membrane, Spectra/Por) was purchased from Repligen Corporation (CA, USA). A PermeaPad® barrier was purchased from innoME GmbH (Espelkamp, Germany). Regenerated cellulose (RC) membrane, 0.45 µm and 15 mm syringe filters were purchased from Phenomenex (CA, USA).

3.2 Quantitative analysis

3.2.1 Quantitation of the model drugs

The amount of dovitinib and dexamethasone was quantified using reverse-phase high performance liquid chromatograph (HPLC). The HPLC apparatus (Ultimate 3000, Thermo Scientific, MA, USA) consisting of a SR-3000 solvent rack, an LPG-3400SD pump with built-in degasser, a WPS-3000SL analytical autosampler, a TCC-3000SD column compartment and a DAD-3000 detector was equipped with a Luna C18, 150 x 4.6 mm, 5 µm column and security guard holder containing a C18, 4 x 3.0 mm cartridge (Phenomenex, CA, USA). Chromatograms were recorded and analyzed using chromatography data system version 7.2.8 (Thermo Scientific Dionex Chromeleon 7, Thermo Fisher Scientific, MA, USA). Mobile phases and HPLC conditions are described below.

Dovitinib: The drug was separated by a gradient program of mobile phases A and B, 0.1 % v/v formic acid in water and acetonitrile, respectively. The gradient program with constant flow rate at 1.0 mL/min was as follows: initial linear gradient from 0.0 to 2.0 mins in 5 % B, linear gradient from 2.0 to 8.0 mins from 5 % B to 95 % B, holding at 95 % B with linear gradient from 8.0 to 12.0 mins, and linear gradient from 12.0 to 14.0 mins from 95 % B to 5 % B. Column temperature was 30°C and injection volume was 20 µL. The detector was at 289 nm. A standard stock solution and samples, if necessary, were diluted with 50 % v/v of acetonitrile in water before determination.

Dexamethasone: The mobile phase consisted of a mixture of acetonitrile, tetrahydrofuran, and water (33:1:66 v/v). The HPLC system was operated under the isocratic mode with flow rate of 1.5 mL/min; injection volume was 20 µL; column temperature was 25°C; and UV detection was at 241 nm. Samples and a standard stock solution were diluted with 25 % v/v of acetonitrile in water before analysis.

3.2.2 Quantitation of γCD

Quantitative determination of γCD was performed on the HPLC-RI system consisting of the same HPLC apparatus as described in section 3.2.1 connected to the second detector, RefractoMax 521 refractive index from ERC INC. (Japan). Kinetex C18, 30 x 4.6 mm, 2.6 µm column with matching ULTRA cartridge guard column (Phenomenex, CA, USA) was installed in the column compartment where temperature was controlled at 30°C. The mobile phase consisted of methanol and water (7:93 v/v) and flow rate was 0.7 mL/min. The temperature of the RI detector was 40°C and injection volume was 20 µL. Sample solutions and standard stock solution were diluted with the mobile phase before injection. In the case of the samples containing the model drugs, the drug was washed off after γCD elution with corresponding mobile phase at a flow rate of 1.0 mL/min. The cleaning mobile phase used the aqueous solution of 33 % v/v acetonitrile for dexamethasone and the mixture of 0.1% v/v formic acid and acetonitrile (75:25 v/v) for dovitinib. The cleaning gradient program started at 2.5 mins until 7 mins and then the column was equilibrated with the mobile phase for γCD for 7 mins before next injection.

3.3 Phase-solubility technique

Phase-solubility technique was used to evaluate complexation and prepare test samples in this study. Briefly, an excess amount of the model drug was added to several concentrations of aqueous CD solutions. Sample suspensions were heated using autoclave method at 121°C for 20 mins (Astell, Kent, UK), then allowed to cool and constantly agitate at 300 rpm under the studied temperature for about 6 to 7 days to reach equilibrium. After that, soluble drug concentrations and other parameters were determined according to the intended purposes. The phase-solubility diagram was plotted between the concentrations of dissolved drug and γCD, which was actual or theoretical concentration, to determine the slope of the linear part. The $K_{1:1}$ and CE were calculated according to Equation (6).

3.4 Preformulation study of dovitinib free base

In this preformulation study, physicochemical properties such as solubility, lipophilicity, and stability of dovitinib free base were evaluated under actual thermodynamic circumstances with the presence of pharmaceutical excipients, for example, counterions, γCD, and buffer salt.

3.4.1 Solubility studies

To improve aqueous solubility of the dovitinib free base, γCD was used as a primary solubilizer in solubility studies. The complex formation of dovitinib free base with γCD was characterized using conventional and simple method, i.e., phase-solubility study. Related studies (Jansook, Praphanwittaya, et al., 2020; Praphanwittaya et al., 2020) reported that addition of counterion to the complexing media of CDs was able to increase the water solubility of dovitinib free base. Therefore, five acidic counterions including HCl, H_3PO_4, lactic, gluconic, and maleic acids were selected based on acid type and pK_a value to investigate the enhancement of aqueous solubility of dovitinib free base with the presence or absence of γCD. Chemical structures and pK_a values of the acids are shown in Table 4.

Table 4. The chemical structure, MW and pK_a value of the acidic counterions used. All data were obtained from Gould (1986) and SciFinder (2022).

Acid	Type	Chemical structure and formular	MW	pK_a
Hydrochloric	Inorganic	HCl	36.46	-6.1
Phosphoric	Inorganic	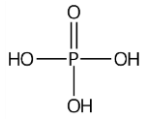 , H_3PO_4	98.00	2.15, 7.20, 12.38
Lactic	Hydroxy	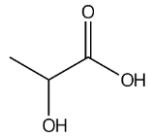 , $C_3H_6O_3$	90.08	3.85
Gluconic	Hydroxy	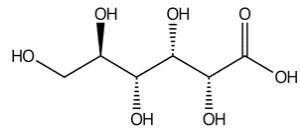 , $C_6H_{12}O_7$	196.16	3.60
Maleic	Carboxylic	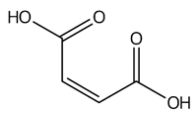 , $C_4H_4O_4$	116.07	1.96, 6.28

3.4.1.1 Phase-solubility study of dovitinib free base

In this present study, phase-solubility technique as mentioned in section 3.3 was used without adjusting pH of complexing media. The excess amount of dovitinib was added to several concentrations of γCD solution in water across the range of 0.25–15 % w/v (eq. to 1.9–115.5 mM). The excess amount of dovitinib which was fixed at 5 mg/mL (eq. to 12.7 mM) was much more than the maximum aqueous solubility of dovitinib in pH-controlled complexing medium reported in related studies, i.e., 0.65 mg/mL (Jansook, Praphanwittaya, et al., 2020). After 7 days of agitation at room temperature (21–22°C), all sample suspensions were filtered through 0.45 µm RC syringe filter and the first 1 mL of the filtrate discarded. Dovitinib and γCD concentration in filtrates and pH of the filtrates were determined using the analytical method stated in section 3.2 and a pH meter (Thermo Scientific, Indonesia), respectively. The sample was prepared in triplicate.

3.4.1.2 pH-solubility studies

The pH-solubility studies were performed by titration of various acidic aqueous solutions with the powder of dovitinib free base. Five acidic counterions mentioned above were used to examine the aqueous solubility of dovitinib free base. Before titration with the dovitinib free base powder, some acidic aqueous solutions and a few diluted NaOH solutions were prepared. A small amount of the drug powder was gradually added to the test tubes containing media until suspensions were formed. All samples were shaken at 300 rpm in an orbital shaker (Edmund Bühler GmbH, Germany) and at room temperature (21–22°C) for 6 to 7 days. During equilibration, physical appearance and pH of the samples were monitored. If necessary, dovitinib powder was added to maintain the excess of the solid drug. When reaching the proper time, the suspensions were centrifuged at 12,000 rpm for 15 mins using a benchtop centrifuge (Thermo Fisher Scientific, P.R. China). The centrifugation and filtration were previously verified and showed no significant difference between both separation methods. Then the dovitinib concentration and the pH of the supernatant were determined using HPLC (section 3.2.1) and the pH meter. The pH-solubility plots were drawn between the concentration of soluble dovitinib and apparent final pH.

3.4.1.3 Improvement of dovitinib aqueous solubility by combined techniques

Two γCD concentrations, 38.6 and 154.2 mM γCD, with three concentrations of each acid and two concentrations of dovitinib free base were used to

investigate the effect of acidic counterions on the aqueous solubility of dovitinib. Three acid concentrations were used in the range of 9.7 to 77.2 mM for both γCD-free sample series and 38.6 mM γCD sample series. The excess amount of dovitinib free base was added to the acidic aqueous solutions or the complexing medium containing different acid concentrations. Unlike the previous sample series, the dovitinib amount was fixed at 76.5 mM in the 154.2 mM γCD sample series, and the acid was varied according to the molar ratio of acid to dovitinib which was from 0.25:1 to 2:1. The samples were prepared using the phase-solubility technique described in section 3.3. After reaching equilibrium under ambient condition (21–22°C), the drug and γCD concentration, and the pH of supernatant were determined (section 3.2). All sample series were performed in triplicate.

3.4.2 Lipophilicity studies

The lipophilicity of dovitinib free base was described by the logarithm of distribution coefficient (log D). The liquid-liquid phase distribution (Másson, Karlsson, Valdimarsdóttir, Magnúsdóttir, & Loftsson, 2007) was used to investigate the distribution coefficient when counterion was present at different pH. The organic phase comprised water-saturated 1-octanol, while the aqueous phase consisted of pure acid in octanol-saturated water or acid/NaOH in octanol-saturated water. The same acids as used in 3.4.1 were used. The 0.4 mg/mL of dovitinib solution was prepared by dissolving the dovitinib free base in the water-saturated octanol. An equal volume of the organic phase containing 0.4 mg/mL of dovitinib, and aqueous phase were pipetted and transferred to a test tube with a cap. Liquid-liquid extraction was performed by shaking the test tube clamped in a horizontal position at 150 rpm for 1 hour. After that, all tubes were placed vertically for a few hours to allow phase separation. The aqueous phase was pipetted to a microcentrifuge tube and centrifuged at 12,000 rpm for 15 mins for complete separation. The concentration of dovitinib in the separated aqueous phase and the octanol stock solution were determined using HPLC as described in 3.2.1. The final pH of the aqueous phase was also measured. The samples were performed in triplicate and the log D was calculated using the following equation:

$$\log D = \log \frac{C_{octanol}}{C_{aqueous}} \quad (7)$$

where $C_{octanol}$ and $C_{aqueous}$ are the concentration of dovitinib in the octanol phase and aqueous phase, respectively.

3.4.3 Stability studies

Six buffer solutions with different pH were used to study the influence of pH and the buffer species on the stability of dovitinib free base. The buffer systems are shown in Table 5. Due to the low aqueous solubility of dovitinib at elevated pH, HPγCD or γCD was added to the media to solubilize dovitinib. A stock solution of dovitinib free base was prepared in DMSO and accurately pipetted to mix with aqueous buffer stock solution to make the test solutions. The test solution contained 0.04 mg/mL dovitinib, 5 % w/v CD, and 100 mM buffer. The concentration of DMSO in all test solutions was 0.8 % v/v. Samples were prepared in triplicate, and the studies were performed at 40±2 and 75±2°C. The dovitinib concentration in the test solution was analyzed using HPLC (section 3.2.1) at different time points until 28 and 5 days for 40 and 75°C, respectively. The pH of the test solutions was monitored throughout the experiment and no significant pH change (>0.5 pH unit) was observed.

Table 5. Buffer systems used in stability studies.

Buffer system	Final concentration (mM)	pH (at 40 °C)
HCl/KCl	100	1.7
H_3PO_4/NaH_2PO_4	100	2.1, 4.0
CH_3COOH/CH_3COONa	100	4.2
NaH_2PO_4/Na_2HPO_4	100	5.9, 8.0

3.4.4 Characterization of solid fraction in the suspensions containing dovitinib, acid, and γCD

3.4.4.1 Determination of dovitinib and γCD contents in solid fraction

The suspensions obtained from the 154.2 mM γCD sample series were investigated. The suspensions were centrifuged at 12,000 rpm for 15 mins to separate solid fraction. The dovitinib and γCD in suspensions and supernatants were determined using HPLC as described in section 3.2. The dovitinib and γCD contents in solid fraction were calculated using the following equation:

$$C_s = C_{ss} - C_{sp} \quad (8)$$

where C_s is the concentration of dovitinib or γCD in the solid fraction, C_{ss} is the concentration of dovitinib or γCD in whole suspension, and C_{sp} is the

concentration of dovitinib or γCD in the supernatant.

3.4.4.2 Size measurement of solid particles in the sample suspension

The particle size of pooled suspensions containing dovitinib, acid, and γCD were determined using a particle size analyzer for micrometer range (Mastersizer 3000, Malvern Panalytical, UK). Pooled sample was used in the measurement of particle size and FTIR spectra because the preparation procedure was initially developed for small-volume sample. The solid fraction obtained from one batch, that is 2 to 3 mL per vial, was not enough for the studies. The pooled sample was prepared by combining 3-mL suspension from 3 vials which were prepared according to section 3.4.1.2 and the following formulae. Two formulae were selected from different acid types including dovitinib/lactic acid (76.5 mM dovitinib/38.6 mM lactic acid/154.2 mM γCD) and dovitinib/phosphoric acid (76.5 mM dovitinib/38.6 mM phosphoric acid/154.2 mM γCD).

A 150-µL aliquot of the pooled sample was pipetted into sample dispersion unit (Malvern Hydro MV, Malvern Panalytical, UK) containing water as a dispersant. The dispersed sample passed through the measurement cell of the optical bench and was measured in duplicate. Particle size of the sample was determined using laser diffraction technique and analyzed by Mastersizer Software. Five data points with stable laser obscuration were chosen from 60 data points obtained from the duplicate measurements to represent particle size distribution of one aliquot. Three aliquots of the pooled sample were determined.

3.4.4.3 Investigation of dovitinib/γCD complex in solid fraction using Fourier-transform infrared spectroscopy (FTIR)

The pooled suspension from section 3.4.4.2 was divided into microcentrifuge tubes and centrifuged at 12,000 rpm for 15 mins. After discarding the supernatant, the solid fraction was washed with water. The opened microcentrifuge tubes were placed in a tight box containing silica gel. The weight of microcentrifuge tubes containing solid fraction was measured until two consecutive weight was constant. Then the solid pellets were crushed and mixed to make a homogeneous sample.

The FTIR spectra of the raw materials including dovitinib free base and γCD, the physical mixture of dovitinib free base and γCD raw materials, and two pooled samples were measured using FTIR spectrometer (Cary 360,

Agilent Technologies, CA, USA). The spectra were recorded from 4000 to 650 cm^{-1}.

3.5 Investigation of the γCD effect on the permeation of lipophilic drugs, and the formulation factor affecting drug permeation

The effect of γCD on the lipophilic drug permeation and the formulation factor influencing the drug permeation were investigated using in-vitro permeation setup consisting of vertical Franz diffusion cell and artificial lipophilic membrane (PermeaPad® barrier).

3.5.1 Preparation of sample solutions

3.5.1.1 Preparation of dexamethasone-saturated aqueous γCD solutions

Dexamethasone was dissolved in solutions of γCD in water to examine $K_{1:1}$ and the dexamethasone solubility at different γCD concentrations over the range of 0.25 to 20 % w/v (eq. to 1.9 to 154.2 mM) as well as to prepare sample solutions for in-vitro permeation study. The phase-solubility procedure as described in section 3.3 and fixed amount of dexamethasone, i.e., 15 mg/mL (eq. to 38.2 mM), were used to prepare the aqueous γCD solutions containing dexamethasone. The sample suspensions were filtrated through 0.45 µm RC syringe filter after agitation at room temperature (21–22°C) for 7 days before determining dissolved dexamethasone and γCD using HPLC (section 3.2). The sample solutions were performed in triplicate. Six dexamethasone-saturated aqueous solutions containing different γCD concentrations, i.e., 7.7, 15.4, 38.6, 57.8, 77.1, and 115.7 mM were selected and used for the permeation study.

3.5.1.2 Preparation of dovitinib-saturated acidic γCD solutions in water

Two aqueous solutions of dovitinib free base were prepared in acidic γCD solutions in water. Excess dovitinib free base, acid stock solution, and γCD stock solution were accurately transferred to make a suspension of the dovitinib base at 1:1 molar ratio of acid to γCD. The sample suspensions were prepared as described in section 3.3. Lactic and phosphoric acid were used in this experiment. When the equilibration reached 7 days, a supernatant was separated using a centrifuge. The concentration of dissolved dovitinib and the final pH of the supernatant were determined. The solubility determinations were performed in triplicate.

An aqueous solution of dovitinib lactate salt was also prepared to compare with the dovitinib-saturated aqueous lactic acid/γCD solution. The amount of dovitinib in the dovitinib lactate solution was equivalent to dovitinib concentration in the aqueous lactic acid/γCD solution prepared using dovitinib free base.

3.5.2 Permeation studies

The permeation studies of the lipophilic model drugs, dexamethasone and dovitinib were carried out in vertical Franz diffusion cells (Perme Gear, SES GmbH, Denmark) comprising donor and receiver compartments. The effective permeable area was 1.77 cm^2. The receiver compartment had volume of 12 mL and was surrounded by a jacket equipped with a water circulating system (CORIO CD, Julabo GmbH, Germany) to control the temperature at 37.0±0.5°C throughout the experiment. The cells were placed in cell holders with the stirrer (SES GmbH, Denmark) underneath it for constant agitation at 500 rpm. The donor and receiver compartments were separated by a lipophilic membrane or PermeaPad® barrier which was an immobilized layer of soya phosphatidylcholine in between two cellulose supporting membranes (MWCO of 6 kD). The membrane was mounted on the receiver compartment containing receiver medium and clamped with donor chamber. The donor chamber contained 1-mL test solution without stirring and was firmly covered with parafilm. The receiver medium was 2 % w/v of γCD aqueous solution and 2.5 % w/v SBEγCD in phosphate buffer saline pH 7.4 for dexamethasone and dovitinib permeation, respectively.

200 µL of the receiver medium was withdrawn at 0.5, 1.0, 1.5, 2.0, 2.5, 3.0, and 4.0 hours and replaced immediately with the same volume of fresh receiver medium. The dexamethasone or dovitinib amounts in the receiver phase and the remaining test solution in the donor phase after the test were determined by HPLC (section 3.2.1). The accumulated drug in the membrane was extracted and analyzed using the same HPLC method. The permeation experiment was performed in six replicates. The leakage was monitored throughout the experiment and the mass balance of all diffusion cells was calculated to verify the validity of the test. The permeation data was included when the mass balance was more than 90%. The steady stated flux (J_{ss}) was obtained from a slope of linear part of permeation profiles (d_q/d_t) and apparent permeation coefficient (P_{app}) was calculated using this Equation (9) (Jansook & Loftsson, 2009).

$$J_{ss} = \frac{d_q}{A \cdot d_t} = P_{app} \cdot C_d \qquad (9)$$

where A is the effective permeable area and C_d is the initial concentration of the model drugs in the donor chamber.

3.5.3 Size measurement of dovitinib/acid/γCD aggregates in the sample solution

The particle size of the aggregate of dovitinib/acid/γCD complexes was determined using a particle size analyzer for nanometer range (NanoSight NS300, Malvern Panalytical, UK). Sample solution without dilution was injected in the top plate O-ring with an infusion rate of 100 and the measurement was performed using dynamic mode with a capture time of 60 seconds per measurement. The solutions containing nanoparticles were measured for five replicates. The size and concentration of the particles was recorded and analyzed based on five measurements using Nanoparticle tracking analysis software.

3.6 Study of drug release from γCD-based drug carrier

Before the test of drug release from γCD-based carrier, dexamethasone solubility in HEPES buffer pH 7.4 at 34°C and the degradation of γCD were investigated. The solubility and degradation studies were performed using phase-solubility technique and enzymatic reaction, respectively. The kinetics of complexation and degradation of γCD was evaluated under simulated eye condition such as tear pH and ocular surface temperature.

3.6.1 Solubility of dexamethasone in HEPES buffer containing γCD

Phase-solubility study was used to determine the solubility of dexamethasone in 20 mM HEPES buffer pH 7.4 (34°C) containing 140 mM NaCl, 2 mM $CaCl_2$, and different γCD concentrations ranging from 0.25 to 154.2 mM. Excess dexamethasone was added to the complexing buffer media and proceeded as described in section 3.3. After equilibration in the temperature-controlled incubator shaker (Lab-Line Instruments, Inc., USA) at 34±1°C for 7 days, all suspensions were filtered through 0.45 µm RC syringe filters and the concentration of dissolved dexamethasone and γCD was determined by HPLC (section 3.2).

3.6.2 Degradation of γCD

Degradation of γCD in the pure buffer solution and the buffer solutions containing dexamethasone/γCD complexes was investigated using enzymatic reaction to mimic the ocular surface condition. The used buffer was the same

as that in the phase-solubility study. Six stock solutions containing different γCD concentrations from 1 to 32 mM and a stock solution of 10 units/mL PPA were prepared in the HEPES buffer. The γCD stock solutions were incubated in an incubator shaker at 34±1°C for about 1 hour. Next, PPA stock solution was accurately transferred to warm γCD stock solutions to prepare the test solution. Final concentrations of substrate and enzyme in the test solution were 95% of initial γCD stock concentration and 1 unit/mL of enzyme, respectively. One-mL sample was taken at 0.5, 1.0, 1.5, 2.0, 2.5, 3.0, 4.0, and 6.0 hours and placed in a preheated test tube in a dry heating block (100°C), capped immediately and heated continuously for further 15 mins to stop the reaction (Lumholdt et al., 2012). The sample was cooled on an ice pack and then the remaining γCD in the samples was analyzed using HPLC (section 3.2.2). For the degradation of γCD in the buffer solution containing dexamethasone/γCD complexes, the stock solutions with the same γCD concentrations were prepared using phase-solubility techniques as described in section 3.6.1 and subjected to the enzymatic reaction as described above. All degradation reactions were performed in triplicate.

The γCD content remaining in the test solution after the reaction was calculated as a percentage of the initial γCD concentration. Michaelis-Menten constants (K_m) and V_{max} were determined by Lineweaver-Burk plot and the turnover number (k_{cat}) was calculated from V_{max} using the following equation: (Berg, Tymoczko, & Stryer, 2002).

$$k_{cat} = V_{max}/[E_t] \quad (10)$$

where $[E_t]$ is total concentration of enzyme in molar.

3.6.3 Drug release

Permeation studies through artificial membranes were used to determine dexamethasone release from aqueous solutions containing complexes of dexamethasone/γCD with or without the PPA. The permeation experiment was performed in the same Franz diffusion cells as mentioned in 3.5.2. However, donor and receiver compartments were separated by a single layer of cellulose ester dialysis membrane which had MWCO of 3.5–5 kD. Before use, the membrane was washed thoroughly with ultrapure water to remove preservative agents and then soaked overnight in 20 mM HEPES buffer pH 7.4 (34°C) containing 140 mM NaCl and 2 mM $CaCl_2$ which was previously sterilized by autoclaving at 121°C for 20 mins. The membrane was equilibrated at 34±0.5°C for about 1 hour after mounting on the receiver compartment containing receiver medium and clamped with donor chamber.

The receiver medium was γCD solution in the HEPES buffer which had the identical γCD concentration as the donor phase. The donor chamber contained 1-mL solution in HEPES buffer of γCD/dexamethasone complexes with or without PPA. The final concentration of γCD was adjusted to 95% of initial concentration by additing PPA stock solution or pure buffer solution. The test solution was mixed and transferred into the donor chamber immediately. PPA concentration in the donor phase was 1 unit/mL in the case of the test solution with PPA. A 150-µL of the receiver medium was withdrawn at 0.5, 1.0, 1.5, 2.0, 2.5, 3.0, 4.0, and 6.0 hours and replaced immediately with the same volume of fresh and warm receiver medium. The dexamethasone content in the receptor phase was determined by HPLC and the permeation was performed in triplicate. The steady stated flux (J_{ss}) and apparent permeation coefficient (P_{app}) were determined as stated in section 3.5.2.

3.6.4 Statistics

The student t-test was used to determine the difference of degradation rate between bound and unbound γCD.

4 Results and discussion

4.1 Preformulation studies of dovitinib free base

The γCD-based drug delivery system has been of interest to pharmaceutical scientists for topical ocular administration because it has shown the potential in the delivery of a lipophilic drug to the posterior segment of the eye (Johannsdottir et al., 2018; Tanito et al., 2011). This present study investigated some physicochemical properties of dovitinib free base with pharmaceutical excipients such as γCD and acidic counterions. The goals were to gain more information regarding formulating factors and seek feasibility of developing γCD-based ophthalmic aqueous formulation.

To achieve therapeutic drug concentration in the intraocular tissues, the drug load in formulation should be optimized to enhance drug availability at the ocular surface. Preparing high lipophilic-drug concentrations in aqueous eye drops is a challenge because an aqueous solubility of lipophilic drug should increase without alteration of its permeability through a biological membrane. The drug must also be chemically stable under the intentionally used excipients and desired formulation. Furthermore, other formulation factors such as sterilization, osmolality, pH etc., should be considered during ophthalmic formulation development. Therefore, fundamental findings of dovitinib in this preformulation study are useful in the formulation development for this drug and contribute substantially to understanding novel γCD-based drug delivery systems.

4.1.1 Improvement of an aqueous solubility of dovitinib free base by the γCD complex and counterions

4.1.1.1 Stability constant, complexation efficiency and phase-solubility diagram of dovitinib free base and γCD

Previous studies prepared dovitinib/γCD complex using an autoclaving method at certain pH (6.5±0.1) and ultrasonic method without controlling pH of samples (Jansook, Praphanwittaya, et al., 2020; Praphanwittaya et al., 2020). They found that γCD and dovitinib free base formed an inclusion complex, and consequently, the aqueous solubility of dovitinib increased. The $K_{1:1}$ was 684 and 865 M^{-1} for the ultrasonic method without pH control and autoclaving method at pH 6.5±0.1 with 0.1 % w/v of ethylenediaminetetraacetate disodium, respectively. The CE obtained from

the autoclaving method (CE = 0.03) was higher than that obtained from the ultrasonic method (CE = 0.01). It revealed that preparation method, pH, and additive influenced $K_{1:1}$ and CE of dovitinib/γCD complexation. In addition, the accuracy of S_0 can affect the $K_{1:1}$ calculated using equation (6) and the slope of the linear part of phase-solubility diagram (Brewster & Loftsson, 2007).

The autoclaving method was used to determine solubility of dovitinib free base in aqueous γCD solutions without pH control in this study. Maximum solubility in the complexing medium was approximately 0.326 mM (eq. to 0.128 mg/mL) when theoretical γCD concentration was 5 % w/v (i.e., added γCD amount to the medium). Figure 6 shows that this batch of dovitinib raw material provided a similar B_s profile and the same order of magnitude of the aqueous solubility as the previous reports (Jansook, Praphanwittaya, et al., 2020; Praphanwittaya et al., 2020). The $K_{1:1}$ and CE, which were calculated based on the apparent intrinsic solubility in water (0.00595±0.00108 mM), were 1830 M^{-1} and 0.01, respectively. The $K_{1:1}$ value in this present study was higher than that in the previous studies. It was because of different ambient condition, drug assay method, and the intrinsic-solubility value. Interestingly, the CE obtained from uncontrolled pH samples was the same in the present and previous studies. This indicated that pH adjustment and additives which affected the ionization of dovitinib influenced the complexation of dovitinib free base with γCD. This finding corresponded with the literature from Brewster and Loftsson (2007) which reviewed the enhancement of CE by improving an intrinsic solubility using drug ionization or salt formation techniques. Although the aqueous solubility of dovitinib free base was improved by γCD, it appeared too low for topical ophthalmic formulation.

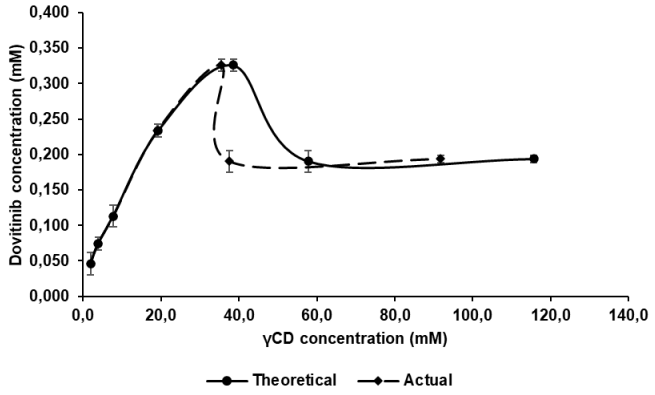

Figure 6. Phase-solubility diagram of dovitinib free base in γCD aqueous solution, the data is shown in mean ± SD.

4.1.1.2 Effect of acidic counterions on aqueous solubility of dovitinib free base

Because the previous studies showed an increase in CE of dovitinib/γCD complexes when pH was adjusted and counterion was added in the media (Jansook, Praphanwittaya, et al., 2020; Praphanwittaya et al., 2020), the effect of acidic counterions on the water solubility of dovitinib was investigated by titration of the studied acid solution and the drug free base. Dovitinib is an ionizable basic drug with two predicted pK_a values, i.e., 7.70 and 9.44 (Table 3). Its aqueous solubility is pH dependent. Therefore, five acids including HCl, H_3PO_4, lactic, gluconic, and maleic acid were chosen to study their effect on dovitinib solubility. The selection was based on pK_a and acid type. The pH-solubility profiles of the drug and acidic counterions are shown in Figure 7A. The study design differed from a general titration, with titration of different fixed concentrations of counterions with the drug powder. The free base was used as a starting material in this experiment. Suspensions of dovitinib free base with pH lower than 7 were prepared in aqueous solution with different acid concentrations, whereas dovitinib suspensions with pH higher than 7 were prepared using a few dilute NaOH solutions. By this experimental design, the pH-solubility profiles of dovitinib free base did not follow the theoretical profile of a basic drug. Those profiles could be divided into three groups according to acid type.

First, HCl and H_3PO_4 are an inorganic acid. HCl is a strong acid with pK_a about -6.1 (Gould, 1986). Thus, it completely ionized across the entire pH-range studied. The solubility of dovitinib sharply increased when pH decreased from approximately 7 to 5.5 (Figure 7B). After that, the dovitinib solubility slightly increased or became about 3 fold between pH 5.5 and 3.4. The profile was nearly flat although the HCl concentration rose 10–100 fold. That is because of the maximum solubility of the dovitinib HCl salt. Surprisingly, a sharp increase of the dovitinib/HCl profile from 19.1 to 46.1 mM of soluble dovitinib was observed within 0.1 pH unit decrease, i.e., pH 3.4 to 3.3. This increment was not expected because in general, the pH-solubility profile of a basic drug in aqueous HCl media will drop after the plateau, owing to the common-ion effect at relatively low pH. It was assumed that ionization of benzimidazole NH lifted the curve of the dovitinib/HCl pH-solubility profile. The dovitinib molecule exists in two ionized forms in acidic aqueous solutions below pH 5. It can form a divalent salt with HCl due to ionization of the N atoms at the piperazine and benzimidazole rings (Figure 8); consequently, the common-ion effect would occur later at very low pH, such as pH 1.

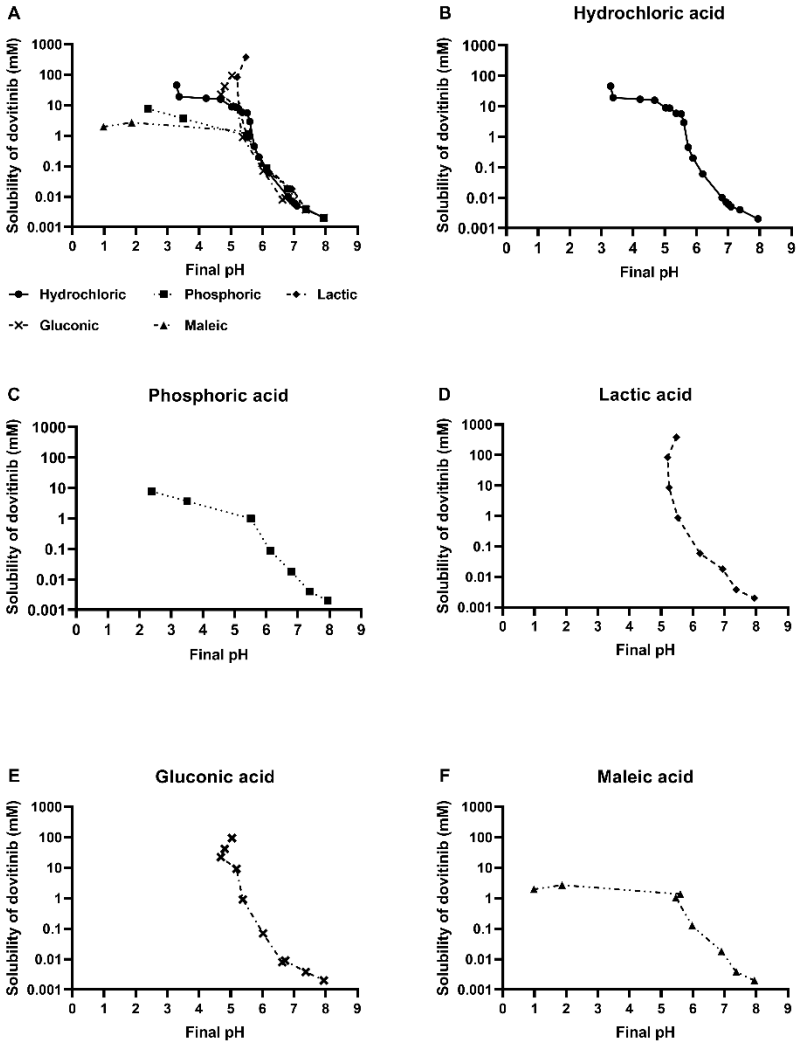

Figure 7. The pH-solubility profiles of dovitinib free base and different acidic counterions.

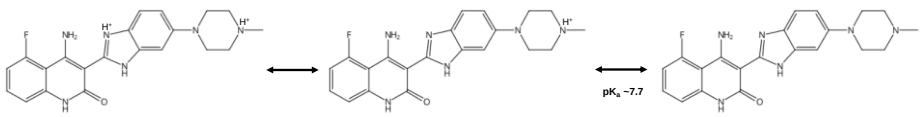

Figure 8. Proposed ionized species of dovitinib with predicted pK_a ~7.7.

H_3PO_4 is a weak inorganic and polyprotic acid. It has three different pK_a values, 2.15, 7.2, and 12.38 (Gould, 1986). The pH-solubility profiles of dovitinib/H_3PO_4 and dovitinib/HCl are quite similar, except for no sharp increase at pH below 2.38 (Figure 7C). Basically, for basic drug, the solubility will be constant then follow by the sharp drop when pH gradually decreases after the pH_{max} where the solubility of the drug reaches maximum level. After pH_{max} (pH 5.51), the H_3PO_4 increased the dovitinib aqueous solubility by 10 fold. The maximum solubility of 7.78 mM at pH 2.38 is close to the pK_a of H_3PO_4. At pH = pK_a = 2.15, the concentrations of the unionized species (H_3PO_4) and the ionized species ($H_2PO_4^-$) are equal. However, the solubility decreased dramatically at pH lower than 2.38 due to limited solubility of dovitinib/H_3PO_4 salt and common-ion effect. The suspension with initial pH 1.72 became semisolid after overnight agitation, preventing determination of the final solution pH and dovitinib solubility.

Second, lactic and gluconic acids are hydroxy acids. They have similar pK_a values of 3.85 and 3.60 for lactic acid and gluconic acid, respectively, but quite different molecular sizes. Lactic and gluconic acids significantly improved the aqueous solubility of dovitinib free base above pH 5. The solubility of dovitinib was increased up to 385.85 mM at pH 5.48, when the initial lactic acid concentration was about 0.5 M (Figure 7D). The highest solubility of dovitinib in aqueous 0.1 M gluconic acid solution was 94.28 mM at pH 5.04 (Figure 7E). The pH at maximum solubility in these hydroxy-acid experiments did not follow the theoretical pH-solubility profile. Unusual right shifting of pH to higher values at the observed maximum solubility was seen in the pH-solubility profiles of dovitinib with lactic or gluconic acid (Figure 7D, 7E).

This behavior of a basic drug has been reported previously (Serajuddin & Rosoff, 1984). The studies determined the pH-solubility profile of papaverine HCl and found that the solubility of papaverine HCl still increased when more concentrated NaOH solution was added to make pH > apparent pH_{max} of 3.9. The solubility of papaverine HCl rose until reaching its maximum at pH 4.5 and then dropped rapidly. This observation was explained by supersaturation at pH between 3.9 and 4.5. The supersaturation hypothesis was verified by adding the papaverine base to the supersaturated solution eliciting precipitation of the papaverine base. One year later, the same researchers also showed that the supersaturation behavior above pH_{max} could occur during titration of either salt or base (Serajuddin & Mufson, 1985). Moreover, they pointed out that the supersaturation of the studied bases would be released when the corresponding salt was added to induce nucleation.

Otherwise, the plateau region expressing the limited solubility of the salt was unobserved. They added the salt of the organic base and the corresponding acidic counterion to the supersaturated solution of the organic base to complete the pH-solubility profile at relatively lower pH than pH_{max}.

In this present study, two pH-solubility profiles of dovitinib/hydroxy acid were accomplished by keeping the excess solid dovitinib base in each concentration of acid. When the concentration of counterion was increased in the presence of excess solid dovitinib base and in equilibrium with dissolved dovitinib, the solution was saturated by the ionized dovitinib that formed a supersaturated solution. In addition, most lactic and gluconic acids were ionized at the supernatants´ pH, i.e., 5–7. The supersaturation of ionized dovitinib resulted in shifting of the pH in the opposite direction from the desired pH; thereby, increasing the aqueous solubility beyond the maximum solubility of dovitinib salt.

Third, maleic acid is a carboxylic acid with two pK_a values, 1.96 and 6.28 (Gould, 1986). It can form a salt with dovitinib free base to increase the aqueous solubility of dovitinib. However, the maleate salt of dovitinib has relatively low solubility compared with the other salts studied (Figure 7F). It improved the solubility by about 100 fold from 0.02 mM at pH 6.90 to 2.71 mM at pH 1.87. Between pH 5.5 and 7, maleic acid enhanced the dovitinib solubility to the same degree as did the other counterion. By contrast, the dovitinib/maleate profile showed the plateau region at pH 1.87 to 5.46, followed by a declining curve at pH 0.98 to 1.87. At pH 1.87 (about pK_a of maleic acid) and lower, the ionized maleate falls below 50% and the unionized form rises, causing a slight decrease of dovitinib solubility.

All studied counterions can improve the aqueous solubility of dovitinib but only lactic acid is able to enhance the water solubility up to many ten-thousand fold. The enhancement depends upon the acid type and concentration, indicating the amount of anion in the solution. For ophthalmic solutions, lactic and gluconic acids may be more suitable than HCl to increase the solubility without lowering the final pH.

4.1.1.3 Enhancement of dovitinib solubility in water through drug/acid/γCD system

The results from earlier sections show a feasibility of improving the aqueous solubility of dovitinib free base using γCD and acidic counterions. γCD affinity for dovitinib was quite good as well as the improving dovitinib aqueous solubility by ionization was great. Loading much more dovitinib content is possible in γCD-based aqueous formulation. Hence, the effect of different concentrations of acidic counterions on dovitinib solubility with or without γCD

was investigated. Three sample sets with respect to γCD concentration, i.e., 0, 38.6, and 154.2 mM were measured. The results of the three sample sets are shown in Figures 9–12.

The aqueous solubility of dovitinib increased 63 and 376 fold when dissolving dovitinib free base in 38.6 and 154.2 mM γCD solution, respectively (Figure 9). Even though the increase in solubility through forming dovitinib/γCD complex was lower than that obtained by salt formation, the final pH of dovitinib/γCD solution was higher than that of dovitinib/counterion solution (Figure 10). Based on the same concentration at 38.6 mM of counterion, the dovitinib solubility trend from low to high concentration was maleic → H_3PO_4 → HCl ~ lactic → gluconic acid.

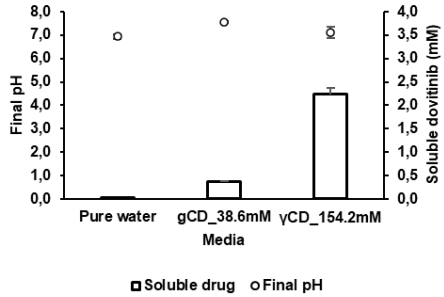

Figure 9. The apparent intrinsic solubility of dovitinib in water and the aqueous solubility and final pH of dovitinib in γCD aqueous solution at room temperature, 21–22 °C (mean ± SD, n = 3).

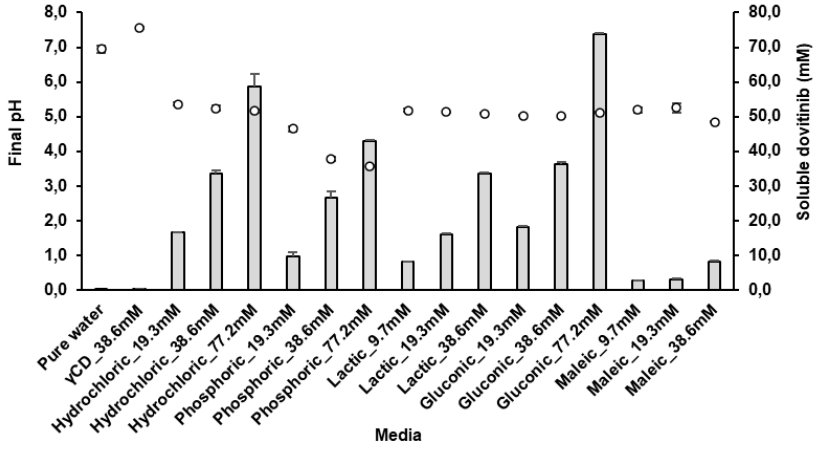

Figure 10. Aqueous solubility and the final pH of the dovitinib in acidic aqueous solution (mean ± SD, n = 3).

For solubility studies in 38.6 mM γCD solution, the acid concentration was varied according to the molar ratio of acid to γCD. As expected, the apparent solubility of dovitinib free base in a ternary system (drug/acid/γCD) increased with increasing acid concentration (Figure 11). The dovitinib solubility in the complexing medium with HCl, lactic, and gluconic acid was quite comparable to that in the corresponding acidic solution. This indicated that the major enhancement of the apparent solubility was due to the observed increase in intrinsic solubility. The slightly increased solubility observed in the aqueous 38.6 mM γCD solution at the highest HCl concentration (77.2 mM) was due to the stabilizing effect of γCD. The degradation peaks that were observed in pure HCl aqueous solution were relatively small when γCD was present. The presence of 38.6 mM γCD in aqueous lactic acid solutions increased the dovitinib solubility through stabilization of dovitinib and the formation of ternary dovitinib/γCD/acid complexes. In all γCD/lactic acid samples, total dovitinib solubility was found to be slightly higher than the combined solubility value in each excipient at the same concentration level. In other words, the effect was synergistic. Additionally, the degradation peaks that used to be seen in the binary system were smaller. Unlike the HCl and lactic acid systems, gluconic acid did not affect the dovitinib solubility in aqueous 38.6 mM γCD solutions. Furthermore, addition of H_3PO_4 or maleic acid to the aqueous 38.6 mM γCD solution resulted in a synergistic increase of dovitinib solubility, regardless of pH. The increment of the aqueous solubility was observed at all acid concentrations. The total solubility in ternary system containing H_3PO_4 or maleic acid was greater than the apparent intrinsic solubility of the corresponding salt, whereas the decrease in the final pH was not proportional to the increase in acid concentration.

The aqueous solubility of dovitinib in the 154.2 mM γCD solution and the acidic aqueous solution with 154.2 mM γCD are illustrated in Figure 12. The dovitinib amount was fixed at 76.5 mM, and the acid concentration varied as follows: 0.25:1, 0.5:1, 1:1, and 2:1 molar ratio of acid to the drug concentration. The results showed that the aqueous solubility of dovitinib increased with increasing acid concentration. However, the dovitinib solubility in the samples with 2:1 and 1:1 molar ratio of acid to drug was constant when the acid was phosphoric and gluconic acid. Presumably, this was due to the limited amount of dovitinib. Interestingly, γCD dissolved more readily with increasing acid concentration. The dovitinib/γCD complex formation was classified as B_s-type (Figure 6). This indicated that the soluble amount of drug and γCD was theoretically less than the dovitinib:γCD molar ratio of 1:1 at relatively high γCD concentration. Moreover, the dovitinib/γCD complexes

could precipitate from the aqueous medium at higher γCD concentration, resulting in lower aqueous solubility of dovitinib. These results suggest the contrary that addition of counterion increases the solubility of both dovitinib itself and that of the dovitinib/γCD complex. The excess addition of acid could affect the final pH and γCD content as seen in the HCl, H_3PO_4, and gluconic samples with highest concentration (152.9 mM). At the highest HCl, H_3PO_4, and gluconic acid concentrations the samples were in solution. The assay of γCD in those solutions after equilibrium should be the same as initial amount, but no such results were observed. At the highest concentration of HCl, H_3PO_4, and gluconic acid, γCD degraded and the remaining γCD is shown as the dissolved γCD concentration in Figure 12. For the lactic and maleic acid systems, the highest dissolved concentration of dovitinib was low compared with the other acids, and all samples were suspensions. Lactic acid was able to increase the aqueous solubility of dovitinib and its complex. Contrasting results were seen in the maleic acid samples, where the aqueous solubility of dovitinib did not change when maleic acid increased. In addition, the synergistic effect of γCD and maleic acid was not observed with the high concentration of γCD; 154.2 mM γCD gave the same result as 38.6 mM γCD.

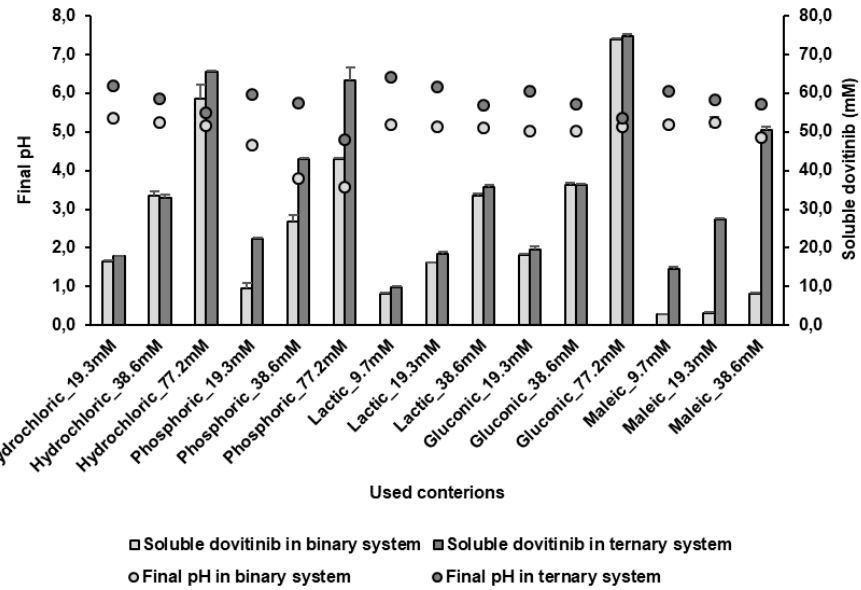

Figure 11. Aqueous solubility and final pH of dovitinib in aqueous binary (drug/acid) and ternary (drug/acid/38.6 mM γCD) system (mean ± SD, n = 3).

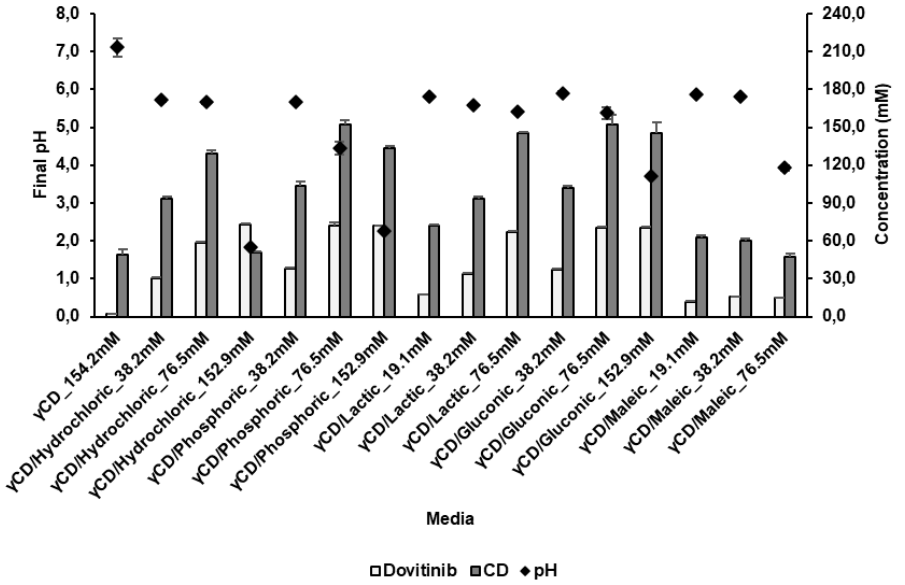

Figure 12. Final pH, soluble dovitinib and dissolved γCD concentration in the ternary system (drug/acid/γCD) at relatively high γCD (154.2 mM) (mean ± SD, n = 3).

The solubilizing effect of γCD on the aqueous solubility of dovitinib was influenced by the counterion type and concentration. The combined techniques of γCD complexation and ionization by acidic counterion can enhance the water solubility of dovitinib to the appropriate concentration for the topical eye drops. The loading dose of the drug in aqueous formulation and the pH can be optimized by changing the acid used and varying the acid concentration.

4.1.2 Effects of pH and acidic counterions on lipophilicity

Not only the solubility but also the lipophilicity of drug is important to drug availability at the site of absorption. Basically, biological membranes consist of an aqueous layer and lipophilic membranes which hampers partition of hydrophilic molecules in the membranes and permeation through them. Lipophilicity of the drug molecule is defined by the partition coefficient and distribution coefficient which is expressed as log P (i.e., the $\log_{10}$ value of the partition coefficient) and log D (i.e., the $\log_{10}$ value of the distribution coefficient), respectively. The dovitinib free base has calculated log P of about 1.31 (Table 3) and its calculated log D values at a certain pH over the pH range 1 to 10 are shown in Figure 13. The distribution coefficient of dovitinib depends upon the pH and indicates that most of the dovitinib was preferred to be in an aqueous phase when the pH is lowered. Generally, an

ionized molecule which is highly water-soluble has low distribution in the organic phase. However, the ion with its pairing-ion can dissolve in the organic phase as a neutral molecule (Comer & Tam, 2007). Therefore, adding counterions to the aqueous phase in the organic/aqueous biphasic mixture can affect the distribution of ionizable dovitinib. The effects of pH and counterion on the lipophilicity of dovitinib were investigated in this study.

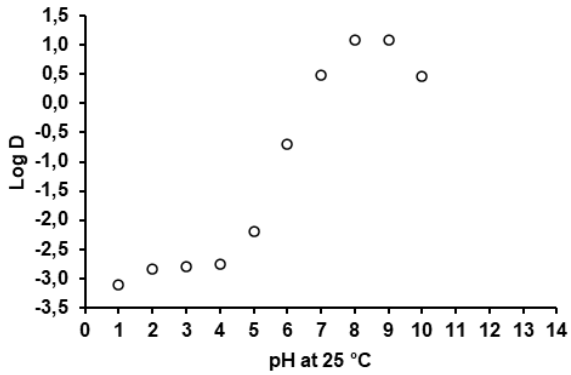

Figure 13. Calculated log D of dovitinib (SciFinder, 2022).

To avoid the effect of other ions used in pH adjustment, some pure acid solutions and some pure NaOH solutions with different concentrations were prepared and used as an aqueous phase. When the extraction and separation were complete, the pH of aqueous phase and the dovitinib concentration were determined. The final pH was plotted against log D of dovitinib and the pH-lipophilicity profiles from all acids used are shown in Figure 14A. The shape of each profile resembled the respective predicted profile (Figure 13), but the curves were shifted upward. The apparent log D values obtained from pure acid or NaOH solutions were about -1.85 to 3.50. These values were higher than the calculated log D. This could happen when a different method is applied to determine the distribution coefficient. Normally, the partition coefficient or distribution coefficient are calculated from the software when the drug candidate is developed. Different software programs use different algorithms to calculate. Accordingly, deviation of the log D values can occur. Similarly, different techniques can provide different log D values. Many other experimental factors can alter the log D values such as ionic strength, the partition of solvent into another phase, the accuracy and sensitivity of a given analytical method, and so on. Another point of difference in the lipophilicity profiles was observed at pH below 4.5 among all counterions. The pH-lipophilicity profiles of the maleic and HCl counterions

deviated from the other three counterions H_3PO_4, lactic, and gluconic acids. Those log D values were not scattered evenly near where the log D values from H_3PO_4, lactic, and gluconic acids were located. Perhaps, this is due to the different H^+ ions in the aqueous phase.

In addition, the higher salt or ionic strength in the aqueous phase can cause higher log D values (Comer & Tam, 2007). As we have seen, the pH-lipophilicity profiles obtained from the aqueous phase containing the mixture of the studied acid and NaOH, the relatively high log D values were also observed especially in the acidic region where pH < 6 (Figure 14B). Those log D values ranged from -1.50 to 3.55. In all, 1 M NaOH was added to adjust pH of the aqueous phase containing a fixed concentration of the counterion at 0.1 M. The addition of NaOH increased the salt in the aqueous phase, consequently the dovitinib free base precipitated and partitioned to the non-aqueous phase. The salting out effect somewhat differed for each counterion due to the different ionizations. Although the experimental log D values of dovitinib differed from the calculated values, they still showed that the dovitinib had a suitable lipophilicity for permeation through a lipophilic membrane. Furthermore, the results confirmed that the pH is the major factor influencing the distribution coefficient of the ionizable drug. The counter ions can affect the log D value of the ionized dovitinib but have a negligible effect on the log D value of the unionized drug.

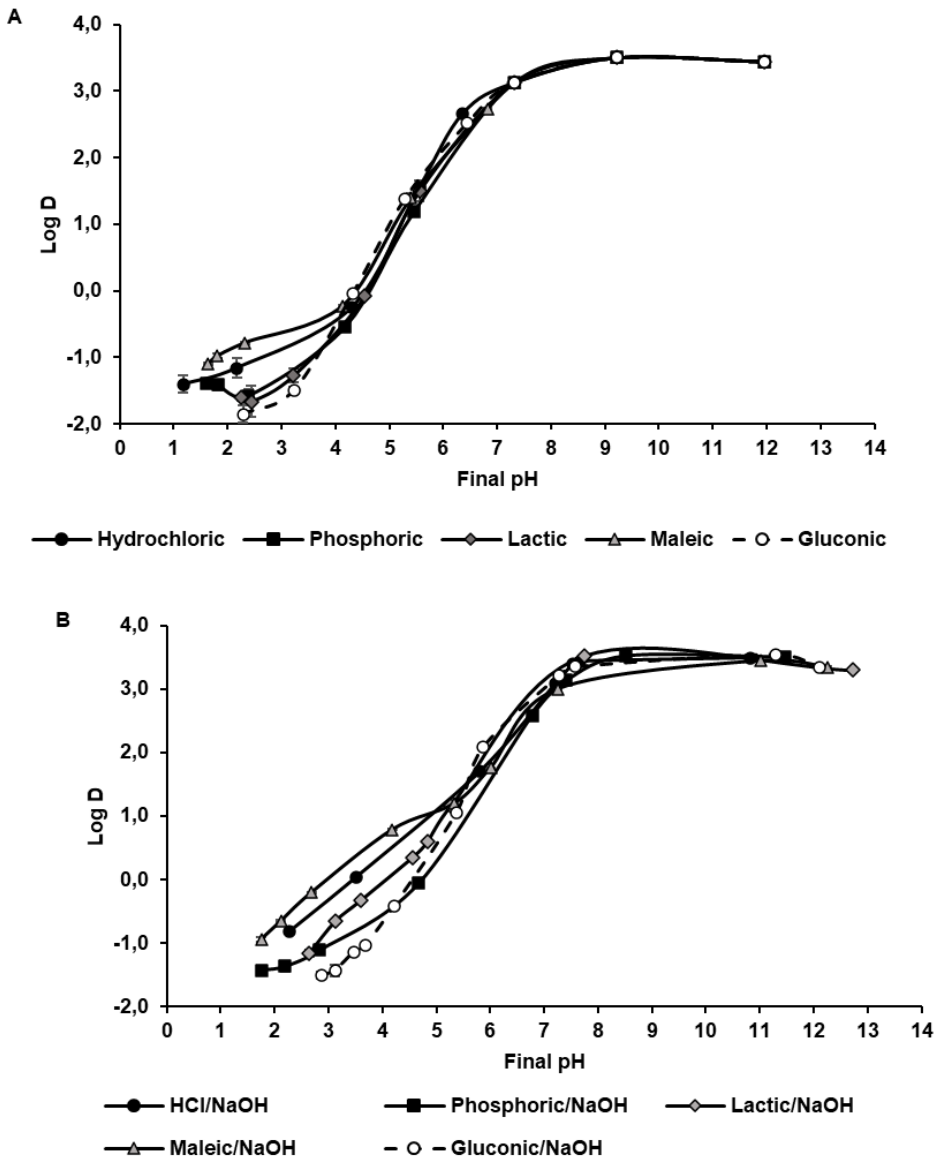

Figure 14. The pH-lipophilicity profiles of dovitinib in the presence of five different counterions. A: the aqueous phase consists of pure acidic counterion in water at different pH. B: the aqueous phase is the mixture of acid and NaOH at different certain pH. The data are showed as mean ± SD (n = 3).

4.1.3 Effects of temperature, pH, and pharmaceutical excipients on stability of dovitinib

The previous study showed that elevated temperature autoclaving (Holding at 121 °C for 20 mins) could accelerate the degradation of dovitinib (Jansook, Praphanwittaya, et al., 2020). In this study, the effect of temperature, pH, buffer species, and solubilizing agent on the stability of dovitinib were investigated. The influence of temperature on the degradation of dovitinib was studied at 40±2 and 75±2 °C. The remaining dovitinib content in the CD buffer solutions at both temperatures is shown in Table 6 and 7. The degradation of dovitinib at high temperature (75°C) was faster than that at low temperature (40°C) in all cases. The effects of pH and solubilizing agent were determined in 100 mM buffer solutions containing 5 % w/v HPγCD or 5 % w/v γCD across the pH range of 2 to 8. Due to the slow degradation of dovitinib at lower temperature (40°C), the effect of pH resulting in the significant decrease of dovitinib was diminished after 2 weeks. About 10 % change in the remaining drug was observed in the solutions of pH 5.9 and 8.0 phosphate buffer with HPγCD at 15 days, whereas a 10 % and greater decrease of dovitinib content was seen at 28 days, when γCD, instead of HPγCD, was used (Table 6). Thus, studies at 75°C were performed to accelerate the reaction. The degradation of dovitinib was investigated using the same buffer systems and solubilizing agents. The percentages of the remaining drug at 1, 3 and 5 days are shown in Table 7. Among four phosphate buffer solutions, dovitinib was the most stable at pH 4 and the least stable at pH 5.9, with both solubilizing agents used. However, the CDs confounded the effect of pH on the degradation of dovitinib at pH 2.1. Notably, γCD stabilized dovitinib in the buffer solution at relatively low pH; consequently, the decrease of dovitinib content was not comparable to that in the buffer solution containing HPγCD. Similar stabilizing effects of γCD were also seen in the other buffer species used, which were HCl/KCl buffer with pH 1.7 and acetate buffer solutions with pH 4.2. The degradation of dovitinib in the HCl/KCl buffer with HPγCD was faster than that in the system with γCD. Forty µg/mL of dovitinib in the HCl/KCl buffer solution with HPγCD completely degraded within 3 days, and the physical appearance of the test solutions of dovitinib in pH 1.7-HCl/KCl buffer with HPγCD obviously changed. The color of the test solutions was darker than the initial color, and some brown precipitate was observed in all the test tubes. Even through the remaining drug obtained from the HCl/KCl buffer solution with γCD was higher than that from HPγCD, the physical appearance in one tube of the γCD system similarly changed, resulting in high standard deviation. In the case of

the acetate buffer with pH 4.2, the % dovitinib remaining in the presence of γCD was quite similar to that of HPγCD. However, at Day 3, a small amount of brown precipitate was observed in one of the test solutions. The outlier sample caused exceedingly high standard deviation of about half the mean of the percentage of drug remaining at Days 3 and 5. When recalculating the percentage of drug remaining using two samples, the mean values were comparable to the values obtained from the pH 4.0-phosphate buffer solution with γCD. The recalculated means ± SD were 96.3±1.1, 88.5±3.1, and 81.1±9.5 for Days 1, 3, and 5, respectively. Therefore, the stabilizing effect of γCD on the degradation of dovitinib was more dominant than the effect of buffer species at relatively low pH.

Table 6. Stability of dovitinib free base in complexing buffer media at different pH and 40±2°C (mean ± SD, n=3).

Time	**Day 7**	**Day 15**	**Day 28**	**Day 7**	**Day 15**	**Day 28**
Solubilizing agent	**HP-γ-CD**			**γ-CD**		
Buffer	**% Drug remaining**			**% Drug remaining**		
pH 1.7 HCl/KCl	99.4 ± 1.3	94.6 ± 1.8	93.8 ± 0.5	103.7 ± 1.1	99.0 ± 0.7	98.3 ± 0.9
pH 2.1 H_3PO_4/NaH_2PO_4	102.9 ± 0.3	99.3 ± 0.1	103.5 ± 0.3	102.6 ± 0.7	100.2 ± 1.2	98.3 ± 1.6
pH 4.0 H_3PO_4/NaH_2PO_4	102.3 ± 1.3	98.7 ± 1.0	103.2 ± 1.2	102.9 ± 0.4	101.0 ± 0.4	97.7 ± 0.4
pH 4.2 CH_3COOH/CH_3COONa	100.5 ± 0.6	95.2 ± 0.5	93.1 ± 0.4	100.9 ± 0.4	98.4 ± 0.8	95.2 ± 1.4
pH 5.9 NaH_2PO_4/Na_2HPO_4	97.2 ± 0.3	87.1 ± 1.4	76.7 ± 1.2	99.2 ± 1.1	96.6 ± 1.3	87.2 ± 1.4
pH 8.0 NaH_2PO_4/Na_2HPO_4	98.2 ± 1.3	90.1 ± 1.3	87.1 ± 0.4	97.8 ± 1.4	93.0 ± 1.9	74.8 ± 1.9

Table 7. Stability of dovitinib free base in complexing buffer media at different pH and 75±2°C (mean ± SD, n = 3).

Time	**Day 1**	**Day 3**	**Day 5**	**Day 1**	**Day 3**	**Day 5**
Solubilizing agent	**HPγCD**			**γCD**		
Buffer	**% Drug remaining**			**% Drug remaining**		
pH 1.7 HCl/KCl	66.4 ± 1.6	0 ± 0.1	NA	94.5 ± 3.3	77.1 ± 8.9	57.3 ± 16.6
pH 2.1 H_3PO_4/NaH_2PO_4	89.3 ± 0.1	71.5 ± 1.3	58.8 ± 1.6	95.4 ± 0.7	88.0 ± 0.3	79.2 ± 0.7
pH 4.0 H_3PO_4/NaH_2PO_4	94.8 ± 0.9	85.2 ± 0.1	79.5 ± 0.6	96.0 ± 1.0	88.8 ± 2.0	82.3 ± 4.2
pH 4.2 CH_3COOH/CH_3COONa	89.6 ± 0.9	61.8 ± 1.9	39.2 ± 1.1	88.2 ± 14.0	69.4 ± 33.1	60.1 ± 37.0
pH 5.9 NaH_2PO_4/Na_2HPO_4	87.0 ± 0.8	63.7 ± 1.1	45.7 ± 0.9	86.2 ± 0.6	63.8 ± 2.5	44.7 ± 7.6
pH 8.0 NaH_2PO_4/Na_2HPO_4	88.1 ± 1.1	74.5 ± 4.3	67.4 ± 3.4	88.0 ± 1.6	68.2 ± 2.8	52.8 ± 2.5

4.1.4 Characterization of solid fraction in the suspensions containing dovitinib, acid, and γCD

A suitable lipophilic drug, polymer and γCD can assemble to form soluble particles which have been used as a drug delivery system, for example, γCD-based eye drops containing telmisartan (Muankaew et al., 2016). In the present solubility studies, suspensions of dovitinib, counterion, and γCD with a unique appearance, i.e., dazzling white-yellow precipitates appeared in some samples during sample preparation. To better understand the appearing solids, the solid fraction was separated and characterized.

4.1.4.1 Dovitinib and γCD contents in solid fraction

Some dazzling white-yellow suspensions spontaneously formed during equilibrating samples in the study of dovitinib solubility in 154.2 mM γCD solution (section 4.1.1.3). The complex formation of γCD and dovitinib has been reported as B_s type profile (Figure 6) indicating that the γCD solubility decreased at relatively high concentration of γCD such as 57.8 and 115.6 mM (eq. to 7.5 and 15 % w/v, respectively) when dovitinib was present. Even though the addition of acidic counterion was able to dissolve more dovitinib and γCD from solid fraction and most dovitinib and γCD were consequently in solution or supernatant, some samples with relatively low acid concentration were seen as suspension.

Therefore, the dovitinib and γCD contents in solid fraction of those suspensions were determined and are shown in Figure 15. The highest γCD content in solid fraction (102.2±18.1 mM) was found in the dovitinib/γCD suspension as expected, while the suspensions of ternary system at the same acid concentration (38.2 mM) had γCD content between 51.0±6.2 mM and 93.4±5.5 mM. All solid fractions contained more γCD content than dovitinib content. Interestingly, the molar ratio of dovitinib to γCD in solid fraction obtained from all studied suspensions was between 1:1.4 and 1:1.9. For the suspension of the ternary system (drug/acid/γCD), the molar ratio of the drug to γCD was from 1:1.4 to 1:1.7. The ratio was quite similar, regardless of acid type. Moreover, the solid fraction decreased with increasing acid concentration. Thus, the proportion of liquid and solid fraction can be adjusted by varying acid concentration.

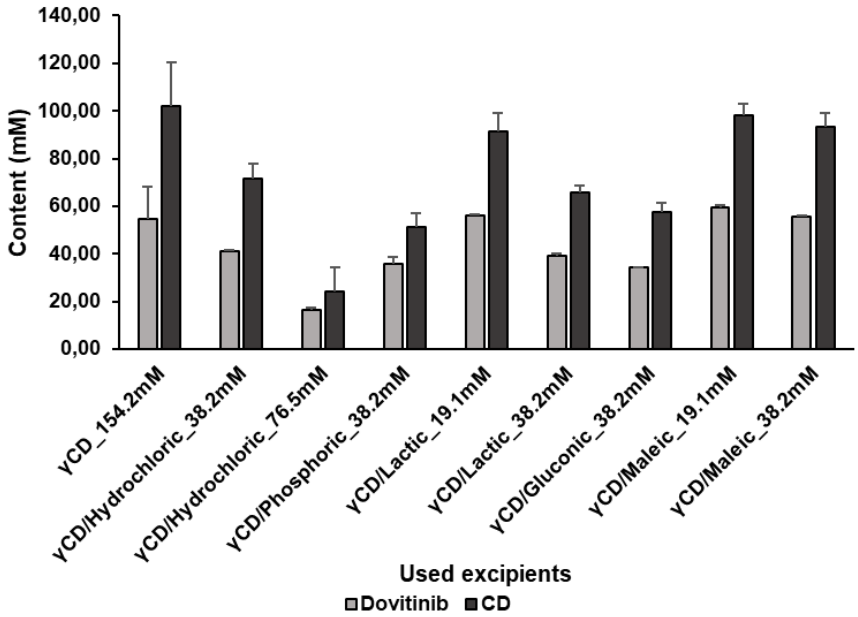

Figure 15. Dovitinib and γCD contents in solid fraction obtained from the suspensions containing dovitinib, acid, and γCD (mean ± SD, n = 3).

4.1.4.2 Particle size distribution of dovitinib/γCD aggregates

Two suspensions of 38.6 mM acid/76.5 mM dovitinib/154.2 mM γCD were selected based on different acid type and the properties, e.g., solubility enhancement, pH, stability, and physical appearance. Lactic and phosphoric acids are from different acid types. The solubility enhancement of dovitinib by

lactic and phosphoric acid when the presence of 38.6 mM γCD was similar; however, they showed the improvement with different degree of synergism based on an apparent intrinsic solubility in the corresponding acidic solution. The synergistic effect of lactic acid/γCD was smaller than that of phosphoric acid/γCD. Both systems provided comparable suspensions in terms of pH and appearance.

The aggregate size of both suspensions was quite similar (Table 8). The particle size of the suspension with phosphoric acid was a bit larger than that of the suspension with lactic acid. The aggregates had small sizes ranging between submicrons and a few microns. Most aggregate sizes of the lactic suspension were within 7 micrometers and the aggregate size of phosphoric suspension was below 8 micrometers (Table 8). Additionally, the size distribution of both samples was quite narrow with the span less than 2 and the pooled sample was homogeneous due to the reproducible particle size obtained from three sample aliquots.

Table 8. Particle size distribution of dovitinib/γCD aggregates in the suspensions containing dovitinib/lactic acid/γCD and dovitinib/phosphoric acid/γCD (mean ± SD, n = 3).

Suspension	Particle size distribution			Span
	Dv (10) (μm)	Dv (50) (μm)	Dv (90) (μm)	
Dovitinib/Lactic/γCD	0,91±0,01	3,16±0,03	6,57±0,07	1,79±0,01
Dovitinib/Phosphoric/γCD	1,16±0,01	3,88±0,06	7,58±0,09	1,65±0,00

Nonetheless, the Mastersizer 3000 can measure the particle size ranging from 0.01 μm to 3500 μm, so the dissolved aggregate of dovitinib/acid/γCD might not be determined due to dilution effect. The aggregate of dovitinib/acid/γCD in liquid fraction of the suspension, which might be in nanometer size, would dissociate immediately when pipetting to 120-mL dispersant (water) and could not be detected.

It was believed that the acid molecule only existed in liquid fraction and was involved in dovitinib/acid/γCD complex formation. The concentration of lactic and phosphoric acid used in this study was relatively low. Based on the pH-solubility studies (section 4.1.1.2), the precipitation of dovitinib salt occurs at lower pH than the apparent pH of the suspension. The previous study has proposed the dovitinib/CD/citric acid complex in aqueous media (Praphanwittaya et al., 2020). Their ^{1}H-NMR results indicated that dovitinib formed inclusion complex with γCD and its derivatives by inserting the quinolinone ring inside the CD cavity and citric acid interacted with H^{+} at the piperazine ring which protruded from the CD cavity. Hence, the results

represented the size of dovitinib/γCD aggregate in solid fraction rather than the size of dovitinib/acid/γCD aggregate in liquid fraction.

Furthermore, the size measurement showed that the microparticle of dovitinib/γCD aggregate of both lactic and phosphoric suspensions was able to dissolve upon dilution. The size of the aggregate and obscuration decreased gradually and rapidly within duplicated measurement (60 second). The aggregate size of lactic suspension reduced from initial size of 6.72 μm at the first sec to the size of 6.04 μm at 60 sec and the obscuration decreased from 12.69% to 9.64%. Similarly, the size observed in the phosphoric suspension decreased even faster. It decreased from 7.69 μm at the beginning to 5.86 μm at last. In addition, the obscuration sharply dropped almost 70% (from 14.30% to 4.45%) within 1 min. This observation implied that the spontaneous solid particles obtained during preparation of dovitinib/acid/γCD suspension are fast soluble dovitinib/γCD aggregates.

4.1.4.3 Dovitinib/γCD complexes in solid fraction by FTIR

FTIR was used to prove that the microparticles of dovitinib/γCD aggregates contain complexes of dovitinib with γCD. The FTIR spectrum provides the information of functional group and the specific bond of molecule which is obtained from the fingerprint region of the spectrum. This technique is used to identify drug/CD complex in solid state (Mura, 2015). When the compound forms complex with CDs, the difference of FTIR spectrum of the free drug and bound drug will be observed such as disappearing peak and decrease in peak intensity. FTIR spectra of dovitinib free base, γCD, physical mixture of 1:2 molar ratio of dovitinib to γCD, and solid fractions obtained from both dovitinib/lactic acid/γCD and dovitinib/phosphoric acid/γCD suspensions are illustrated in Figure 16.

The FTIR spectrum of dovitinib free base raw material showed six interesting peaks in the functional group region (4000–1500 cm^{-1}) and high intense peaks in the fingerprint region (1500–650 cm^{-1}). Two small peaks with extremely low intensity at 3507 and 3345 cm^{-1} corresponded to the stretching vibration of primary amine (NH_2) which is located at the quinolinone ring. A board peak with a little tip at 2788 cm^{-1} on elevated baseline between 3000 and 2600 cm^{-1} was a C-H stretching vibration related to the methyl group and C-H in the aromatic ring. A carbonyl group is connected to the amine group and conjugated with carbon double bond in the dovitinib molecule; consequently, the absorption of the carbonyl stretching vibration was shifted and appeared at 1634 cm^{-1}. Similarly, the adjacent peaks at 1610 and 1586 cm^{-1} represented the vibration of C=C (stretching) and N-H (bending) in aromatic rings and were affected by neighboring bond in the dovitinib molecule. The high absorption peaks at 1407 and 792 cm^{-1}

corresponded to bending vibration of the C-H bond of the methyl group and aromatic ring. While the dovitinib spectrum showed many specific vibration peaks, the γCD spectrum had fewer absorption bands including board peak from 3000 to 3600 cm^{-1} due to stretching O-H of the glucose ring, 2941 cm^{-1} due to the stretching C-H of the CH_2, and 1019 cm^{-1} due to the stretching C-O and bending C-H out-of-plane (Maksimowski & Rumianowski, 2016; Muankaew et al., 2016; Suharyani et al., 2021).

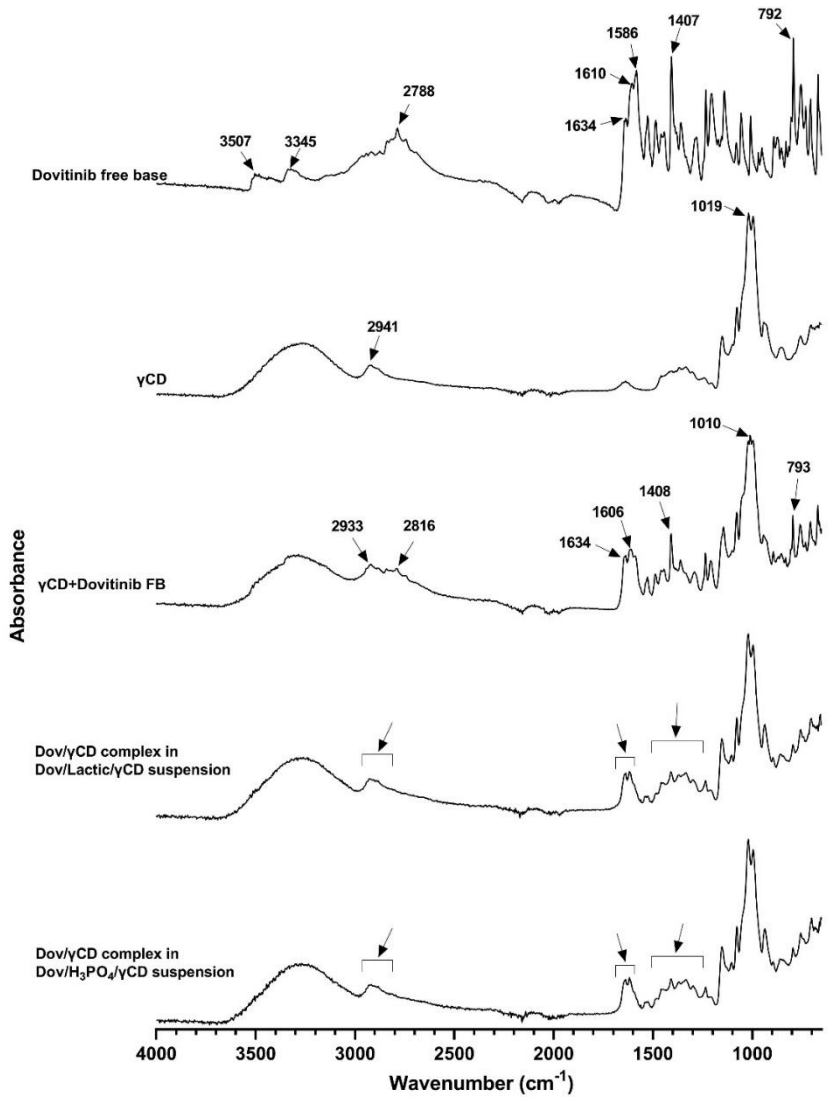

Figure 16. FTIR spectra of dovitinib free base, γCD, the physical mixture of 1:2 molar ratio of dovitinib free base to γCD, the solid fractions containing dovitinib/γCD complexes obtained from the suspension consisted of 76.5 mM dovitinib, 38.6 mM acid (lactic or phosphoric acid), and 154 mM γCD.

The physical mixture of drug and CD is used to demonstrate the mixture of two compounds without complex formation. The physical mixture of dovitinib free base and γCD was prepared by mixing dovitinib with γCD at 1:2 molar ratio of the drug to γCD in a mortar. The amount of dovitinib and γCD in the mixture was equivalent to the content of dovitinib and γCD found in the solid fraction of the suspension containing dovitinib, acid, and 154.2 mM γCD. The FTIR spectrum of the physical mixture illustrated the peaks from both dovitinib and γCD. The vibration peaks related to dovitinib were less intense than that to γCD owing to a lower amount of dovitinib in the mixture. Unlike the physical mixture spectrum, the FTIR spectrums of dovitinib/γCD aggregates obtained from both lactic and phosphoric suspensions showed characteristics of the complex with γCD. The vibration peaks with respect to dovitinib at 2788, 1586, 1407, and 792 cm^{-1} disappeared, and the peaks related to C=O and C=C stretching vibration at 1634 and 1610 cm^{-1} had exceptionally low intensity. The sample obtained from both lactic and phosphoric suspensions provided remarkably similar FTIR spectrum. This indicated that the microparticles of dovitinib/γCD aggregates contained dovitinib/γCD complexes.

Based on the results in this preformulation study, γCD can solubilize, stabilize, and encapsulate the lipophilic ionizable drug such as dovitinib. It is a versatile excipient with many functions in one formulation. The study also demonstrated how to incorporate the drug in γCD complex and how to develop γCD-based aqueous formulation. γCD successfully formulates with dovitinib and can be carrier for dovitinib. However, the capability of γCD to deliver the drug need to be further investigated.

4.2 Factors affecting drug permeation through lipophilic membrane

γCD has shown that it can increase the in-vitro permeation of lipophilic drugs through semipermeable and artificial lipophilic membranes (Jansook, Kurkov, et al., 2010; Muankaew, Jansook, & Loftsson, 2017). It also enhances drug permeation in ex-vivo experiments and drug absorption in in vivo studies (Johannsdottir et al., 2018; Lorenzo-Veiga, Diaz-Rodriguez, Alvarez-Lorenzo, Loftsson, & Sigurdsson, 2020). This is because γCD improves an aqueous solubility of lipophilic drugs and the drug concentration in UWL such as an aqueous-mucin layer of tear film (T. Loftsson, 2012). γCD function can change from one to another when different drug and excipients are present, thus the ability to enhance drug permeation through a lipophilic membrane may be affected. Besides that, are there any γCD-related factors which can

enhance or hamper the drug permeation? To better understand the effect of γCD and formulation factor on the permeability of lipophilic drugs, the in-vitro permeation studies were carried out. Two lipophilic drugs, dexamethasone and dovitinib, were used as a model drug in the studies due to the ability to form a complex with γCD and a similar molecular mass. However, they have different ionized states at desired pH ranges, i.e., pH 5 to 8. The effects of γCD, solubility, particle size etc. on drug permeation were studied using the experimental designs which simulated the UWL at ocular surface and maximized thermodynamic activity of the dissolved drugs. In an unstirred donor phase, vehicles can influence a chemical potential of drug through a fraction of the dissolved drug described with the thermodynamic activity according to Higuchi and Kunst and Lee (Flynn, Carpenter, & Yalkowsky, 1972; Higuchi, 1960; Kunst & Lee, 2016). The vehicle with an ability to increase the difference of chemical drug potential between the aqueous phase in donor chamber and the lipophilic phase of membrane will promote greater drug permeation into lipophilic membrane, and subsequently higher drug partition to the receiver phase. Therefore, the γCD effect and relevant formulation factor were discussed how they manage the lipophilic drug permeations.

4.2.1 Effects of γCD and the solubility on dexamethasone permeation

The effect of γCD on the solubility and permeability of dexamethasone was observed in this study. The solubility results showed that the overall solubility of dexamethasone increased when adding γCD to the aqueous media although the solubility of γCD decreased at relatively high concentration. Basically, the γCD has limited solubility in water or 249 mg/mL at 25°C (Sabadini, Cosgrove, & Egídio, 2006). We found that the γCD solubility was lowered to about 8.48 mM (eq. to 11 mg/mL) when dexamethasone was added to the aqueous γCD complexation medium. Consistently, adding lipophilic drugs to aqueous γCD solutions decreases its solubility to, for example, about 14 mg/mL when a steroid like hydrocortisone is added to the medium (Saokham & Loftsson, 2017).

The phase-solubility diagram of dexamethasone in the aqueous γCD solution showed B_S type characteristic with an initial linear increase in dexamethasone solubility, followed by a kind of plateau and then a decline when excess γCD is present (Figure 17A). $K_{1:1}$ of the complex formation was 13600 m^{-1} calculated from 0 to 11.6 mM of γCD. The phase-solubility study was intentionally performed by adding fixed amount of dexamethasone, i.e.,

38.2 mM to 0–154.2 mM γCD solutions in water. The fixed amount was much more than the apparent intrinsic solubility in water (0.19±0.00 mM). The initial linear increase in dexamethasone solubility happened at low γCD concentration where all added γCD is in solution, followed by a plateau where the aqueous solution is saturated with the dexamethasone/γCD complex and then an increase in dissolved γCD when all dexamethasone in the medium has formed a complex with γCD (Figure 17B). The initial linear increment indicates formation of a 1:1 dexamethasone/γCD complex. In the plateau region, the molar ratio of dissolved dexamethasone and γCD is 1.0:1.3 indicating that about 77% of the dissolved γCD molecules are forming a 1:1 complex with dexamethasone. In the last part, the decline in dexamethasone solubility was in inverse relation to the dissolved γCD in solution (Figure 17).

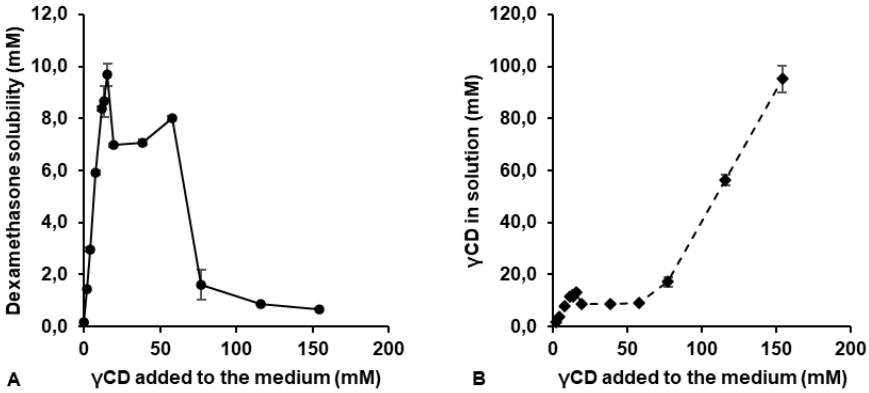

Figure 17. A: Phase-solubility diagram of dexamethasone in aqueous γCD solutions (mean ± SD), B: A plot of actual γCD dissolved in phase-solubility media versus γCD added to the media (mean ± SD).

Here the apparent $K_{1:1}$ is determined from a phase-solubility diagram where the molar concentration of dissolved dexamethasone is plotted against the molar concentration of γCD in solution. This differs from the conventional method where the molar concentration of dissolved dexamethasone is plotted against the total concentration of γCD added to the aqueous media, i.e., γCD in both solution and solid precipitate. Thus, the apparent $K_{1:1}$ was high compared with reported values on dexamethasone/γCD complexes in pure water or in aqueous eye drops at room temperature, i.e., 22–23°C (Jansook & Loftsson, 2008). The previous reported $K_{1:1}$ in pure water and in aqueous eye drops were 1210 M^{-1} and 1320 M^{-1}, respectively. In addition, formation of drug/CD complexes in aqueous media is a dynamic equilibrium process; and

thus, the different ambient conditions will affect the $K_{1:1}$ value (Brewster & Loftsson, 2007).

Permeation studies of dexamethasone were performed using six saturated solutions of dexamethasone in aqueous solutions containing 7.7, 15.4, 38.6, 57.8, 77.1, and 115.7 mM of γCD which were prepared like the solution sample in the phase-solubility study of dexamethasone. The six γCD concentrations were selected from the concentration across different regions of the phase-solubility profile. The permeation results showed that γCD increased the dexamethasone flux through the artificial lipophilic membrane with a sharp maximum at γCD concentration of 15.4 mM where the dexamethasone/γCD complex displayed maximum solubility (Figures 17 and 18A). This was followed by a sharp decrease due to the drop of the dexamethasone solubility as clearly observed when the drug flux was plotted against the concentration of dissolved γCD (Figure 18B). To clarify the decrease in the drug flux when the γCD increased, the dexamethasone flux versus the concentration of dissolve dexamethasone (Figure 18C) and the dexamethasone solubility versus the concentration of dissolved γCD (Figure 18D) were plotted. The drug flux increased when increasing the dissolved dexamethasone concentration in an unstirred donor chamber (Figure 18C), but the increase in dissolved dexamethasone was not directly proportional to the increase of dissolved γCD at relatively high added γCD-concentration (Figure 18D). The molar ratio of the dissolve dexamethasone to the dissolved γCD was 1.0:10.7 and 1.0:63.8 for 77.1 mM and 115.7 mM γCD, respectively. In other words, the dexamethasone/γCD complex precipitated out when γCD concentration was relatively high. This finding indicated that the saturated solutions of dexamethasone in the aqueous solutions containing high γCD concentrations, i.e., concentrations in the decline region of B_s-type solubility profile, had unnecessary γCD for the drug permeation or excess solubilizer. Similarly, the very soluble CD derivative, HPγCD increased the permeation of difluprednate through the same membrane type (Sripetch, Prajapati, & Loftsson, 2022). The HPγCD increased the difluprednate flux when the dissolved difluprednate and the HPγCD concentration increased. The increase of difluprednate flux with increased solubilizer concentration was found when the donor chambers contained saturated media of difluprednate in different HPγCD concentrations. The difluprednate flux dropped sharply when the donor chamber consisted of unsaturated solutions of the drug in relatively high HPγCD concentrations.

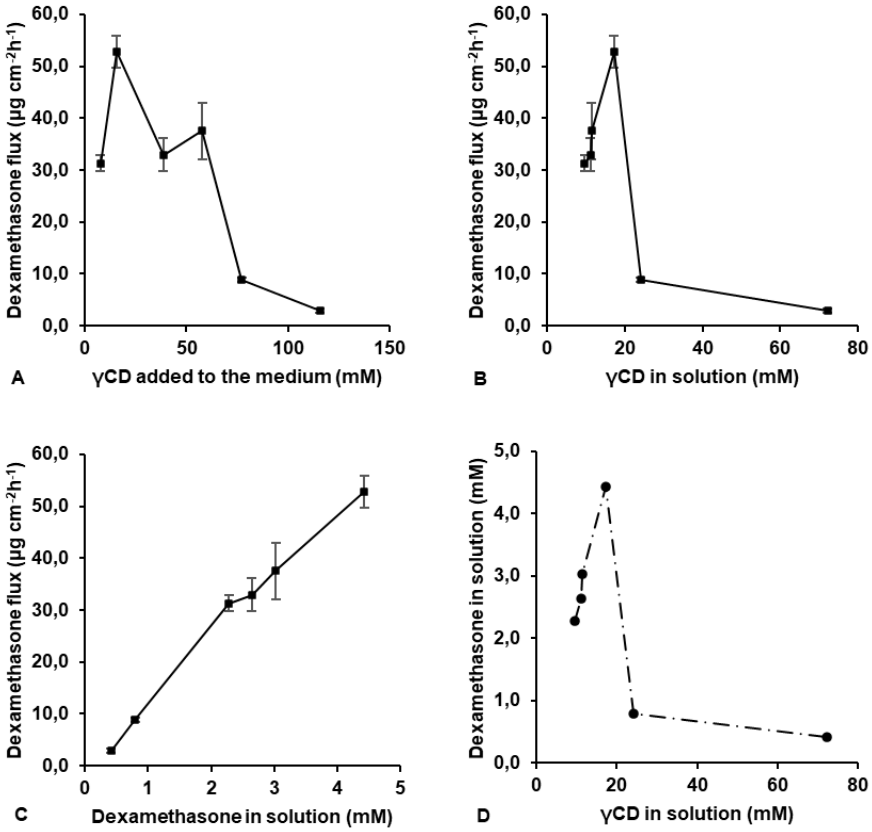

Figure 18. A: Flux of dexamethasone from the aqueous γCD media through a PermeaPad® membrane at 37°C; B: The flux plotted against the concentration of dissolved γCD, i.e., both dissolved unbound γCD and bound in a dissolved dexamethasone/γCD complex; C: The flux plotted against the concentration of dissolved dexamethasone, i.e., both apparent intrinsic solubility and dissolved bound dexamethasone/γCD complex; D: The concentration of dissolved dexamethasone in the aqueous γCD solutions plotted against the concentration of dissolved γCD in the aqueous γCD solutions. The data points represent the mean ± SD (n = 3–5).

The thermodynamic activity of the dissolved drug in a saturated solution, assumed to be maximum and constant among different solvent concentrations, is a factor contributing to the ability of drug partition from the exterior aqueous layer to the lipophilic membrane. The observation of dexamethasone-saturated aqueous solution containing high γCD concentration suggested elaborated assumption to the thermodynamic activity issue that is maximum drug flux will obtain when both the thermodynamic activity and concentration of the drug are at their maximum

value. Therefore, the consideration of the thermodynamic activity of the drug in the system like γCD should not be presumed based on the saturated condition for the entire range of solubilizer concentration.

As we know, γCD tends to form self-aggregate structure which is concentration dependent (Thorsteinn Loftsson, 2014). The self-assemble behavior is also found when the γCD forms complexes with lipophilic drugs and consequent nano or micro particles of γCD/drug complex aggregates exist (Thorsteinn Loftsson, Saokham, & Sá Couto, 2019). This behavior might appear in the excess γCD in the dexamethasone/γCD aqueous solution at relatively high γCD concentration and could contribute to the decrease in dexamethasone flux. The self-assemble nanoparticles of drug/γCD complexes were also studied and discussed in the following section.

4.2.2 Effect of γCD-based nanoparticles on dovitinib permeation

The dovitinib permeation through the artificial lipophilic membrane demonstrated the effect of γCD-related factor on the drug flux and permeation coefficient. Due to extremely limited solubility of its free base, dovitinib is marketed as the more water-soluble dovitinib lactate. Table 9 shows the dovitinib flux from three different aqueous solutions. One sample was an aqueous dovitinib lactate solution containing equivalent to 33.0 mM of dovitinib free base at pH 5.65. This is close to a saturated solution of the drug. Other two samples were saturated solutions of the dovitinib free base. The former was an equivalent composition of dovitinib, lactic acid, and γCD, and the latter close to an equivalent composition of dovitinib, phosphoric acid, and γCD. Despite similar concentrations of dissolved dovitinib, and similar thermodynamic activity, i.e., all three solutions were close to being saturated with the drug, the dovitinib flux through the lipophilic membrane was fastest from the pure dovitinib lactate solution but slowest from the dovitinib-saturated solution containing phosphoric acid (Table 9). Similarly, the P_{app} from highest to lowest value was of dovitinib lactate solution, dovitinib-saturated aqueous γCD solution containing lactic acid, and dovitinib-saturated aqueous γCD solution containing phosphoric acid. Thus, the differences in the drug flux and permeation coefficient must be due to some other differences in the donor media. Because the natural γCD and its complexes have a high tendency to self-assemble to form nano and microparticles (Thorsteinn Loftsson et al., 2005). Thus, the nano-size analyzer was used to detect nanoparticles with diameter from 10 to 1000 nm in the aqueous solution studied. No nanoparticles were detected in the aqueous dovitinib lactate solution, but the other two solutions contained high concentrations of nanoparticles (Table 10). Only free dovitinib molecules permeate the lipophilic membrane (Thorsteinn Loftsson et al., 2005); and

therefore, formation of nanoparticles can explain the low drug flux from the two γCD aqueous solution compared with the dovitinib solution and why the solution with more numerous large particles provides slower flux than the one with less numerous and smaller particles.

Besides the physiochemical properties of lipophilic drugs, the formulation factor which is resulted by the drug and excipients used also play a significant role in drug permeation. Here γCD can enhance or hamper the drug permeation through lipophilic membrane by different mechanism, and its effect is concentration dependent.

Table 9. The steady state flux (J_{ss}) and apparent permeability coefficient (P_{app}) of dovitinib from an unsaturated aqueous solution of dovitinib lactate and saturated solutions of dovitinib free base in aqueous 38.6 mM γCD solution through artificial lipophilic membrane at 37°C (mean ± SD, n = 3-5).

Sample	**Initial dovitinib concentration**		**pH**[a]	**J_{ss} ± SD** ($\mu g\ cm^{-2}\ h^{-1}$)	**P_{app} ± SD**[b] (cm/h)
	mg/mL	mM			
Dovitinib lactate solution in water	12.95	33.0	5.65	28.0 ± 1.3	2.16 ± 0.10 ($x10^{-3}$)
Saturate solution of dovitinib free base in aqueous solution containing 38.6 mM lactic acid and 38.6 mM γCD	12.81	32.6	6.48	19.2 ± 2.7	1.50 ± 0.21 ($x10^{-3}$)
Saturate solution of dovitinib free base in aqueous solution containing 38.6 mM phosphoric acid and 38.6 mM γCD	15.74	40.1	6.20	10.5 ± 1.3	0.67 ± 0.08 ($x10^{-3}$)

[a]Measured at room temperature (20–22 °C).
[b]Calculated from the flux and the initial total concentration of dissolved drug according to equation 9.

Table 10. Size distribution and concentration of nanoparticles in three dovitinib aqueous solutions (mean ± SD, n = 5).

Sample	**Mean diameter ± SD** (nm)			**Concentration** (particles/mL)
	D10	D50	D90	
Dovitinib lactate solution in water	-	-	-	~0
Saturate solution of dovitinib free base in aqueous solution containing 38.6 mM lactic acid and 38.6 mM γCD	157.7 ± 3.3	223.6 ± 5.1	386.2 ± 5.7	2.98 ± 0.13 ($x10^{8}$)
Saturate solution of dovitinib free base in aqueous solution containing 38.6 mM phosphoric acid and 38.6 mM γCD	152.9 ± 5.9	281.4 ± 8.8	421.9 ± 6.5	3.44 ± 0.22 ($x10^{8}$)

4.3 Study of drug release from γCD-based drug carrier

The preformulation and permeation studies of dovitinib and dexamethasone have shown how to incorporate the drug in γCD-based carrier and how the γCD-based carrier manages the drug permeation. We know that only free drug molecule can permeate into the lipophilic membrane. Before this, the drug must leave the CD cavity. γCD has been reported that it can be hydrolyzed faster when α-amylase enzyme is present, but guest molecules such as lipophilic drug can hamper the reaction (Lumholdt et al., 2012). Therefore, due to the α-amylase was found in tear fluid, that might affect a γCD-based drug carrier in delivering a drug to the ocular epithelium. This study focused on what happened to the drug in aqueous-mucin layer when the α-amylase was present. The experiment was designed to investigate the effect of α-amylase on drug release under the condition simulating tear pH and ocular surface temperature. To determine the specific effect precisely, a vertical Franz diffusion cell with a semipermeable membrane was used instead of complicated setup such as small volume of artificial tear with a lipophilic membrane. The simplified setup also included the test solution which was saturated solutions of dexamethasone in HEPES buffer solutions containing different γCD concentrations. The dexamethasone was dissolved in the γCD aqueous buffer solution pH 7.4 (34°C) to simulate when the dexamethasone/γCD complex is topically delivered to the ocular surface. The test solution was prepared and characterized by phase-solubility technique and the α-amylase enzyme function was checked under the test condition before the drug release experiment.

4.3.1 Solubility of dexamethasone in HEPES buffer

Phase-solubility diagram of dexamethasone and γCD in 20 mM HEPES buffer pH 7.4 (34°C) containing 140 mM NaCl, 2 mM $CaCl_2$ (Figures 19) was similar to that in water. The γCD affinity for dexamethasone under the test condition in this study ($K_{1:1}$ = 12887 M^{-1}) was a bit lower than that in water in the section 4.2.1 ($K_{1:1}$ = 13600 m^{-1}). A maximum dexamethasone solubility in the buffer solution at 34±1 °C was at 32 mM γCD. It has been well known that CD complex formation is a dynamic equilibrium process and affected by temperature and pH (Brewster & Loftsson, 2007). Thus, such difference was observed. The effect of buffer, temperature, and pH did not change the pattern of phase-solubility diagram of dexamethasone/γCD complexes. That means the γCD can still improve aqueous solubility of dexamethasone at relatively low γCD concentration even in the presence of an organic salt and some electrolytes.

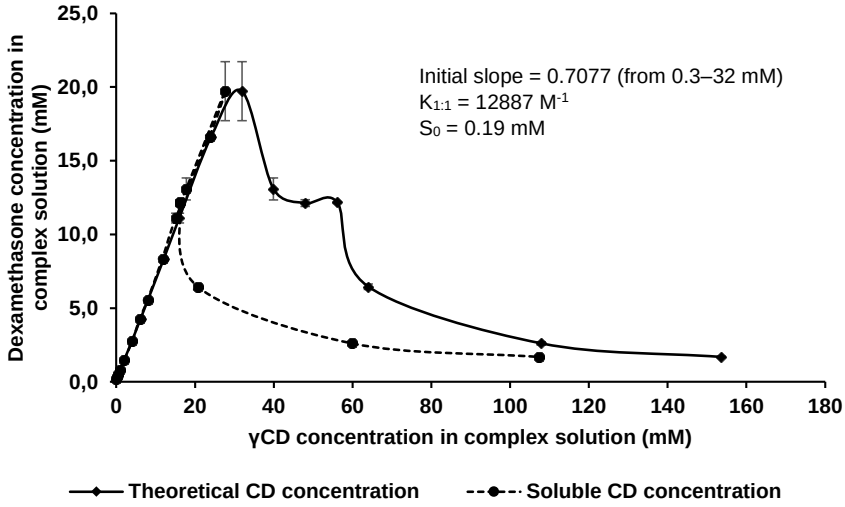

Figure 19. Phase-solubility diagram of dexamethasone and γCD in 20 mM HEPES buffer pH 7.4 containing 140 mM NaCl and 2 mM $CaCl_2$ at 34±1°C.

4.3.2 Degradation of γCD

The α-amylase enzyme catalyzes the hydrolysis of γCD through formation of an α-amylase/γCD complex. When the γCD molecule has been cleaved by α-amylase maltotriose, maltose or glucose are produced afterward via a multiple attack mechanism, that is, α-amylase randomly binds to another γCD molecule or intermediate oligosaccharides (Kondo et al., 1990). PPA was used in this study owing to lack of commercial α-amylase from tear fluid. K_m and V_{max} of this enzyme, under the described test conditions, were determined to be 3.24±0.23 mM and 0.00979±0.00037 mM/min, respectively (Figure 20).

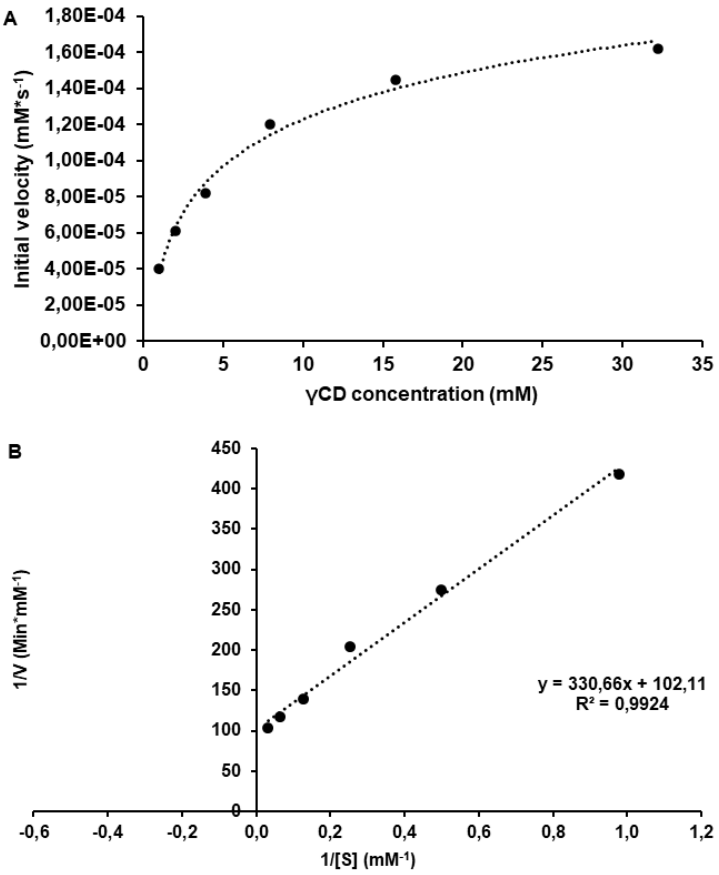

Figure 20. Plots of γCD degradation when no drug was present; A: Michaelis-Menten plot, B: Lineweaver-Burk plot.

The K_m was higher, and V_{max} was lower than those reported by Lumholdt et al. (2012) investigating γCD degradation under conditions that mimic intestinal fluid (pH 6.5, 37°C). Lumholdt et al. (2012) found that the K_m was 0.54±0.07 mM, and the V_{max} was 17.01±3.11 mM/min. The enzyme activity is very sensitive to many factors such as pH, temperature, substrate and enzyme concentrations, substrate type, and coenzyme. (Bisswanger, 2014). Consequently, its catalytic activity will be affected by the test condition (Kazuhiko Ishikawa, Matsui, Honda, Kobayashi, & Nakatani, 1991).

Furthermore, the apparent optimum pH and temperature for PPA depends on the type of substrate. It has been stated in the supplier´s certificate of analysis that the optimum pH and temperature for 1% starch are pH 6.9 and 45°C, respectively. However, the maximum activity of PPA is at pH 7.0

(Anitha Gopal & Muralikrishna, 2009). For γCD hydrolysis, the optimum pH for k_{cat} was shifted to pH 5.2 (at 30°C) and the turnover number, which depends on pH, was about 17 s^{-1} (Ishikawa, Matsui, Honda, & Nakatani, 1990). Ishikawa et al. (1990) found a deviation around pH 7 and a slower catalytic rate when pH increased. They obtained k_{cat} between 3 and 5 s^{-1} at pH 7–7.5. In this study, the initial hydrolysis of γCD was determined by monitoring the disappearance of γCD at a certain time point for 6 hours (Figure 21A). The present k_{cat} was 853 s^{-1} calculated using equation (5) where enzyme concentration was approximately 191 nM and the PPA´s molecular mass was 51–54 kD according to the manufacturer´s certificate of analysis. Under the present conditions, PPA had a higher turnover number than what Ishikawa et al. (1990) found but lower than what Lumholdt et al. (2012) reported (1668 s^{-1}). Lumholdt et al. (2012) determined hydrolytic rate by monitoring formation of reducing-end product, i.e., maltose, while here we monitored the disappearance of γCD. Based on the multiple attack mechanism of PPA (Robyt & French, 1967), quantitation of the reducing-end product reflected all hydrolysis including γCD ring-opening and repetitive digestion of linear oligosaccharides. Consequently, the rate values will depend on the method used to monitor the degradation process.

Figure 21 shows that the PPA catalyzed γCD hydrolysis in solutions containing dexamethasone/γCD complexes was slower than that in solutions containing pure γCD. For the dexamethasone-free media, the percentage of γCD degradation after 6 hours was determined to be 54.5, 44.3, 33.5, 24.3, 15.5, and 10.8% at γCD concentration of 1, 2, 4, 8, 16 and 32 mM, respectively. Whereas, for the dexamethasone-containing media (containing dexamethasone/γCD complexes) the percent of γCD degraded after 6 hours was determined to be 11.0% for the 1 mM γCD solution and less than 10% for 2 to 32 mM γCD solutions. The degradation of free γCD under the present studied condition was about half that observed by Kondo et al. (1990) at 37°C, 50 nM of PPA and 6.18 mM γCD in 50 mM sodium glycerophosphate buffer pH 6.9 containing 25 mM NaCl. In addition, the present results are lower than those of Lumholdt et al. (2012). The initial velocity of PPA catalysis of γCD degradation when unoccupied γCD increased with increasing γCD concentration up to γCD concentration of about 8 mM or 1 % w/v (Figure 20A). The initial degradation rates gradually decreased from 14.04 to 5.45% remaining of γCD per hour when γCD concentration increased from 1 to 8 mM (Figure 22A), while the initial degradation rate of γCD in complex solution was exceptionally low and did not depend on the total concentration of γCD (Figure 21B). The highest rate was observed in the

dexamethasone complex solution containing 1 mM γCD showing 2.33% remaining of γCD per hour (Figure 22A). The degradation studies illustrate that formation of dexamethasone/γCD complex prevented the PPA-catalyzed γCD hydrolysis.

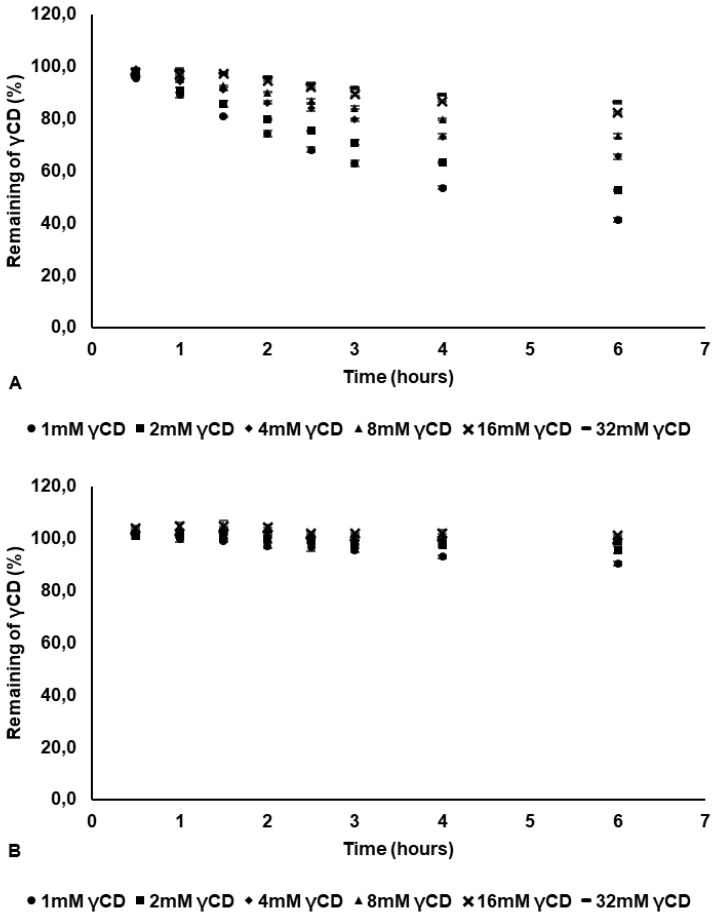

Figure 21. A: Degradation profiles of pure γCD solution, B: Degradation of γCD in the solution containing dexamethasone/γCD complex where γCD concentration varied from 1 to 32 mM, Each point is the mean ± SD (n = 3).

Although only free γCD is degraded by PPA, we observed some γCD degradation in dilute dexamethasone/γCD complex solutions, i.e., 1–8 mM γCD, under the present condition. That was due to the presence of free γCD in the solutions. The drug-saturated γCD solutions contained not only dissolved drug/γCD complex but also some free drug and unbound γCD

(Schönbeck, Madsen, Peters, Holm, & Loftsson, 2017). The phase-solubility study showed that the necessary dexamethasone concentration to saturate 1 mM γCD solution was 0.8 mM. Thus, only about 0.6 mM of dexamethasone will be in a complex calculated from the apparent intrinsic solubility (0.2 mM, see Figure 19). Based on the $K_{1:1}$, the estimated γCD in the complex is approximately 0.6 mM but the rest, i.e., 0.4 mM, is free. The amount of free γCD in the complex media will remain essentially constant (about 32–39% of soluble free γCD compared with added γCD) in the dexamethasone-saturated γCD solution evaluated, although the concentration of dexamethasone/γCD complex will increase with increasing γCD concentration.

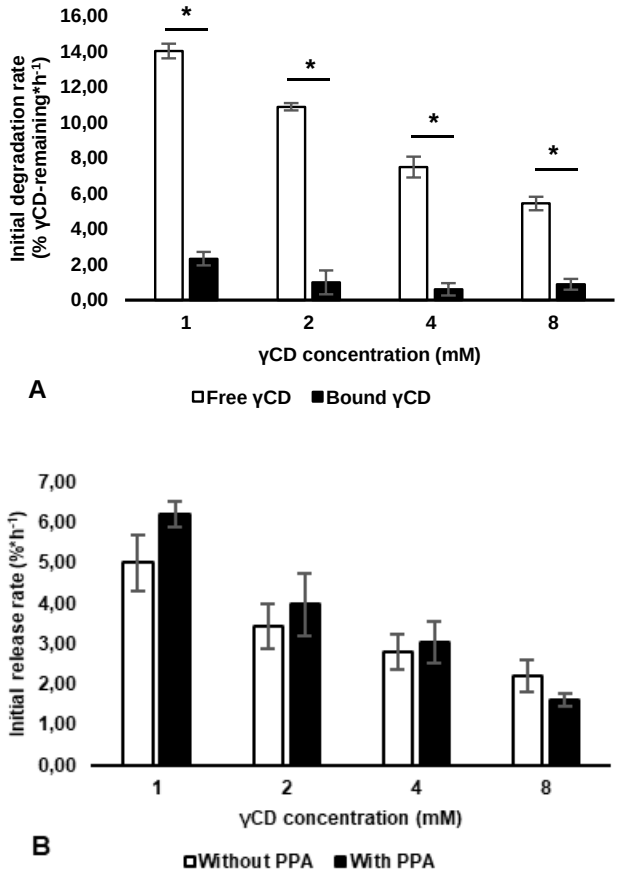

Figure 22. A: Degradation rate of free γCD and bound γCD; B: Release rate of dexamethasone from complex solution without PPA and with PPA; Data shown is the mean ± SD (n = 3).

4.3.3 The effect of dilution and α-amylase on dexamethasone release from γCD-based carrier

As mentioned earlier, in an aqueous drug/CD complex solution, the complex is in a dynamic equilibrium where the complex constantly associates and dissociates. No covalent bonds involve in the complex formation (Brewster & Loftsson, 2007). In the aqueous complex solutions, free γCD is degraded by PPA and subsequently its concentration decreases. This should shift the complex equilibrium and promote drug release from the complex. Thus, it has been hypothesized that the presence of PPA in the complexation media would enhance dexamethasone release from the dexamethasone/γCD complex. Consequently, the dexamethasone bioavailability will be enhanced by aqueous γCD solutions. To test that hypothesis, the dexamethasone flux and permeation coefficient of dexamethasone from media containing the dexamethasone/γCD complex were determined, both in the presence and absence of PPA. The dexamethasone permeation profiles (Figure 23) from solutions containing 1 to 8 mM of γCD illustrate that the percentage of dexamethasone that permeated through the artificial membrane over 6 hours was inversely proportional to the initial γCD concentration. The dexamethasone contents after 6 hours in the receiver compartment were approximately 30, 20, 15, and 10% for 1, 2, 4 and 8 mM of γCD, respectively. The final concentration of dexamethasone in complex solution (or test solution in the donor chamber) was kept at 95% of saturation of the initial drug concentration. Therefore, thermodynamic activity of dexamethasone was identical in all complex solutions tested. The permeation of dexamethasone was slower from the solutions containing higher γCD concentration than that from solutions containing lower γCD concentration (Figure 23). The apparent permeation coefficients showed that γCD was more efficient in delivery of dexamethasone when γCD concentration was low (Figure 24B). The results agreed with the fact that media dilution is the main mechanism of drug release from CD complexes and the fact that in aqueous CD solutions the fraction of drug bound to CD decreases with decreasing CD concentration (Stella et al., 1999). On the contrary, within the studied range of γCD concentrations, i.e., 1–8 mM, the total dexamethasone flux increased when γCD concentration increased and PPA was absent (Figure 24A). The greater solubility of dexamethasone due to higher γCD concentration contributed to total flux increase because both free drug and drug/γCD complex which has combined MW less than 5 kD can permeate the semipermeable membrane. However, that was not observed in the 8 mM γCD solution containing PPA. When PPA was present in the donor, the total

dexamethasone flux rose in 1, 2 and 4 mM γCD complex solutions and then dropped in the 8 mM γCD solution. Self-assembly of drug/γCD complexes was considered to have caused the decrease in flux of 8 mM γCD solution when PPA was present. However, particle size analysis using dynamic light scattering technique showed no particles larger than 1.3 nm from all γCD concentrations solution tested. The size measurement was performed at 34°C after filtration through 0.45 µm RC filter and incubation at 34°C for 3, 6, and 9 hours to represent the condition of the drug/γCD complexes solution in the donor compartment. That might because the fraction of small aggregates, less than 5 kD, was extraordinarily little. In other words, most dexamethasone/γCD complexes in this test solution were in monomer or dimer form. A previous study on self-aggregation of free γCD and hydrocortisone/γCD complexes using Slide-A-Lyzer™ MINI Dialysis units reported the critical aggregation concentration of both free γCD and hydrocortisone/γCD complex were 0.93 % w/v or 7.17 mM (Saokham, Sá Couto, Ryzhakov, & Loftsson, 2016). This study differed from the previous study in terms of the drug, the analytical technique, temperature, sample preparation, additives, and storage time. High temperature, electrolytes such as NaCl, filtration and high pH affect the self-aggregation of γCD (Messner, Kurkov, Palazón, et al., 2011; Puskás, Schrott, Malanga, & Szente, 2013; Szente, Szejtli, & Kis, 1998). The factor of self-assembly of γCD and drug/γCD complexes was not excluded from contributing factors to the dropping flux at 8 mM γCD when PPA was present. However, self-aggregation was not the dominant factor in this circumstance. Concentration of enzyme and affinity of dexamethasone to γCD can also be involved in the decrease of permeation. The equilibrium of drug and γCD in buffer media was lost when PPA was present. PPA was added immediately before transferring to the donor chamber and starting permeation studies. The concentration of PPA was equal in all γCD concentrations, whereas free γCD in all γCD concentration was approximate 35%. This means higher γCD concentrations would have more substrates for enzymes. Therefore, the transient increase of free dexamethasone in the donor compartment of the complex solution with higher γCD concentration did not occur as rapidly as that with lower γCD concentration. The rising of free dexamethasone in 8 mM γCD solution was insufficient for increase in driving force for drug diffusion through membrane within the studied time-period. Moreover, the high affinity of γCD for dexamethasone based on phase-solubility data might induce reformation of dexamethasone/γCD complexes in the donor compartment rather than permeation or precipitation. The observation in donor compartment after stopping permeation did not see solid appearance.

Although the mechanism of drug release was unclear, this result indicated that a negative effect on drug permeation when PPA was present at high γCD concentrations. The permeation results for complex solutions containing 1, 2 and 4 mM γCD showed that dexamethasone was released faster when PPA was present than when absent (Figure 22B and Figure 23). The highest drug release rate was observed from the 1 mM γCD complex solution, that is, at the lowest γCD concentration used in this study. This revealed the additive effect of PPA and dilution on drug release.

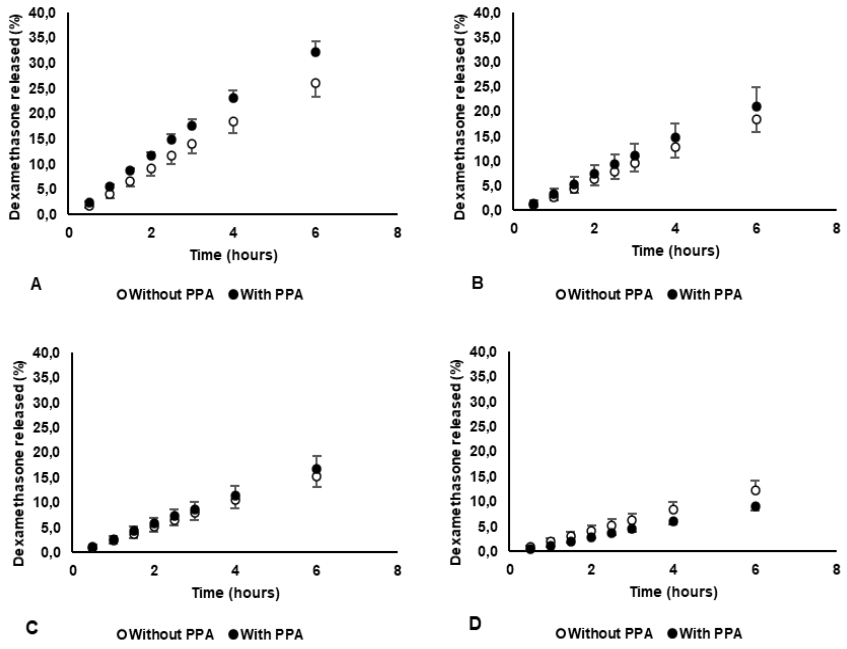

Figure 23. Permeation profiles of dexamethasone/γCD complex solution with PPA and without PPA; A: 1 mM γCD; B: 2 mM γCD; C: 4 mM γCD; D: 8 mM γCD. Data point represented as mean ± SD (n = 3).

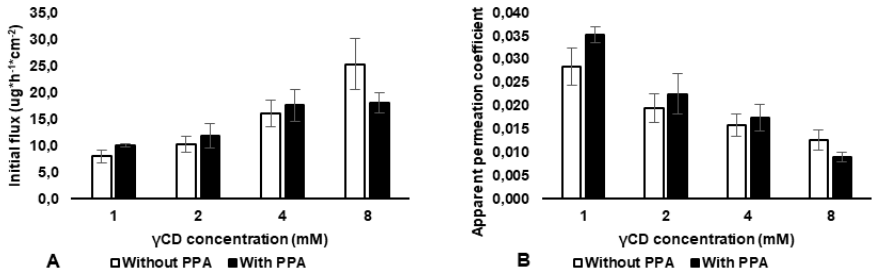

Figure 24. A: Total dexamethasone flux of dexamethasone/γCD complex solution without PPA and with PPA; B: apparent permeation coefficient of dexamethasone/γCD complex solution without PPA and with PPA; Data showed is the mean ± SD (n = 3).

The findings from all studies suggest that γCD is an enabling excipient for ocular drug delivery. It can carry a lipophilic drug within its hydrophobic cavity and self-assemble particle. When an ophthalmic formulation containing drug loaded in γCD-based carrier is applied to the eye the aqueous-mucin layer of tear film is saturated with the dissolved drug and γCD. The gradient of chemical potential with respect to the dissolved drug will promote the drug permeation to intraocular tissues. Although the self-assemble microparticles of the drug/γCD complexes will be removed from ocular surface rapidly, drug-saturated tear film would act as a reservoir and the tear α-amylase could accelerate drug release from the dissolved drug/γCD complexes resulting in a transient supersaturation of the drug and consequently faster absorption of the drug to the eyes.

5 Summary and conclusions

This dissertation focused on the application of γCD as a drug carrier for topical administration to the eyes. The investigation of γCD application for ocular drug delivery covered three topics as follows: preformulation study, the effect of γCD on drug permeation and the study of drug release from a γCD-based drug carrier. First, the preformulation study was the study of complex formation with γCD and developing γCD-based drug carrier using dovitinib as a representative of poorly water-soluble and ionizable basic drugs. The physicochemical properties of the dovitinib including water solubility, lipophilicity, and stability were also investigated with γCD and other pharmaceutical excipients during the development. After the optimization, the γCD-based carrier was successful in incorporating dovitinib as much as desired. In addition, the γCD-based carrier for dovitinib was able to switch between solution and suspension by adjusting γCD and counterion concentration. Second, the γCD effect on drug permeation and formulation factor affecting drug permeation through lipophilic membrane were examined. The study was conducted in the in-vitro Franz diffusion cell equipped with an artificial lipophilic membrane to simulate the drug permeation from UWL to the lipophilic part of the biological membrane. The effects of γCD and solubility were evaluated using several dexamethasone-saturated aqueous solutions containing different γCD concentration, whereas the formulation factor, i.e., self-assembled γCD nanoparticles was assessed regarding their impact on dovitinib permeation. Third, the study of dexamethasone release from a γCD-based carrier in the presence of PPA was performed under the simulated condition of tear pH and ocular surface temperature. The degradation of γCD with or without complexation with dexamethasone by enzymatic reaction provided the kinetic information of the PPA under the described condition. Then a drug release test in the presence and absence of the α-amylase enzyme was determined and explained. All mentioned studies made these following observations:

- The γCD formed an inclusion complex with dovitinib free base and provided good affinity for dovitinib. However, the aqueous solubility of dovitinib/γCD complexes was lower than that of salt formation with counterions.
- Screening of salt formation was carried out by titration of acid solution

with a solid dovitinib base. This experimental design provided pH-solubility profiles that did not follow theoretical profile of a basic drug. The acidic counterions with suitable pK_a, that comprised about 2 to 3 of pH unit differences between acid and base, showed very high enhancement of water solubility of the dovitinib. The hydroxy acids, i.e., lactic and gluconic acid, dramatically increased the aqueous solubility of dovitinib without lowering final pH of the solution. The extreme solubility of dovitinib in hydroxy acid solutions was because of supersaturation of ionized dovitinib.

- The improved aqueous solubility of dovitinib with combined techniques of γCD complexation and ionization by acidic counterion showed great results and produced an unexpected effect. At low concentration of γCD, the ternary system of dovitinib/acid/γCD increased the aqueous solubility of dovitinib beyond the solubility in a binary system (acid/drug or γCD/drug). Lactic, phosphoric, and maleic acid contributed synergistic enhancement with γCD at all levels of acid concentration. For the high concentration of γCD, the acid dissolved more dovitinib and dovitinib/γCD complexes with increasing acid concentration. Consequently, less solid fraction was found at relatively high concentrations of acid. The increase in water solubility of dovitinib depended on acid type, acid concentration, and γCD concentration. However, the excess of acid could cause dovitinib degradation.
- The ternary system of dovitinib/acid/γCD is readily alterable. The system can become a solution or suspension when changing acid and γCD concentration. Drug loading can be increased and decreased with optimizing only two excipients. The final pH is also adjustable by choosing acid type and concentration.
- The solid fraction of spontaneous suspension of dovitinib/acid/γCD contained dovitinib and γCD and was found that to have more γCD content than dovitinib content. The suspension of the ternary system obtained from lactic and phosphoric acids contained self-assembled microparticles of dovitinib/γCD complexes. Moreover, both solution and suspension of the dovitinib ternary-system contained self-assembled particles in nano or micrometer size range.
- The experimental log D values of dovitinib differed from the calculated values; however, the curve of the experimented log D was quite similar to that of the calculated log D. The experimental log D curve

shifted upward compared with the calculated one. It indicated that dovitinib has a suitable lipophilicity for permeation through a lipophilic membrane. The pH was the major factor influencing the distribution coefficient of dovitinib. The counterions can affect the log D value of the ionized dovitinib but produce a negligible effect on the log D value of the unionized drug.

- The accelerated degradation of dovitinib was performed at high temperatures including 40±2 °C and 75±2 °C. The stability was investigated across a range of pH 2 to 8, three buffer species, and in the presence of two CDs, γCD and HPγCD. Dovitinib was most stable at pH 4 in phosphate buffer, and γCD showed a stabilizing effect. At relatively low pH, the stabilizing effect of γCD was more dominant than the effect of buffer species.
- The solubility of dexamethasone, another model drug in this study, in water and HEPES buffer pH 7.4 (34 °C) revealed that the medium composition and temperature affected the complex formation of unionized lipophilic drug with γCD. Furthermore, the deviation of $K_{1:1}$ and CE values between the studies was due to many factors, for example, intrinsic solubility value, analytical method, calculation method.
- γCD enhanced the drug flux through the artificial lipophilic membrane in the in-vitro vertical Franz diffusion cell. The enhancement of drug permeation was because of the increase in drug aqueous solubility. Based on dexamethasone permeation, the flux increased with increasing dissolved dexamethasone and γCD until reaching the highest concentration of dissolved dexamethasone. The dexamethasone flux decreased sharply afterward where the dissolved γCD was in excess. It indicated that the highest flux obtained when both thermodynamic activity of the drug and the soluble drug concentration reached maximum.
- According to dovitinib permeation, the formulation factor, i.e., self-assembled nanoparticles, hampered drug permeation and decreased both drug flux and permeability coefficient although the thermodynamic activity and the dissolved concentration of the drug was at maximum.
- The hydrolysis of γCD was catalyzed by the α-amylase enzyme, but the complex formation with a lipophilic drug such as dexamethasone,

could prevent the enzyme catalysis. In addition, the degradation rate of pure γCD depended on the γCD concentration, enzyme activity, and studied condition.

- The release of dexamethasone from the γCD-based carrier was faster when the γCD concentration was lower. It indicated that drug/γCD complex dissociated upon dilution. The presence of α-amylase enzyme with aqueous solutions of dexamethasone/γCD complexes promoted the drug release from the γCD-based carrier. This suggested that the faster release of dexamethasone at relatively low concentrations of γCD was due to the additive effect of dilution and α-amylase catalysis.

To conclude, the results have shown that γCD can form a complex with poorly water-soluble drugs and consequently improve aqueous solubility of the drug. It exhibits functional flexibility as an excipient depending on its concentration and the presence of additives. The γCD-based drug carrier can enhance or hamper the drug permeation through the lipophilic membrane. Both opposite effects resulted from formulation characteristics. Also, the media dilution and presence of α-amylase enzyme constitutes an additive driving force of the drug release from the γCD-based carrier under simulated tear conditions. All of these suggest that γCD can be used as a drug carrier for topical drug delivery to the eyes. This topic can be further investigated regarding the interaction between γCD, acid, and dovitinib in a solution with outstanding effect of solubilization for better understanding. The promising ternary system could be developed into aqueous eye drops and further tested in animal model. Lastly, various permeation setups should be used to elucidate the mechanism of drug release from the γCD-based carrier and driving force of drug partition from external aqueous-mucin layer into the next lipophilic membrane.

References

Abelson, M. B., Udell, I. J., & Weston, J. H. (1981). Normal Human Tear pH by Direct Measurement. *Archives of Ophthalmology, 99*(2), 301-301. doi:10.1001/archopht.1981.03930010303017

Agrahari, V., Mandal, A., Agrahari, V., Trinh, H. M., Joseph, M., Ray, A., . . . Mitra, A. K. (2016). A comprehensive insight on ocular pharmacokinetics. *Drug Delivery and Translational Research, 6*(6), 735-754. doi:10.1007/s13346-016-0339-2

Anderson, J. A., & Leopold, I. H. (1979). Enzymatic Activities Found in Human Tears. In O. Hockwin & W. B. Rathbun (Eds.), *Progress in Anterior Eye Segment Research and Practice: Volume in Honour of Prof. John E. Harris, Ph. D., M. D.* (pp. 333-340). Dordrecht: Springer Netherlands.

Angevin, E., Lopez-Martin, J. A., Lin, C.-C., Gschwend, J. E., Harzstark, A., Castellano, D., . . . Escudier, B. (2013). Phase I Study of Dovitinib (TKI258), an Oral FGFR, VEGFR, and PDGFR Inhibitor, in Advanced or Metastatic Renal Cell Carcinoma. *Clinical Cancer Research, 19*(5), 1257-1268. doi:10.1158/1078-0432.Ccr-12-2885

Anitha Gopal, B., & Muralikrishna, G. (2009). Porcine Pancreatic α-Amylase and its Isoforms: Purification and Kinetic Studies. *International Journal of Food Properties, 12*(3), 571-586. doi:10.1080/10942910801947755

Armstrong, R. A., & Cubbidge, R. P. (2014). Chapter 1 - The Eye and Vision: An Overview. In V. R. Preedy (Ed.), *Handbook of Nutrition, Diet and the Eye* (pp. 3-9). San Diego: Academic Press.

Augusteyn, R. C., Nankivil, D., Mohamed, A., Maceo, B., Pierre, F., & Parel, J.-M. (2012). Human ocular biometry. *Experimental Eye Research, 102*, 70-75. doi:https://doi.org/10.1016/j.exer.2012.06.009

Bachu, R. D., Chowdhury, P., Al-Saedi, Z. H. F., Karla, P. K., & Boddu, S. H. S. (2018). Ocular Drug Delivery Barriers—Role of Nanocarriers in the Treatment of Anterior Segment Ocular Diseases. *Pharmaceutics, 10*(1), 28. Retrieved from https://www.mdpi.com/1999-4923/10/1/28

Berg, J. M., Tymoczko, J. L., & Stryer, L. (2002). *The Michaelis-Menten Model Accounts for the Kinetic Properties of Many Enzymes*.

Bisswanger, H. (2014). Enzyme assays. *Perspectives in Science, 1*(1), 41-55. doi:https://doi.org/10.1016/j.pisc.2014.02.005

Brewster, M. E., & Loftsson, T. (2007). Cyclodextrins as pharmaceutical solubilizers. *Advanced Drug Delivery Reviews, 59*(7), 645-666. doi:https://doi.org/10.1016/j.addr.2007.05.012

Chang, A. Y., & Purt, B. (2022). Biochemistry, Tear Film. In *StatPearls*. Treasure Island (FL): StatPearls Publishing

Copyright © 2022, StatPearls Publishing LLC.

Cholkar, K., Dasari, S. R., Pal, D., & Mitra, A. K. (2013). 1 - Eye: anatomy, physiology and barriers to drug delivery. In A. K. Mitra (Ed.), *Ocular Transporters and Receptors* (pp. 1-36): Woodhead Publishing.

Coles, W. H., & Jaros, P. A. (1984). Dynamics of ocular surface pH. *Br J Ophthalmol, 68*(8), 549-552. doi:10.1136/bjo.68.8.549

Comer, J. E. A., & Tam, K. Y. (2007). *Lipophilicity Profiles: Theory and Measurement*.

Das, M., Padda, S. K., Frymoyer, A., Zhou, L., Riess, J. W., Neal, J. W., & Wakelee, H. A. (2015). Dovitinib and erlotinib in patients with metastatic non-small cell lung cancer: A drug–drug interaction. *Lung Cancer, 89*(3), 280-286. doi:https://doi.org/10.1016/j.lungcan.2015.06.011

Delamere, N. A. (2005). Ciliary Body and Ciliary Epithelium. In J. Fischbarg (Ed.), *Advances in Organ Biology* (Vol. 10, pp. 127-148): Elsevier.

Diebold, Y., & García-Posadas, L. (2021). Is the Conjunctiva a Potential Target for Advanced Therapy Medicinal Products? *Pharmaceutics, 13*(8). doi:10.3390/pharmaceutics13081140

Fautsch, M. P., Johnson, D. H., & Group, t. S. A. P. R. I. W. (2006). Aqueous Humor Outflow: What Do We Know? Where Will It Lead Us? *Investigative Ophthalmology & Visual Science, 47*(10), 4181-4187. doi:10.1167/iovs.06-0830

Flynn, G. L., Carpenter, O. S., & Yalkowsky, S. H. (1972). Total Mathematical Resolution of Diffusion Layer Control of Barrier Flux. *Journal of Pharmaceutical Sciences, 61*(2), 312-314. doi:https://doi.org/10.1002/jps.2600610248

Furuishi, T., Takahashi, S., Ogawa, N., Gunji, M., Nagase, H., Suzuki, T., . . . Tomono, K. (2017). Enhanced dissolution and skin permeation profiles of epalrestat with β-cyclodextrin derivatives using a cogrinding method. *European Journal of Pharmaceutical Sciences, 106*, 79-86. doi:https://doi.org/10.1016/j.ejps.2017.05.047

Galloway, N. R., Amoaku, W. M. K., Galloway, P. H., & Browning, A. C. (2016). Basic Anatomy and Physiology of the Eye. In *Common Eye Diseases and their Management* (pp. 7-16). Cham: Springer International Publishing.

Gaudana, R., Ananthula, H. K., Parenky, A., & Mitra, A. K. (2010). Ocular Drug Delivery. *The AAPS Journal, 12*(3), 348-360. doi:10.1208/s12248-010-9183-3

Goel, M., Picciani, R. G., Lee, R. K., & Bhattacharya, S. K. (2010). Aqueous humor dynamics: a review. *The open ophthalmology journal, 4*, 52-59. doi:10.2174/1874364101004010052

Gordon, D. M. (1960). USE OF DEXAMETHASONE IN EYE DISEASE. *Journal of the American Medical Association, 172*(4), 311-312. doi:10.1001/jama.1960.03020040009003

Gote, V., Sikder, S., Sicotte, J., & Pal, D. (2019). Ocular Drug Delivery: Present Innovations and Future Challenges. *Journal of Pharmacology and Experimental Therapeutics, 370*(3), 602-624. doi:10.1124/jpet.119.256933

Gould, P. L. (1986). Salt selection for basic drugs. *International Journal of Pharmaceutics, 33*(1), 201-217. doi:https://doi.org/10.1016/0378-5173(86)90055-4

Harangi, J., Béke, G., Harangi, M., & Mótyán, J. A. (2012). The digestable parent cyclodextrin. *Journal of Inclusion Phenomena and Macrocyclic Chemistry, 73*(1), 335-339. doi:10.1007/s10847-011-0061-0

Higuchi, T. (1960). *Physical Chemical analysis of Percutaneous Absorption Process from Creams and Ointments*.

Higuchi, T., & Connors, K. A. (1965). A phase solubility technique. *Adv. Anal. Chem. Instrum., 4*, 117-211.

Hosoya, K.-i., Lee, V. H. L., & Kim, K.-J. (2005). Roles of the conjunctiva in ocular drug delivery: a review of conjunctival transport mechanisms and their regulation. *European Journal of Pharmaceutics and Biopharmaceutics, 60*(2), 227-240. doi:https://doi.org/10.1016/j.ejpb.2004.12.007

Ishikawa, K., Matsui, I., Honda, K., Kobayashi, S., & Nakatani, H. (1991). The pH dependence of the action pattern in porcine pancreatic α-amylase-catalyzed reaction for maltooligosaccharide substrates. *Archives of Biochemistry and Biophysics, 289*(1), 124-129. doi:https://doi.org/10.1016/0003-9861(91)90451-N

Ishikawa, K., Matsui, I., Honda, K., & Nakatani, H. (1990). Substrate-dependent shift of optimum pH in porcine pancreatic alpha-amylase-catalyzed reactions. *Biochemistry, 29*(30), 7119-7123. doi:10.1021/bi00482a025

Jansook, P., Hnin, H. M., Praphanwittaya, P., Loftsson, T., & Stefansson, E. (2022). Effect of salt formation on γ-cyclodextrin solubilization of irbesartan and candesartan and the chemical stability of their ternary complexes. *Journal of Drug Delivery Science and Technology, 67*, 102980. doi:https://doi.org/10.1016/j.jddst.2021.102980

Jansook, P., Kurkov, S. V., & Loftsson, T. (2010). Cyclodextrins as solubilizers: Formation of complex aggregates. *Journal of Pharmaceutical Sciences, 99*(2), 719-729. doi:https://doi.org/10.1002/jps.21861

Jansook, P., & Loftsson, T. (2008). γCD/HPγCD: Synergistic solubilization. *International Journal of Pharmaceutics, 363*(1), 217-219. doi:https://doi.org/10.1016/j.ijpharm.2008.07.011

Jansook, P., & Loftsson, T. (2009). CDs as solubilizers: Effects of excipients and competing drugs. *International Journal of Pharmaceutics, 379*(1), 32-40. doi:https://doi.org/10.1016/j.ijpharm.2009.06.005

Jansook, P., & Loftsson, T. (2022). Self-assembled γ-cyclodextrin as nanocarriers for enhanced ocular drug bioavailability. *International Journal of Pharmaceutics, 618*, 121654. doi:https://doi.org/10.1016/j.ijpharm.2022.121654

Jansook, P., Ogawa, N., & Loftsson, T. (2018). Cyclodextrins: structure, physicochemical properties and pharmaceutical applications. *International Journal of Pharmaceutics, 535*(1), 272-284. doi:https://doi.org/10.1016/j.ijpharm.2017.11.018

Jansook, P., Prajapati, M., Pruksakorn, P., & Loftsson, T. (2020). Antifungal activity of econazole nitrate/cyclodextrin complex: Effect of pH and formation of complex aggregates. *International Journal of Pharmaceutics, 574*, 118896. doi:https://doi.org/10.1016/j.ijpharm.2019.118896

Jansook, P., Praphanwittaya, P., Sripetch, S., & Loftsson, T. (2020). Solubilization and in vitro permeation of dovitinib/cyclodextrin complexes and their aggregates. *Journal of Inclusion Phenomena and Macrocyclic Chemistry, 97*(3), 195-203. doi:10.1007/s10847-020-00995-y

Jansook, P., Ritthidej, G. C., Ueda, H., Stefánsson, E., & Loftsson, T. (2010). γCD/HPγCD Mixtures as Solubilizer: Solid-State Characterization and Sample Dexamethasone Eye Drop Suspension. *Journal of Pharmacy & Pharmaceutical Sciences, 13*(3), 336-350. doi:10.18433/J3M88B

Joensuu, H., Blay, J.-Y., Comandone, A., Martin-Broto, J., Fumagalli, E., Grignani, G., . . . Le Cesne, A. (2017). Dovitinib in patients with gastrointestinal stromal tumour refractory and/or intolerant to imatinib. *British Journal of Cancer, 117*(9), 1278-1285. doi:10.1038/bjc.2017.290

Jóhannesson, G., Moya-Ortega, M. D., Asgrímsdóttir, G. M., Agnarsson, B. A., Lund, S. H., Loftsson, T., & Stefánsson, E. (2014). Dorzolamide cyclodextrin nanoparticle suspension eye drops and Trusopt in rabbit. *J Ocul Pharmacol Ther, 30*(6), 464-467. doi:10.1089/jop.2013.0164

Jóhannesson, G., Moya-Ortega, M. D., Ásgrímsdóttir, G. M., Lund, S. H., Thorsteinsdóttir, M., Loftsson, T., & Stefánsson, E. (2014). Kinetics of γ-cyclodextrin nanoparticle suspension eye drops in tear fluid. *Acta Ophthalmologica, 92*(6), 550-556. doi:https://doi.org/10.1111/aos.12334

Johannsdottir, S., Jansook, P., Stefansson, E., Kristinsdottir, I. M., Fulop, Z., Asgrimsdottir, G. M., . . . Loftsson, T. (2018). Topical drug delivery to the posterior segment of the eye: Dexamethasone concentrations in various eye tissues after topical administration for up to 15 days to rabbits. *Journal of Drug Delivery Science and Technology, 45*, 449-454. doi:https://doi.org/10.1016/j.jddst.2018.04.007

Jóhannsdóttir, S., Jansook, P., Stefánsson, E., & Loftsson, T. (2015). Development of a cyclodextrin-based aqueous cyclosporin A eye drop formulations. *International Journal of Pharmaceutics, 493*(1), 86-95. doi:https://doi.org/10.1016/j.ijpharm.2015.07.040

Joussen, A. M., Wolf, S., Kaiser, P. K., Boyer, D., Schmelter, T., Sandbrink, R., . . . Boettger, M. K. (2019). The Developing Regorafenib Eye drops for neovascular Age-related Macular degeneration (DREAM) study: an open-label phase II trial. *Br J Clin Pharmacol, 85*(2), 347-355. doi:10.1111/bcp.13794

Kels, B. D., Grzybowski, A., & Grant-Kels, J. M. (2015). Human ocular anatomy. *Clinics in Dermatology, 33*(2), 140-146. doi:https://doi.org/10.1016/j.clindermatol.2014.10.006

Kim, H. M., & Woo, S. J. (2021). Ocular Drug Delivery to the Retina: Current Innovations and Future Perspectives. *Pharmaceutics, 13*(1), 108. Retrieved from https://www.mdpi.com/1999-4923/13/1/108

Kim, K. B., Chesney, J., Robinson, D., Gardner, H., Shi, M. M., & Kirkwood, J. M. (2011). Phase I/II and Pharmacodynamic Study of Dovitinib (TKI258), an Inhibitor of Fibroblast Growth Factor Receptors and VEGF Receptors, in Patients with Advanced Melanoma. *Clinical Cancer Research, 17*(23), 7451-7461. doi:10.1158/1078-0432.Ccr-11-1747

King-Smith, P. E., Fink, B. A., Fogt, N., Nichols, K. K., Hill, R. M., & Wilson, G. S. (2000). The Thickness of the Human Precorneal Tear Film: Evidence from Reflection Spectra. *Investigative Ophthalmology & Visual Science, 41*(11), 3348-3359.

Kondo, H., Nakatani, H., & Hiromi, K. (1990). In vitro action of human and porcine α-amylases on cyclomalto-oligosaccharides. *Carbohydrate Research, 204*, 207-213. doi:https://doi.org/10.1016/0008-6215(90)84036-T

Konrádsdóttir, F., Ogmundsdóttir, H., Sigurdsson, V., & Loftsson, T. (2009). Drug targeting to the hair follicles: a cyclodextrin-based drug delivery. *AAPS PharmSciTech, 10*(1), 266-269. doi:10.1208/s12249-009-9205-6

Ku, M. S. (2008). Use of the Biopharmaceutical Classification System in early drug development. *The AAPS Journal, 10*(1), 208-212. doi:10.1208/s12248-008-9020-0

Kunst, A., & Lee, G. (2016). Release and Skin Permeation of Scopolamine From Thin Polymer Films in Relation to Thermodynamic Activity. *Journal of Pharmaceutical Sciences, 105*(4), 1496-1500. doi:https://doi.org/10.1016/j.xphs.2016.02.004

Kurkov, S. V., & Loftsson, T. (2013). Cyclodextrins. *International Journal of Pharmaceutics, 453*(1), 167-180. doi:https://doi.org/10.1016/j.ijpharm.2012.06.055

Lipinski, C. A. (2000). Drug-like properties and the causes of poor solubility and poor permeability. *Journal of Pharmacological and Toxicological Methods, 44*(1), 235-249. doi:https://doi.org/10.1016/S1056-8719(00)00107-6

Lipinski, C. A., Lombardo, F., Dominy, B. W., & Feeney, P. J. (1997). Experimental and computational approaches to estimate solubility and permeability in drug discovery and development settings. *Advanced Drug Delivery Reviews, 23*(1), 3-25. doi:https://doi.org/10.1016/S0169-409X(96)00423-1

Löbenberg, R., & Amidon, G. L. (2000). Modern bioavailability, bioequivalence and biopharmaceutics classification system. New scientific approaches to international regulatory standards. *European Journal of Pharmaceutics and Biopharmaceutics, 50*(1), 3-12. doi:https://doi.org/10.1016/S0939-6411(00)00091-6

Loftsson, T. (2012). Drug permeation through biomembranes: cyclodextrins and the unstirred water layer. *Pharmazie, 67*(5), 363-370.

Loftsson, T. (2014). Self-assembled cyclodextrin nanoparticles and drug delivery. *Journal of Inclusion Phenomena and Macrocyclic Chemistry, 80*(1), 1-7. doi:10.1007/s10847-013-0375-1

Loftsson, T., & Brewster, M. E. (2012). Cyclodextrins as Functional Excipients: Methods to Enhance Complexation Efficiency. *Journal of Pharmaceutical Sciences, 101*(9), 3019-3032. doi:https://doi.org/10.1002/jps.23077

Loftsson, T., Jarho, P., Másson, M., & Järvinen, T. (2005). Cyclodextrins in drug delivery. *Expert Opinion on Drug Delivery, 2*(2), 335-351. doi:10.1517/17425247.2.1.335

Loftsson, T., Moya-Ortega, M. D., Alvarez-Lorenzo, C., & Concheiro, A. (2015). Pharmacokinetics of cyclodextrins and drugs after oral and parenteral administration of drug/cyclodextrin complexes. *Journal of Pharmacy and Pharmacology, 68*(5), 544-555. doi:10.1111/jphp.12427

Loftsson, T., Saokham, P., & Sá Couto, A. R. (2019). Self-association of cyclodextrins and cyclodextrin complexes in aqueous solutions. *International Journal of Pharmaceutics, 560*, 228-234. doi:https://doi.org/10.1016/j.ijpharm.2019.02.004

Loftsson, T., & Stefánsson, E. (2022). Aqueous eye drops containing drug/cyclodextrin nanoparticles deliver therapeutic drug concentrations to both anterior and posterior segment. *Acta Ophthalmologica, 100*(1), 7-25. doi:https://doi.org/10.1111/aos.14861

Lorenzo-Veiga, B., Diaz-Rodriguez, P., Alvarez-Lorenzo, C., Loftsson, T., & Sigurdsson, H. H. (2020). In Vitro and Ex Vivo Evaluation of Nepafenac-Based Cyclodextrin Microparticles for Treatment of Eye Inflammation. *Nanomaterials, 10*(4), 709. Retrieved from https://www.mdpi.com/2079-4991/10/4/709

Lumholdt, L. R., Holm, R., Jørgensen, E. B., & Larsen, K. L. (2012). In vitro investigations of α-amylase mediated hydrolysis of cyclodextrins in the presence of ibuprofen, flurbiprofen, or benzo[a]pyrene. *Carbohydrate Research, 362*, 56-61. doi:https://doi.org/10.1016/j.carres.2012.09.018

M9 Biopharmaceutics classification system-based biowaiver. (2021). The international council for harmonisation of technical requirements for pharmaceuticals for human use Retrieved from https://www.fda.gov/regulatory-information/search-fda-guidance-documents/m9-biopharmaceutics-classification-system-based-biowaivers

Maksimowski, P., & Rumianowski, T. (2016). Properties of the gamma-cyclodextrin/CL-20 system. *Central European Journal of Energetic Materials, 13*(1), 217--229.

Mannermaa, E., Vellonen, K.-S., & Urtti, A. (2006). Drug transport in corneal epithelium and blood–retina barrier: Emerging role of transporters in ocular pharmacokinetics. *Advanced Drug Delivery Reviews, 58*(11), 1136-1163. doi:https://doi.org/10.1016/j.addr.2006.07.024

Martola, E.-L., & Baum, J. L. (1968). Central and Peripheral Corneal Thickness: A Clinical Study. *Archives of Ophthalmology, 79*(1), 28-30. doi:10.1001/archopht.1968.03850040030009

Másson, M., Karlsson, F. J., Valdimarsdóttir, M., Magnúsdóttir, K., & Loftsson, T. (2007). Cyclodextrins and the liquid-liquid phase distribution of progesterone, estrone and prednicarbate. *Journal of Inclusion Phenomena and Macrocyclic Chemistry, 57*(1), 481-487. doi:10.1007/s10847-006-9238-3

McDermott, A. M. (2013). Antimicrobial compounds in tears. *Experimental Eye Research, 117*, 53-61. doi:https://doi.org/10.1016/j.exer.2013.07.014

Messner, M., Kurkov, S. V., Brewster, M. E., Jansook, P., & Loftsson, T. (2011). Self-assembly of cyclodextrin complexes: Aggregation of hydrocortisone/cyclodextrin complexes. *International Journal of Pharmaceutics, 407*(1), 174-183. doi:https://doi.org/10.1016/j.ijpharm.2011.01.011

Messner, M., Kurkov, S. V., Palazón, M. M., Fernández, B. Á., Brewster, M. E., & Loftsson, T. (2011). Self-assembly of cyclodextrin complexes: Effect of temperature, agitation and media composition on aggregation. *International Journal of Pharmaceutics, 419*(1), 322-328. doi:https://doi.org/10.1016/j.ijpharm.2011.07.041

Mishima, S., Gasset, A., Klyce, S. D., Jr., & Baum, J. L. (1966). Determination of Tear Volume and Tear Flow. *Investigative Ophthalmology & Visual Science, 5*(3), 264-276.

Mochizuki, T., & Masai, I. (2014). The lens equator: A platform for molecular machinery that regulates the switch from cell proliferation to differentiation in the vertebrate lens. *Development, Growth & Differentiation, 56*(5), 387-401. doi:10.1111/dgd.12128

Morrison, P. W., & Khutoryanskiy, V. V. (2014). Advances in ophthalmic drug delivery. *Ther Deliv, 5*(12), 1297-1315. doi:10.4155/tde.14.75

Motzer, R. J., Porta, C., Vogelzang, N. J., Sternberg, C. N., Szczylik, C., Zolnierek, J., . . . Escudier, B. (2014). Dovitinib versus sorafenib for third-line targeted treatment of patients with metastatic renal cell carcinoma: an open-label, randomised phase 3 trial. *The Lancet Oncology, 15*(3), 286-296. doi:https://doi.org/10.1016/S1470-2045(14)70030-0

Muankaew, C., Jansook, P., & Loftsson, T. (2017). Evaluation of γ-cyclodextrin effect on permeation of lipophilic drugs: application of cellophane/fused octanol membrane. *Pharmaceutical Development and Technology, 22*(4), 562-570. doi:10.1080/10837450.2016.1180394

Muankaew, C., Jansook, P., Sigurđsson, H. H., & Loftsson, T. (2016). Cyclodextrin-based telmisartan ophthalmic suspension: Formulation development for water-insoluble drugs. *International Journal of Pharmaceutics, 507*(1), 21-31. doi:https://doi.org/10.1016/j.ijpharm.2016.04.071

Muankaew, C., Jansook, P., Stefánsson, E., & Loftsson, T. (2014). Effect of γ-cyclodextrin on solubilization and complexation of irbesartan: Influence of pH and excipients. *International Journal of Pharmaceutics, 474*(1), 80-90. doi:https://doi.org/10.1016/j.ijpharm.2014.08.013

Mura, P. (2015). Analytical techniques for characterization of cyclodextrin complexes in the solid state: A review. *Journal of Pharmaceutical and Biomedical Analysis, 113*, 226-238. doi:https://doi.org/10.1016/j.jpba.2015.01.058

Musolino, A., Campone, M., Neven, P., Denduluri, N., Barrios, C. H., Cortes, J., . . . André, F. (2017). Phase II, randomized, placebo-controlled study of dovitinib in combination with fulvestrant in postmenopausal patients with HR+, HER2− breast cancer that had progressed during or after prior endocrine therapy. *Breast Cancer Research, 19*(1), 18. doi:10.1186/s13058-017-0807-8

Nayak, K., & Misra, M. (2018). A review on recent drug delivery systems for posterior segment of eye. *Biomedicine & Pharmacotherapy, 107*, 1564-1582. doi:https://doi.org/10.1016/j.biopha.2018.08.138

Ohira, A., Hara, K., Jóhannesson, G., Tanito, M., Ásgrímsdóttir, G. M., Lund, S. H., . . . Stefánsson, E. (2015). Topical dexamethasone γ-cyclodextrin nanoparticle eye drops increase visual acuity and decrease macular thickness in diabetic macular oedema. *Acta Ophthalmologica, 93*(7), 610-615. doi:https://doi.org/10.1111/aos.12803

Ohtani, Y., Irie, T., Uekama, K., Fukunaga, K., & Pitha, J. (1989). Differential effects of α-, β- and γ-cyclodextrins on human erythrocytes. *European Journal of Biochemistry, 186*(1-2), 17-22. doi:https://doi.org/10.1111/j.1432-1033.1989.tb15171.x

Okhamafe, A., Chou, J., Gullapalli, R., Harwood, E., Ryckman, D., Zhu, S., & Shang, X. (2005). W. I. P. Organization.

Pei, Y. F., & Rhodin, J. A. (1971). Electron microscopic study of the development of the mouse corneal epithelium. *Invest Ophthalmol, 10*(11), 811-825.

Pflugfelder, S. C., & Stern, M. E. (2020). Biological functions of tear film. *Experimental Eye Research, 197*, 108115. doi:https://doi.org/10.1016/j.exer.2020.108115

Popielec, A., Agnes, M., Yannakopoulou, K., Fenyvesi, É., & Loftsson, T. (2018). Self-assembled cyclodextrin-based nanoparticles for meropenem stabilization. *Journal of Drug Delivery Science and Technology, 45*, 20-27. doi:https://doi.org/10.1016/j.jddst.2018.02.018

Prajapati, M., Christensen, G., Paquet-Durand, F., & Loftsson, T. (2021). Cytotoxicity of β-Cyclodextrins in Retinal Explants for Intravitreal Drug Formulations. *Molecules (Basel, Switzerland), 26*(5), 1492. doi:10.3390/molecules26051492

Prajapati, M., & Loftsson, T. (2022). Stabilization and solubilization of difluprednate in aqueous cyclodextrin solution and its characterization for ophthalmic delivery. *Journal of Drug Delivery Science and Technology, 69*, 103106. doi:https://doi.org/10.1016/j.jddst.2022.103106

Praphanwittaya, P., Jansook, P., & Loftsson, T. (2020). Aqueous solubility of kinase inhibitors: III the effect of acidic counter ion on the dovitinib/γ-cyclodextrin complexation. *Journal of Inclusion Phenomena and Macrocyclic Chemistry, 98*(1), 57-67. doi:10.1007/s10847-020-01009-7

Puskás, I., Schrott, M., Malanga, M., & Szente, L. (2013). Characterization and control of the aggregation behavior of cyclodextrins. *Journal of Inclusion Phenomena and Macrocyclic Chemistry, 75*(3), 269-276. doi:10.1007/s10847-012-0127-7

Regenxbio. RGX-314 Subretinal. Retrieved from https://www.regenxbio.com/therapeutic-programs/

Reinstein, D. Z., Archer, T. J., Gobbe, M., Silverman, R. H., & Coleman, D. J. (2009). Stromal Thickness in the Normal Cornea: Three-Dimensional Display with Artemis Very High-Frequency Digital Ultrasound. *Journal of Refractive Surgery, 25*(9), 776-786. doi:doi:10.3928/1081597X-20090813-04

Robyt, J. F., & French, D. (1967). Multiple attack hypothesis of α-amylase action: Action of porcine pancreatic, human salivary, and Aspergillus oryzae α-amylases. *Archives of Biochemistry and Biophysics, 122*(1), 8-16. doi:https://doi.org/10.1016/0003-9861(67)90118-X

Rolando, M., & Zierhut, M. (2001). The Ocular Surface and Tear Film and Their Dysfunction in Dry Eye Disease. *Survey of Ophthalmology, 45*, S203-S210. doi:https://doi.org/10.1016/S0039-6257(00)00203-4

Ruan, X., Liu, Z., Luo, L., & Liu, Y. (2020). Structure of the lens and its associations with the visual quality. *BMJ Open Ophthalmology, 5*(1), e000459. doi:10.1136/bmjophth-2020-000459

Rüfer, F., Schröder, A., & Erb, C. (2005). White-to-white corneal diameter: normal values in healthy humans obtained with the Orbscan II topography system. *Cornea, 24*(3), 259-261. doi:10.1097/01.ico.0000148312.01805.53

Sabadini, E., Cosgrove, T., & Egídio, F. d. C. (2006). Solubility of cyclomaltooligosaccharides (cyclodextrins) in H2O and D2O: a comparative study. *Carbohydrate Research, 341*(2), 270-274. doi:https://doi.org/10.1016/j.carres.2005.11.004

Saokham, P., & Loftsson, T. (2017). γ-Cyclodextrin. *International Journal of Pharmaceutics, 516*(1), 278-292. doi:https://doi.org/10.1016/j.ijpharm.2016.10.062

Saokham, P., Sá Couto, A., Ryzhakov, A., & Loftsson, T. (2016). The self-assemble of natural cyclodextrins in aqueous solutions: Application of miniature permeation studies for critical aggregation concentration (cac) determinations. *International Journal of Pharmaceutics, 505*(1), 187-193. doi:https://doi.org/10.1016/j.ijpharm.2016.03.049

Schäfer, N., Gielen, G. H., Kebir, S., Wieland, A., Till, A., Mack, F., . . . Glas, M. (2016). Phase I trial of dovitinib (TKI258) in recurrent glioblastoma. *Journal of Cancer Research and Clinical Oncology, 142*(7), 1581-1589. doi:10.1007/s00432-016-2161-0

Schönbeck, C., Madsen, T. L., Peters, G. H., Holm, R., & Loftsson, T. (2017). Soluble 1:1 complexes and insoluble 3:2 complexes – Understanding the phase-solubility diagram of hydrocortisone and γ-cyclodextrin. *International Journal of Pharmaceutics, 531*(2), 504-511. doi:https://doi.org/10.1016/j.ijpharm.2017.05.024

SciFinder. (2022). SciFinder. Retrieved from https://scifinder-n.cas.org. https://scifinder-n.cas.org

Serajuddin, A. T. M., & Mufson, D. (1985). pH-Solubility Profiles of Organic Bases and Their Hydrochloride Salts. *Pharmaceutical Research, 2*(2), 65-68. doi:10.1023/A:1016382426347

Serajuddin, A. T. M., & Rosoff, M. (1984). pH-Solubility Profile of Papaverine Hydrochloride and Its Relationship to the Dissolution Rate of Sustained-Release Pellets. *Journal of Pharmaceutical Sciences, 73*(9), 1203-1208. doi:https://doi.org/10.1002/jps.2600730905

Shirasaki, Y. (2008). Molecular Design for Enhancement of Ocular Penetration. *Journal of Pharmaceutical Sciences, 97*(7), 2462-2496. doi:https://doi.org/10.1002/jps.21200

Soe, H. M. S. H., Sripetch, S., Loftsson, T., Stefánsson, E., & Jansook, P. (2022). Effect of Soluplus® on γ-cyclodextrin solubilization of irbesartan and candesartan and their nanoaggregates formation. *Pharmaceutical Development and Technology, 27*(1), 9-18. doi:10.1080/10837450.2021.2017968

Sripetch, S., & Loftsson, T. (2021). Topical drug delivery to the posterior segment of the eye: Thermodynamic considerations. *International Journal of Pharmaceutics, 597*, 120332. doi:https://doi.org/10.1016/j.ijpharm.2021.120332

Sripetch, S., Prajapati, M., & Loftsson, T. (2022). Cyclodextrins and Drug Membrane Permeation: Thermodynamic Considerations. *Journal of Pharmaceutical Sciences, 111, 2571-2580*. doi:https://doi.org/10.1016/j.xphs.2022.04.015

Stella, V. J., Rao, V. M., Zannou, E. A., & Zia, V. (1999). Mechanisms of drug release from cyclodextrin complexes. *Advanced Drug Delivery Reviews, 36*(1), 3-16. doi:https://doi.org/10.1016/S0169-409X(98)00052-0

Subrizi, A., del Amo, E. M., Korzhikov-Vlakh, V., Tennikova, T., Ruponen, M., & Urtti, A. (2019). Design principles of ocular drug delivery systems: importance of drug payload, release rate, and material properties. *Drug Discovery Today, 24*(8), 1446-1457. doi:https://doi.org/10.1016/j.drudis.2019.02.001

Suharyani, I., Muchtaridi, M., Mohammed, A. F. A., Elamin, K. M., Wathoni, N., & Abdassah, M. (2021). α-Mangostin/γ-Cyclodextrin Inclusion Complex: Formation and Thermodynamic Study. *Polymers, 13*(17), 2890. Retrieved from https://www.mdpi.com/2073-4360/13/17/2890

Svitova, T. F., & Lin, M. C. (2016). Dynamic interfacial properties of human tear-lipid films and their interactions with model-tear proteins in vitro. *Advances in Colloid and Interface Science, 233*, 4-24. doi:https://doi.org/10.1016/j.cis.2015.12.009

Szente, L., Szejtli, J., & Kis, G. L. (1998). Spontaneous Opalescence of Aqueous γ-Cyclodextrin Solutions: Complex Formation or Self-Aggregation? *Journal of Pharmaceutical Sciences, 87*(6), 778-781. doi:https://doi.org/10.1021/js9704341

Tanito, M., Hara, K., Takai, Y., Matsuoka, Y., Nishimura, N., Jansook, P., . . . Ohira, A. (2011). Topical Dexamethasone-Cyclodextrin Microparticle Eye Drops for Diabetic Macular Edema. *Investigative Ophthalmology & Visual Science, 52*(11), 7944-7948. doi:10.1167/iovs.11-8178

Tiffany, J. M. (2008). The normal tear film. *Dev Ophthalmol, 41*, 1-20. doi:10.1159/000131066

Urtti, A. (2006). Challenges and obstacles of ocular pharmacokinetics and drug delivery. *Advanced Drug Delivery Reviews, 58*(11), 1131-1135. doi:https://doi.org/10.1016/j.addr.2006.07.027

van Haeringen, N. J., Ensink, F., & Glasius, E. (1975). Amylase in human tear fluid: Origin and characteristics, compared with salivary and urinary amylases. *Experimental Eye Research, 21*(4), 395-403. doi:https://doi.org/10.1016/0014-4835(75)90049-4

Varela-Fernández, R., Díaz-Tomé, V., Luaces-Rodríguez, A., Conde-Penedo, A., García-Otero, X., Luzardo-Álvarez, A., . . . Otero-Espinar, F. J. (2020). Drug Delivery to the Posterior Segment of the Eye: Biopharmaceutic and Pharmacokinetic Considerations. *Pharmaceutics, 12*(3), 269. Retrieved from https://www.mdpi.com/1999-4923/12/3/269

Wanko, T., Lloyd, B. J., Jr, & Matthews, J. (1964). The Fine Structure of Human Conjunctiva in the Perilimbal Zone. *Investigative Ophthalmology & Visual Science, 3*(3), 285-301.

Watsky, M. A., Jablonski, M. M., & Edelhauser, H. F. (1988). Comparison of conjunctival and corneal surface areas in rabbit and human. *Current Eye Research, 7*(5), 483-486. doi:10.3109/02713688809031801

Willoughby, C. E., Ponzin, D., Ferrari, S., Lobo, A., Landau, K., & Omidi, Y. (2010). Anatomy and physiology of the human eye: effects of mucopolysaccharidoses disease on structure and function – a review. *Clinical & Experimental Ophthalmology, 38*(s1), 2-11. doi:https://doi.org/10.1111/j.1442-9071.2010.02363.x

Woei-A-Jin, F. J. S. H., Weijl, N. I., Burgmans, M. C., Fariña Sarasqueta, A., Tom van Wezel, J., Wasser, M. N. J. M., . . . Osanto, S. (2021). Neoadjuvant Treatment with Angiogenesis-Inhibitor Dovitinib Prior to Local Therapy in Hepatocellular Carcinoma: A Phase II Study. *The Oncologist, 26*(10), 854-864. doi:10.1002/onco.13901

Yeh, S., Khurana, R. N., Shah, M., Henry, C. R., Wang, R. C., Kissner, J. M., . . . Noronha, G. (2020). Efficacy and Safety of Suprachoroidal CLS-TA for Macular Edema Secondary to Noninfectious Uveitis: Phase 3 Randomized Trial. *Ophthalmology, 127*(7), 948-955. doi:https://doi.org/10.1016/j.ophtha.2020.01.006

Original publications

Paper I

Paper II

Paper III

Paper IV

Paper V

Paper VI